# MB 2019-01

U-Pb Geochronology of Zircon and Monazite by LA-ICPMS in Samples from Northern Quebec

**Documents complémentaires**

***Additional Files***

**Licence**

***License***



*Énergie et Ressources naturelles*
Québec

# U-Pb Geochronology of Zircon and Monazite by LA-ICPMS in Samples from Northern Quebec

Donald W. Davis and Chelsea N. Sutcliffe

MB 2019-01

Énergie et Ressources naturelles
Québec

# U-Pb Geochronology of Zircon and Monazite by LA-ICPMS in Samples from Northern Quebec

## June 1, 2018


## D W. Davis and C.N. Sutcliffe
## Department of Earth Sciences
## University of Toronto
## 22 Russell St.
## Toronto ON Canada M5S 3B1


### 1. SAMPLES

New U-Pb geochronological data are reported on zircon from eighteen samples of Precambrian metasedimentary, volcanic and plutonic rocks from northern Quebec. Ages were determined on selected crystal domains by analyzing U and Pb isotopes using laser ablation inductively coupled plasma mass spectrometry (LA-ICPMS). A sample list, grouped by region, is given below.

| | **Sample** | **Lithostratigraphic unit** | **Region** |
|---|---|---|---|
| 1 | 17FM2013A | Felsic metavolcanic, Roman Formation, René Group | James Bay |
| 2 | 17JF5071A | Polymictic conglomerate, Bohier Group | James Bay |
| 3 | 17JM6010A | Lapilli tuff, Érasme Formation, René Group | James Bay |
| 4 | 17JM6017A | Tonalite, Île Bohier Pluton | James Bay |
| 5 | 17JM6027A | Clast supported polymict conglomerate, Bohier Group | James Bay |
| 6 | 17JM6059A | Granodiorite, Cadieux Suite | James Bay |
| 7 | 17CB1073B | Pegmatitic granite, Aveneau Suite | Labrador Trough |
| 8 | 17CB1099B | Quartzite, Arnaud Complex | Labrador Trough |
| 9 | 17WC4222A | Tonalite, Ungava Complex | Labrador Trough |
| 10 | 17BC6068A | Monzodiorite, Sainte-Hélène Complex | Ungava area |
| 11 | 17LP2065A | Tonalite, Kovic Complex | Ungava area |
| 12 | 17SM4102A | Opdalite, Navvaataaq Suite | Ungava area |
| 13 | 17MP1013A | Quartz diorite with orthopyroxene, Pingasualuit Complex | Ungava area |
| 14 | 17LP2023A | Monzodiorite, Nallujuaq Suite | Ungava area |
| 15 | 17LP2157A | Monzonite, Suluraaq Suite | Ungava area |
| 16 | 17MP1092A | Quartz monzodiorite, Suluraaq Suite | Ungava area |
| 17 | 17CT5021A | Enderbite, Pingasualuit Complex | Ungava area |
| 18 | 17BC6021A | Tonalite, Sainte-Hélène Complex | Ungava area |

## 2. METHODS

Following crushing and pulverization, initial separation of heavy minerals was carried out on a Wilfley table. This was followed by paramagnetic separations with the Frantz isodynamic separator and density separations using methylene iodide. Final sample selection for geochronology was by hand picking under a microscope, choosing the freshest, least cracked grains.

Grains from all samples were mounted in epoxy and polished. Grains were imaged with backscattered electrons (BSE) using a JEOL JSM6610-Lv scanning electron microscope in order to detect phases of growth that may have different ages. Cathodoluminescence (CL) imaging was not used on highly damaged zircon grains, since radiation damage and alteration quench fluorescence. Monazite does not fluoresce and typically shows little structure under BSE.

Imaged grains were partially ablated using either a 213 nm New Wave laser attached to a Plasmaquad ICPMS equipped with a large rotary pump (S-option) for enhanced sensitivity, or a 193 nm New Wave excimer laser and an Agilent 7900 ICP-MS. The lasers were generally operated at 5 Hz and about 5 J/cm$^2$ fluence with typical beam diameter of 20-60 microns, depending on the sample. Data were collected on $^{88}$Sr (10 ms), $^{206}$Pb (30 ms), $^{207}$Pb (70 ms), $^{232}$Th (10 ms) and $^{238}$U (20 ms). Prior to analyses, spots were pre-ablated with a larger beam diameter for 1 sec (5 pulses) to clean the surface. Following a 10 sec period of baseline accumulation, the laser sampling beam was turned on and data were collected for 25 seconds followed by a washout period. About 150 measurement cycles per sample were produced and ablation pits are about 15 microns deep.

Data were edited and reduced using custom VBA software (UtilLAZ program) written by D. W. Davis. $^{206}$Pb/$^{238}$U ratios show increasing fractionation for zircon caused by loss of refractory U with increasing penetration depth through the run while the $^{207}$Pb/$^{206}$Pb profile is usually flat. No corrections were made for common Pb, since the $^{204}$Pb peak is too small to be measured precisely and common Pb is usually insignificant for unaltered Precambrian zircon and monazite. If present, common Pb would have the effect of pushing data to the right away from the concordia curve along a shallow mixing line with slope determined by the isotopic composition of the common Pb contaminant. $^{88}$Sr was monitored from zircon in order to detect intersection of the beam with zones of alteration or inclusions and data showing high Sr or irregular time resolved profiles were either averaged over restricted time windows or rejected. In some cases, high Sr is due to ablation of small apatite inclusions, and does not significantly affect the U-Pb analysis.

The Th/U ratio of zircon can be a useful petrogenetic indicator and was also measured, although it is only a rough estimate because the ratio is not constant in the standard. Low Th/U (<0.1) is characteristic of metamorphic and hydrothermal zircon whereas most zircon crystallized from felsic melts has Th/U in the range 0.1-1.0.

Two zircon standards were used: DD85-17, from a quartz diorite from the Marmion batholith in northwest Ontario previously dated at 3002 +/- 2 Ma by isotope dilution thermal ionization mass spectrometry (ID-TIMS; Tomlinson et al., 2003) and DD91-1, a monzodiorite from the Pontiac province of Quebec dated at 2682 ± 1 Ma (Davis, 2002). The monazite standard was from DD90-26A, a sample of the Lac

LaCroix granite in the western Superior province of Minnesota previously dated at 2671 +/- 2 Ma (D.W. Davis unpublished data). Sets of 4-5 sample measurements are bracketed by measurements on standards. Differences between standards are time interpolated to correct sample measurements.

## 3. RESULTS

Results of U-Pb isotopic analyses by LA-ICPMS are given in Table 1 and data are plotted on figures below. Average age errors in the text and error ellipses on figures are given at 2 sigma (twice the 1 sigma errors given in Table 1). These were calculated and plotted using the Isoplot program of Ludwig (1998, 2003). MSWD (mean square of weighted deviations) would be expected to be around 1 or slightly higher with correctly chosen analytical errors for $^{207}Pb/^{206}Pb$ ages if the age population is unimodal. Since Pb/U errors do not include possible biases from compositional differences between samples and standard, scatter above and below concordia may be more pronounced, but it should not affect $^{207}Pb/^{206}Pb$, which is fractionated only in the plasma.

U decay constants are taken from Jaffey et al. (1971). For Paleoproterozoic and Archean samples, $^{207}Pb/^{206}Pb$ ages are more precise than $^{206}Pb/^{238}U$ ages, and are also much less susceptible to fractionation biases between samples and standards. Therefore, ages are based on $^{207}Pb/^{206}Pb$ ratios.

Representative images for individual samples are presented in the sections below.

Zircon populations from all samples were often cracked and altered. BSE is enhanced by radiation damage in zircon, resulting in brighter domains. Alteration shows as darker amorphous domains that may follow high-U zones. BSE also shows cracks. Both are avoided during targeting but the beam can penetrate into subsurface alteration. Typically, alteration is associated with high levels of Ca as well as common Pb so $^{88}Sr$, which follows Ca but with a lower background, is used to indicate its presence. Analyses showing high Sr levels or irregular time-resolved profiles were rejected or limited to short segments where Sr is low. Large variations in U content and damage can introduce sample-standard bias for the Pb/U ratio. A more serious bias, which may account for reverse discordance, is the necessity of averaging the time-resolved data profile over a limited window to avoid altered (high Sr) domains. Because the Pb/U profile increases with time, the sample profile may differ from that used to measure the standard. Such biases should be insignificant for $^{207}Pb/^{206}Pb$ ages, which is why this ratio is selected as the preferred geochronometer. Analyses of altered zircon domains generally produce data that plot well below concordia because of Pb loss. The $^{207}Pb/^{206}Pb$ age may be too young, because of non-zero Pb loss, but may also be too old if significant amounts of common Pb are present. Accordingly, excessively discordant data (>10%) are usually rejected.

### *3-1 17FM2013A, Felsic metavolcanic, Formation de Roman, Groupe de René, James Bay area*

This sample yielded generally cracked, subrounded prismatic zircon (Fig 1-1). BSE images show a consistent pattern of broad zonation without clear evidence of cores (Fig 1-2A-C). U-Pb isotopic analyses of spots on 41 grains give $^{207}Pb/^{206}Pb$ ages that scatter only slightly outside of error with a mean age of 2770 ± 3 Ma (Fig 1-3). This is the best estimate for the age of crystallization of the rhyolite, which appears to have been derived from a uniform source.

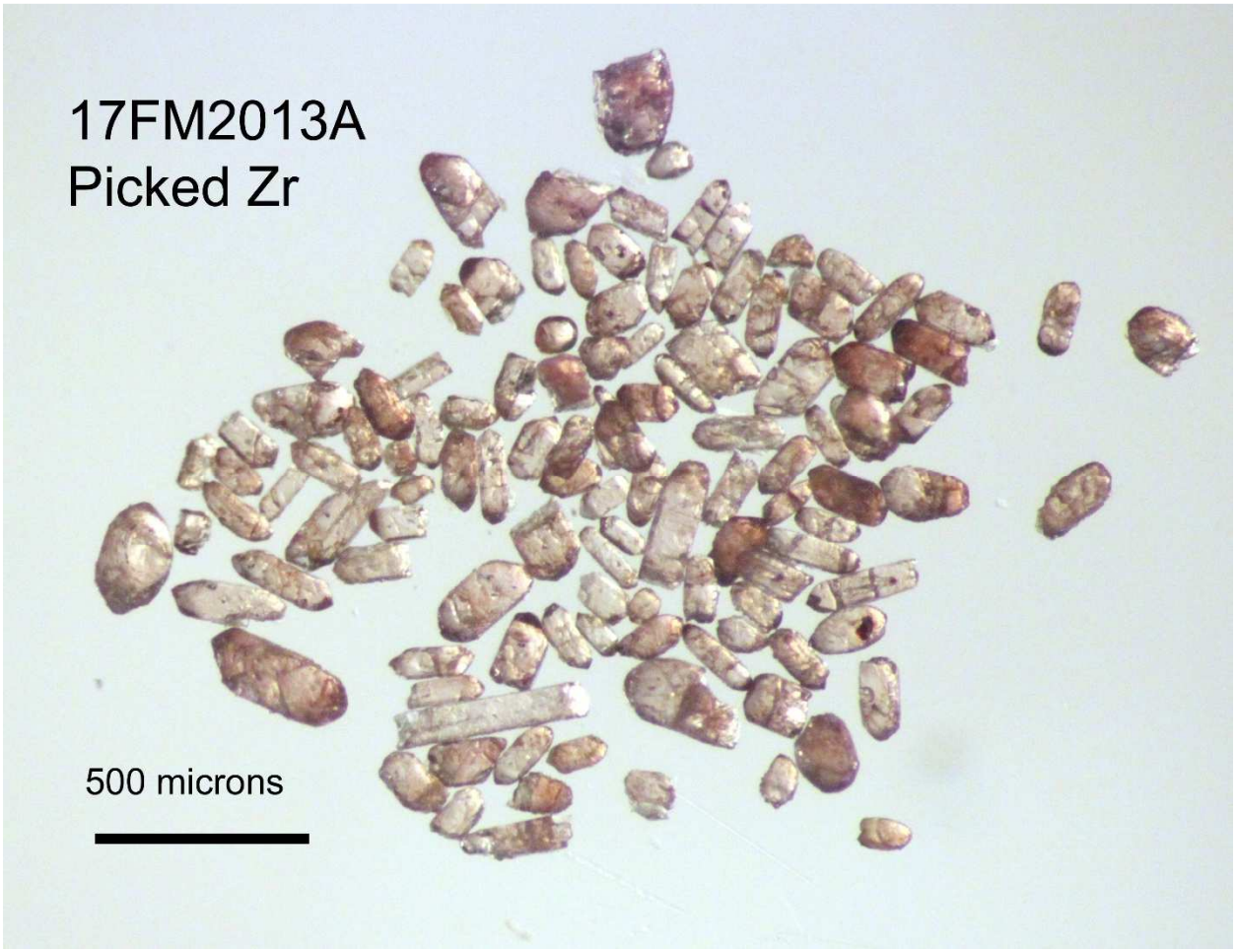


Fig 1-1. Picked zircon from rhyolite sample 1FM2013A.

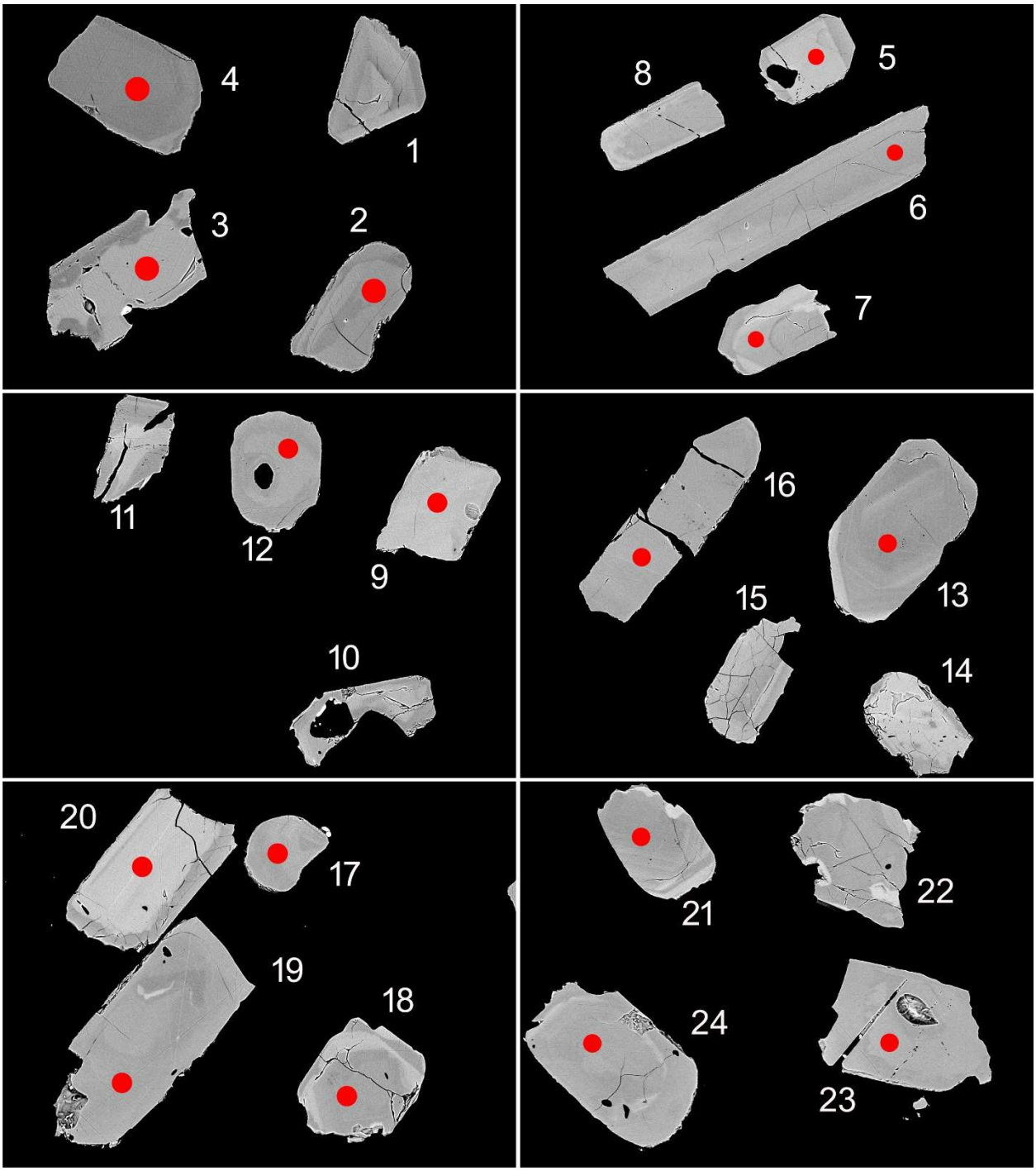


Fig 1-2-1. BSE images of selected grains from rhyolite sample 17FM2013A. The red spots represent the approximate locations of 20 micron diameter laser ablation pits.

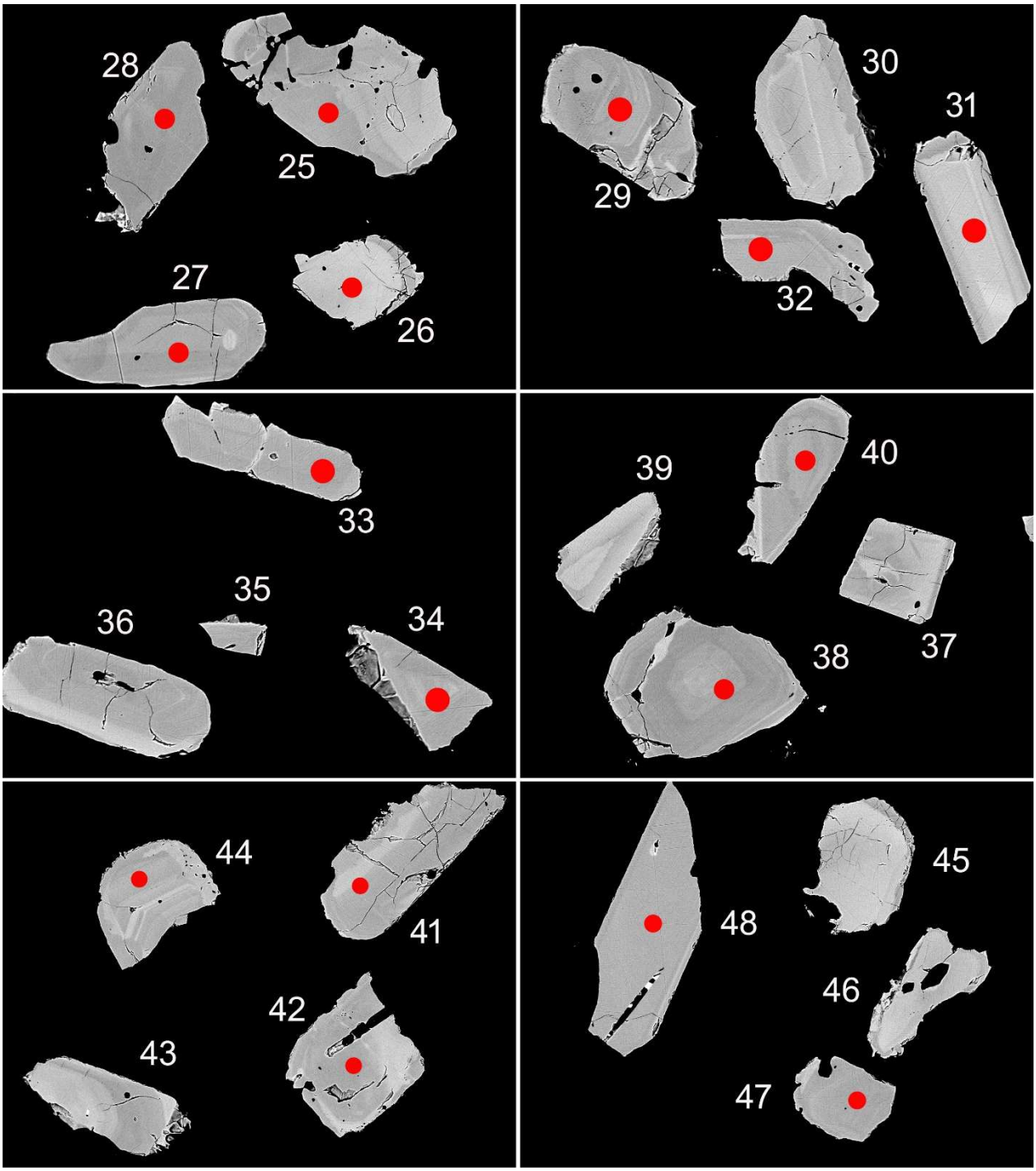


Fig 1-2-2. BSE images of selected grains from rhyolite sample 17FM2013A. The red spots represent the approximate locations of 20 micron diameter laser ablation pits.

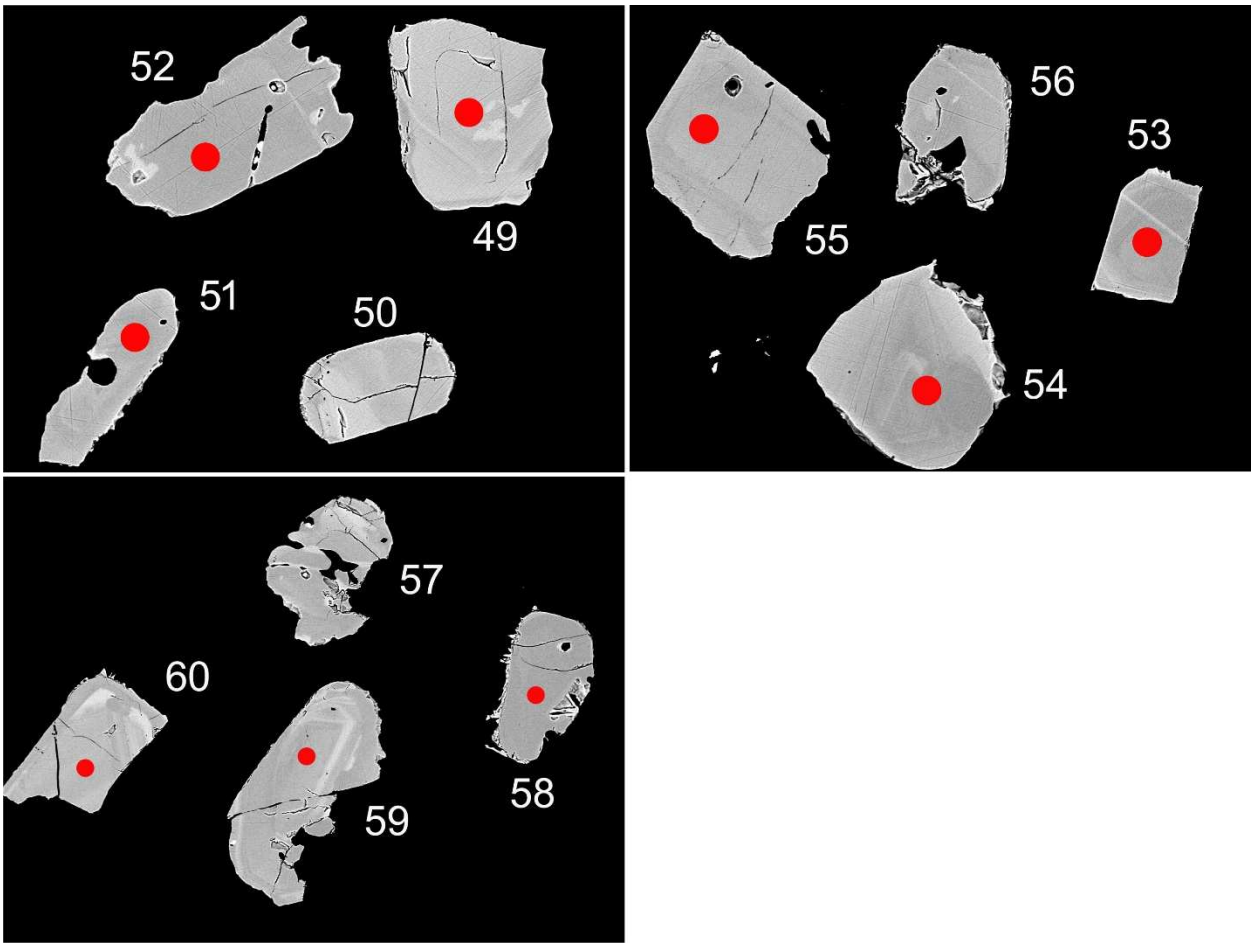


Fig 1-2-3. BSE images of selected grains from rhyolite sample 17FM2013A. The red spots represent the approximate locations of 20 micron diameter laser ablation pits.

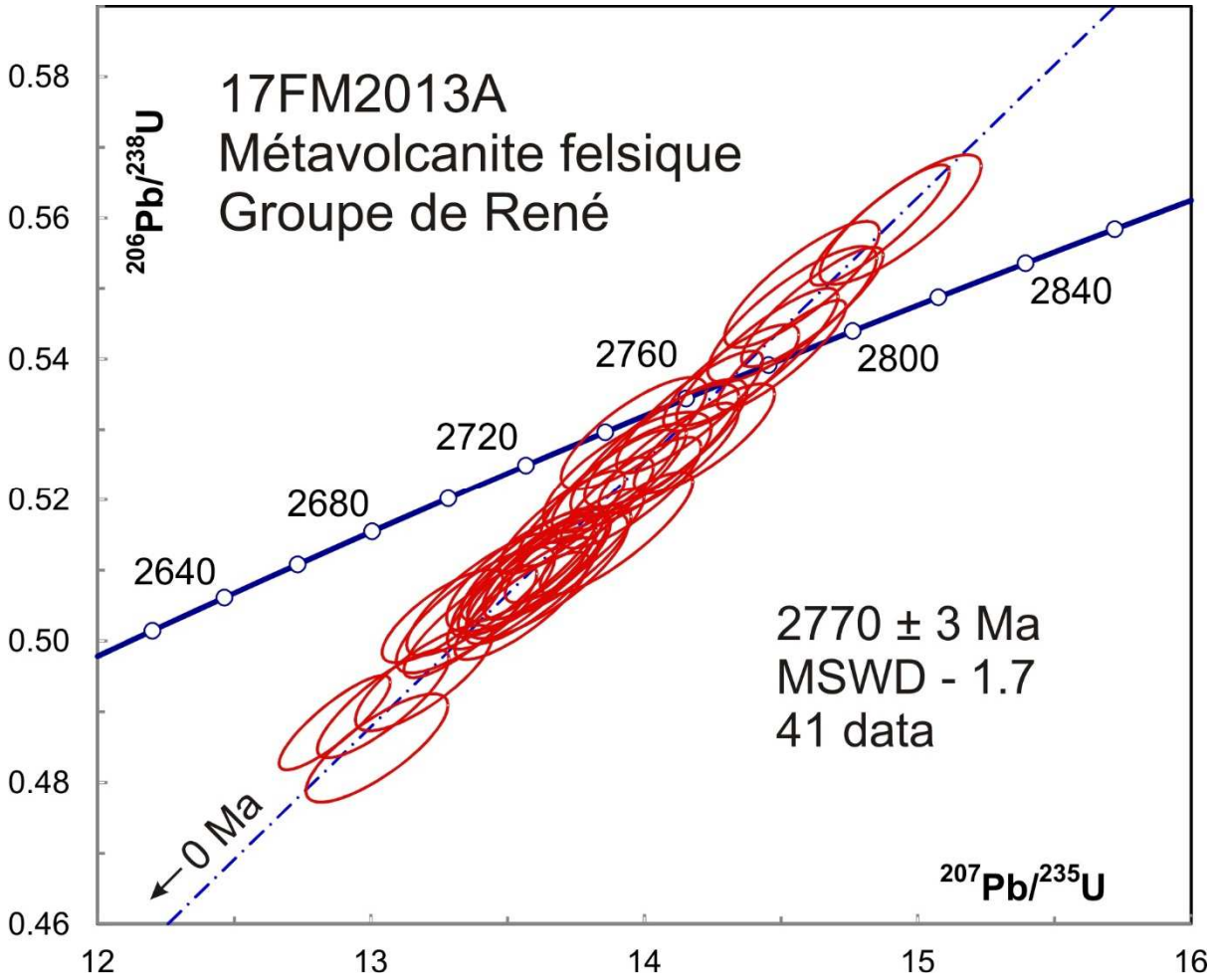


Fig 1-3. Concordia plot showing U-Pb isotopic data on polished zircon from rhyolite sample 17FM2013A.

### *3-2 17JF5071A, Polymictic conglomerate, Groupe de Bohier, James Bay area*

This sample yielded a small amount of zircon with diverse morphologies (Fig 2-1). The larger grains are generally damaged, restricting the number available for geochronology. BSE images of polished grains show a variety of oscillatory and patchy zoning patterns (Fig 2-2).

U-Pb analyses of 33 spots on polished grains show two main clusters of $^{207}Pb/^{206}Pb$ ages scattering around 2712 Ma and 2836 Ma (Fig 2-3) with one somewhat discordant datum giving an age of 3245 ± 14 Ma (Table 1). The smaller grains are more numerous in the population making it easier to find relatively clear, unfractured crystals. Because of their small size, these were mounted for ablation onto double sided tape (Fig 2-4). U-Pb analyses on 70 grains define a similar distribution as for the polished grains with two clusters and an oldest age being 3036 ± 10 Ma (Fig 2-5). A relative probability density plot of the combined data set shows two main peaks around 2710 Ma and 2830 Ma, although the peaks are somewhat assymetrical suggesting that they each contain at least one other unresolved age component (Fig 2-6). The youngest acceptable analyses with magmatic Th/U ratios are 2663 ± 14 Ma for a polished grain, although it appears somewhat discordant, and 2678 ± 10 Ma for an unpolished grain.

Analyses of unpolished grains are sensitive to the presence of thin overgrowths and allow depth profiling where the age of an overgrowth can be measured during the early part of an analysis and that of a core as the beam penetrates deeper. The Th/U ratio provides a sensitive indicator of penetration into a metamorphic phase. A number of analyses show high U signals accompanied by Th/U < 0.1 during the initial few seconds of the 30 second time resolved profile (Fig 2-7). The sample areas were previously cleaned by 15 laser shots to remove alteration that is often present on grain surfaces (equivalent to 1.5 seconds of pre-ablation). If these sections of the time resolved profile show no significant Sr signal, they can be used to determine a U-Pb datum for the rim, provided an equivalent Pb/U window is chosen on the standards ($^{207}Pb/^{206}Pb$ does not change with depth so this entire window can be averaged on the standard). Ten analyses were processed in this way from the unpolished grains (Table 1). In addition, one analysis on polished grain 29 showed low Th/U over the entire profile, as did, coincidentally, unpolished grain 29, which is a separate grain. Only the unpolished grains gave data that are sufficiently concordant to be meaningful. These data show a significant range of ages (Fig 2-8) from 2591 ± 12 Ma to two overlapping data at 2820 Ma. There are also several data around 2730 Ma and 2660 Ma (Table 1). Low Th/U zircon can result from crystallization of S-type magmas as well as metamorphism. The low Th/U overgrowth on grain 60 (2821 Ma) was beneath the surface of the grain (Fig 2-7), which suggests that it represents an old metamorphic overgrowth on a detrital core. There is a possibility that the beam intersected both metamorphic and magmatic phases, and therefore gave a mixed age. Profiles that show changing Th/U values were avoided for this reason but some profiles had to be made very short so mixing cannot be ruled out.

The youngest magmatic detrital ages of around 2670 Ma put an older age estimate on deposition of the unit. Older low Th/U phases may record earlier episodes of metamorphism or be mixtures between a post-depositional metamorphic phase and older detrital ages. However, low Th/U rims were only found on a minority of grains.

Some rims could have been removed during pre-ablation but BSE images (Fig 2-2) show no consistent evidence for high-U metamorphic overgrowths. Had metamorphism post-dated deposition, it might be expected to have affected all the grains. This suggests that the youngest 2591 Ma phase may also be detrital in which case it would be an older limit on deposition.


Fig 2-1. Picked zircon from conglomerate sample 17JF5071A.

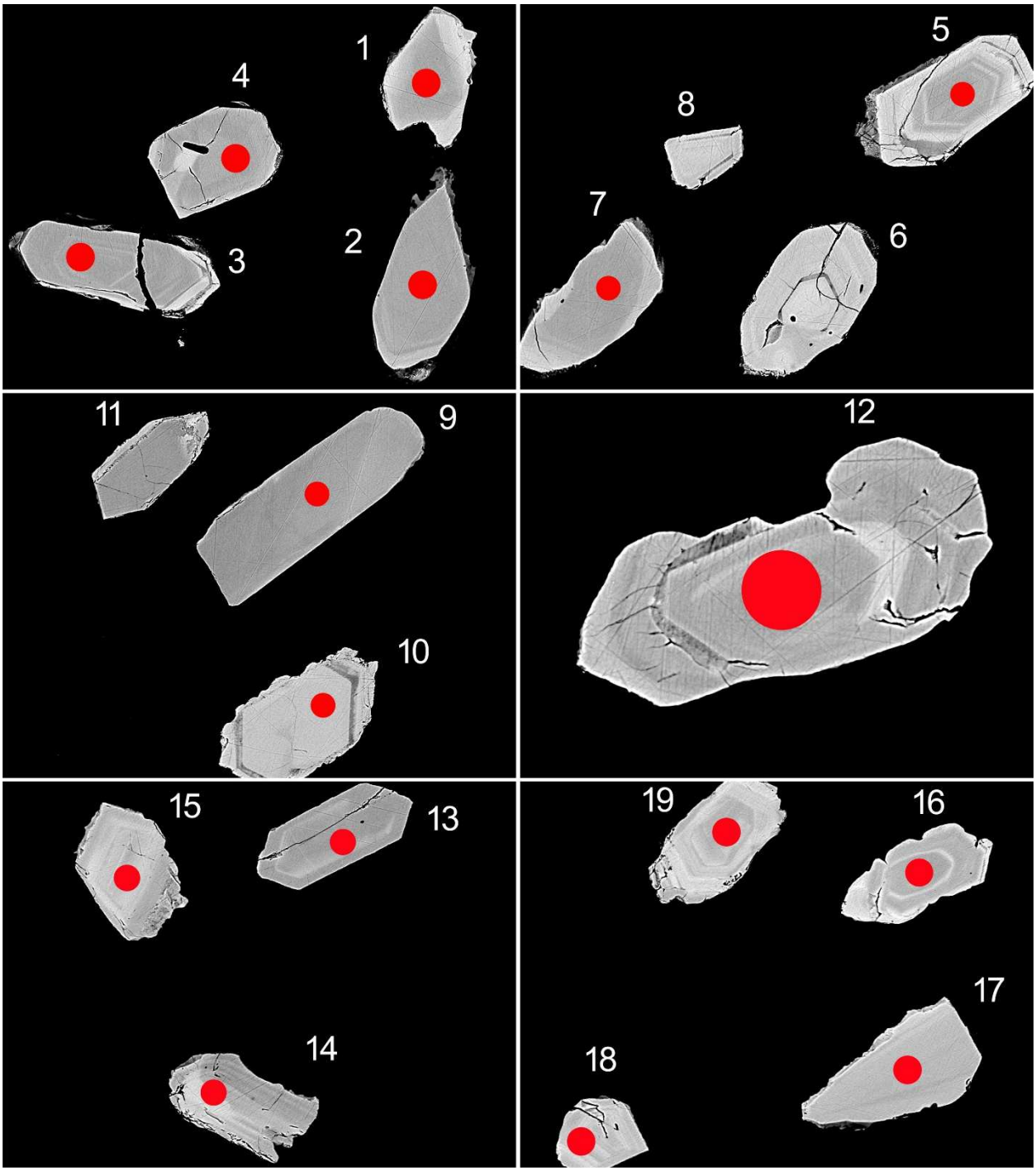


Fig 2-2-1. BSE images of selected grains from conglomerate sample 17JF5071A. The red spots represent the approximate locations of 20 micron diameter laser ablation pits.

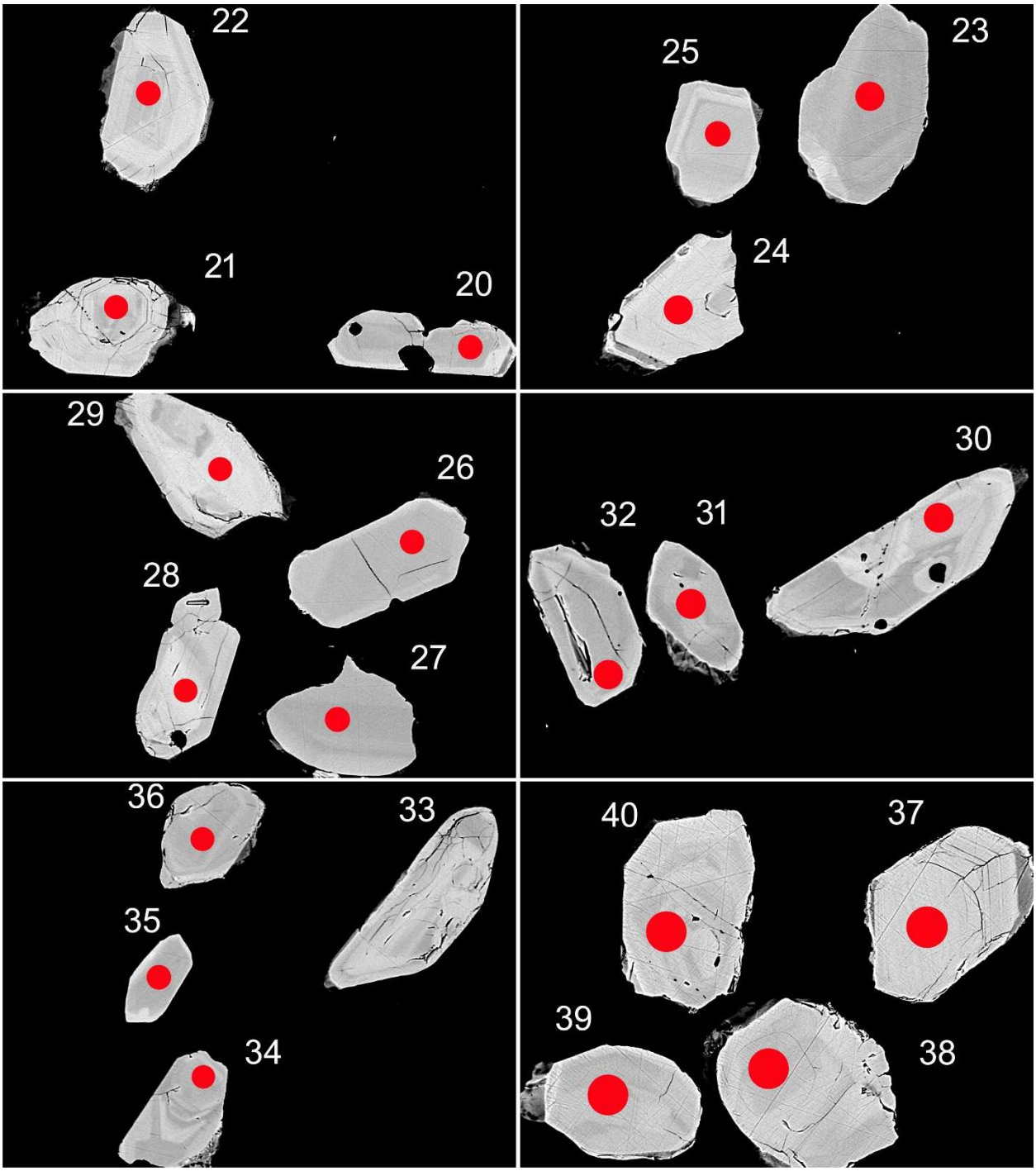


Fig 2-2-2. BSE images of selected grains from conglomerate sample 17JF5071A. The red spots represent the approximate locations of 20 micron diameter laser ablation pits.

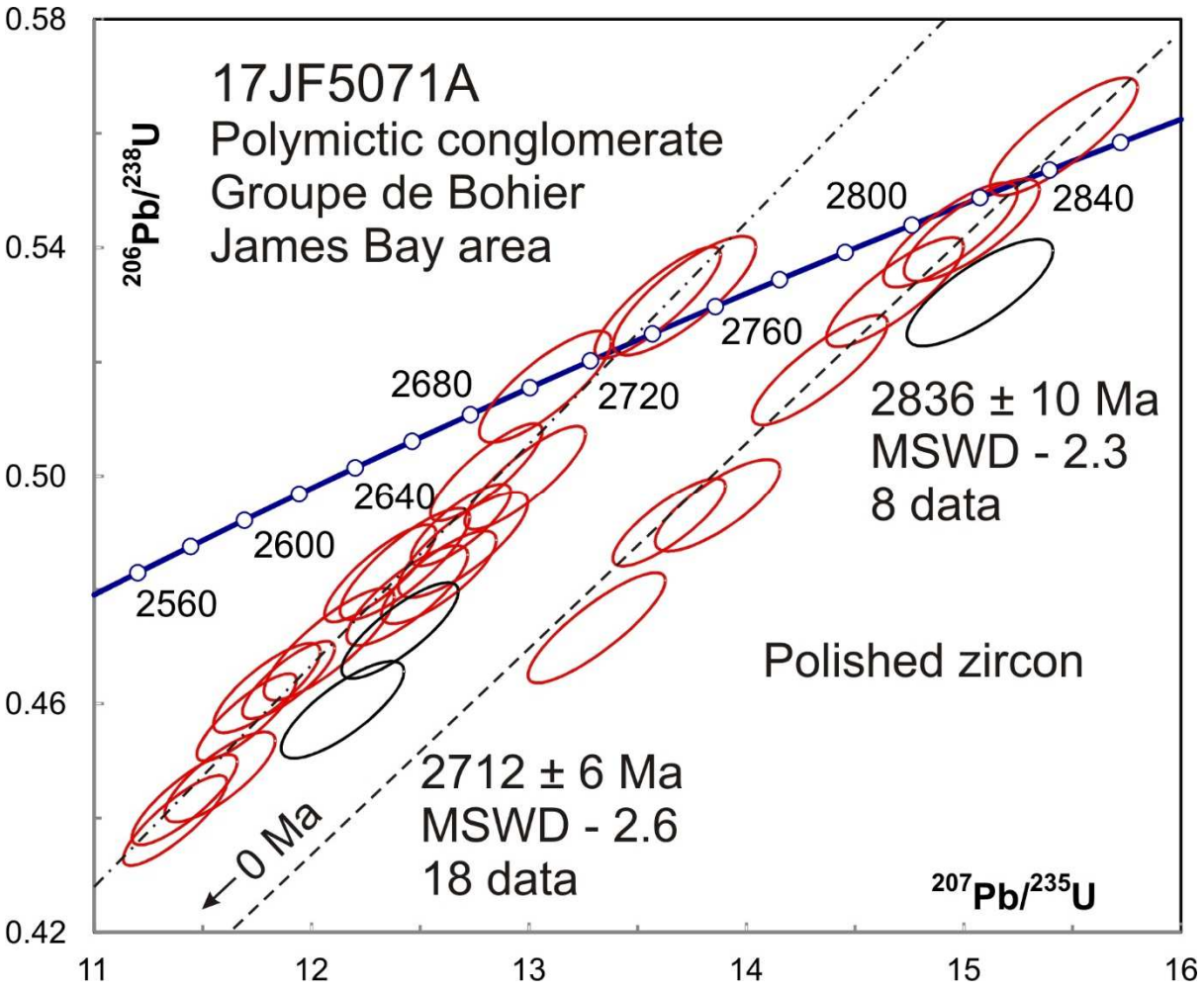


Fig 2-3. Concordia plot showing U-Pb isotopic data on polished zircon from conglomerate sample 17JF5071A.

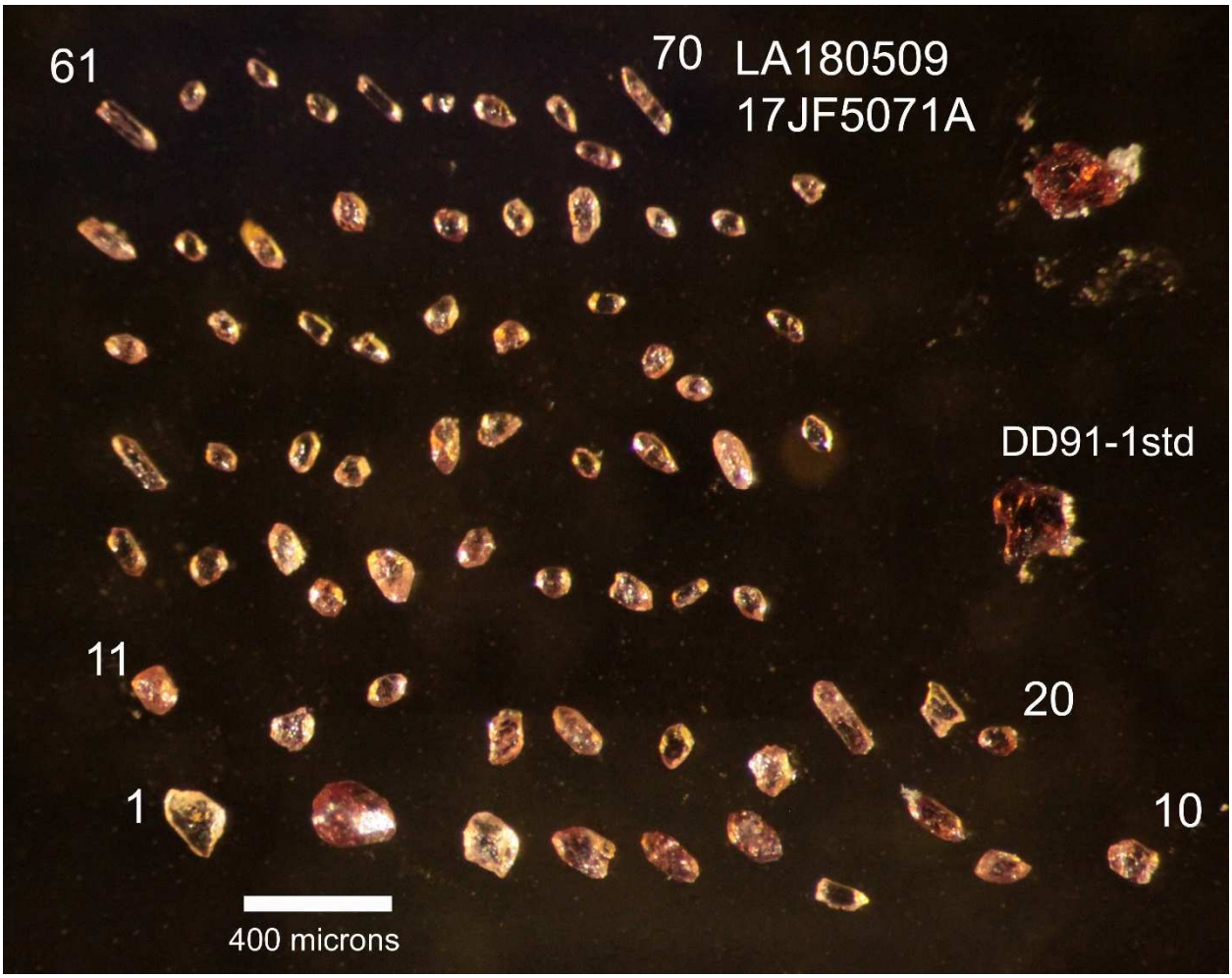


Fig 2-4. Mounted whole grain (unpolished) zircon from conglomerate sample 17JF5071A.

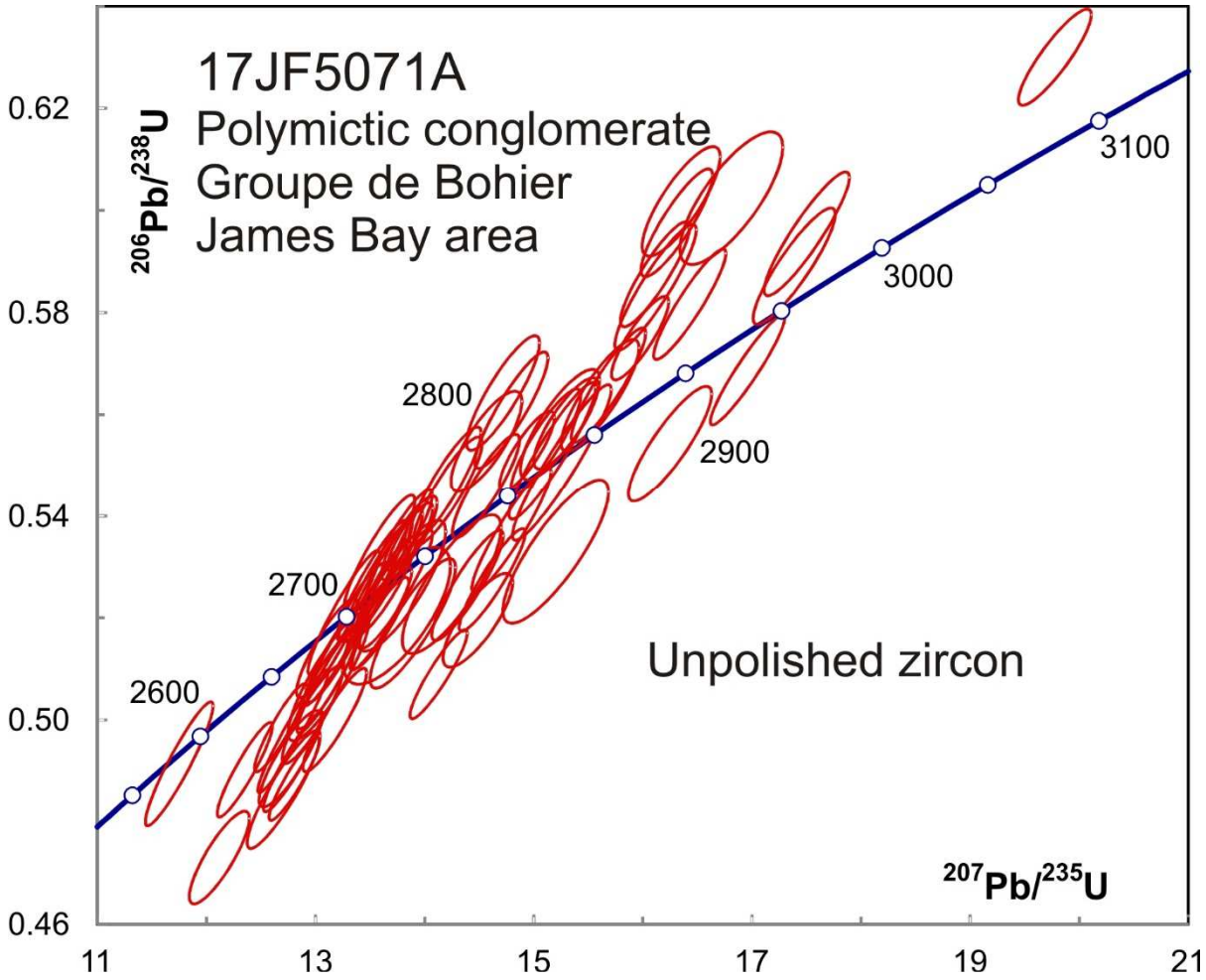


Fig 2-5. Concordia plot showing U-Pb isotopic data on whole grain (unpolished) zircon from conglomerate sample 17JF5071A.

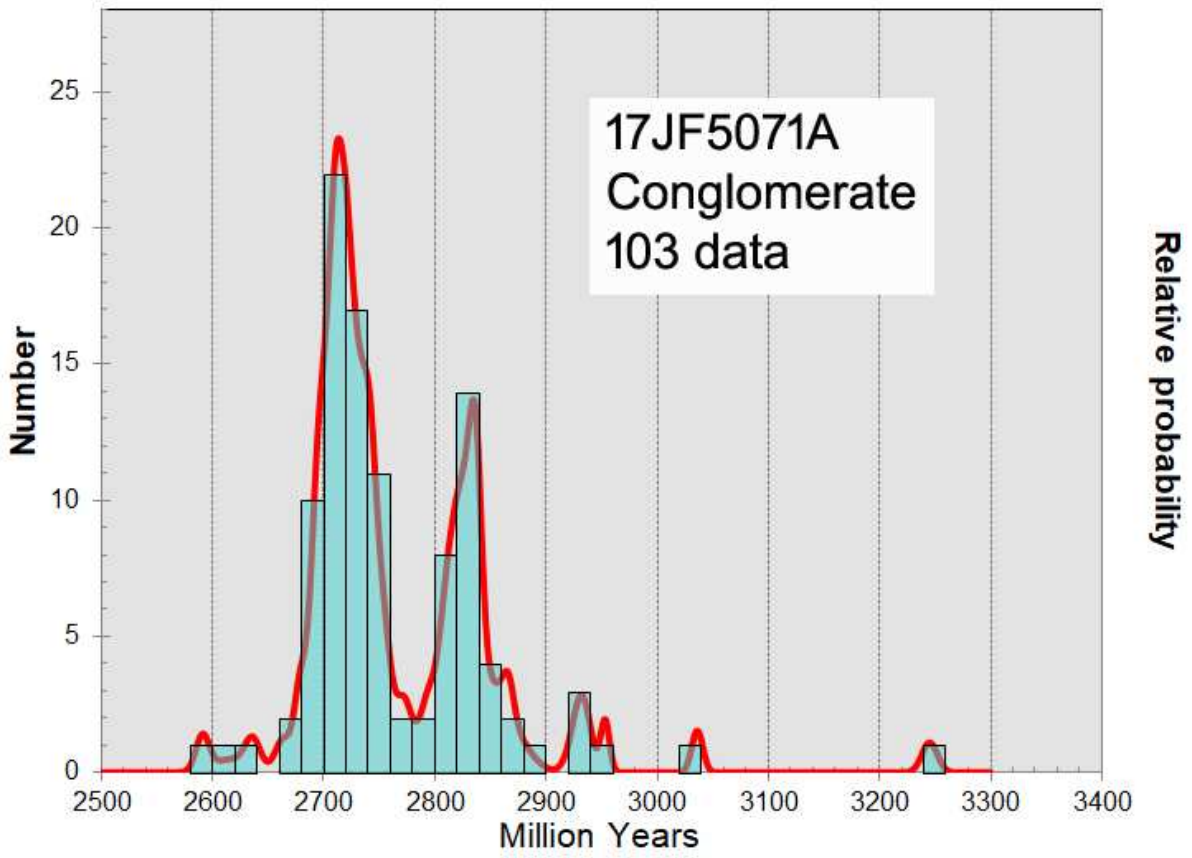


Fig 2-6. Relative probability density distribution of $^{207}Pb/^{206}Pb$ ages of polished and unpolished zircon from conglomerate sample 17JF5071A.

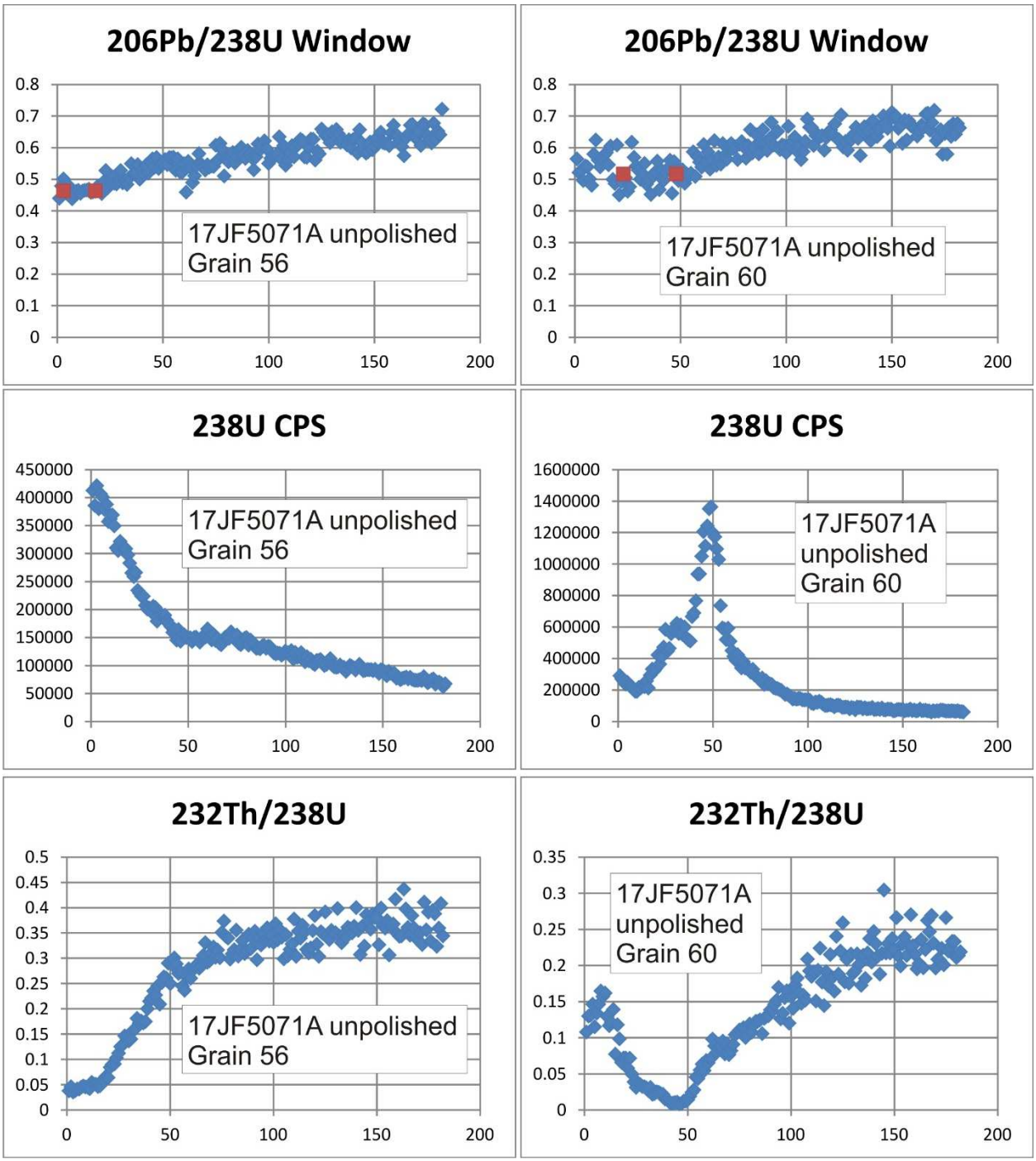


Fig 2-7. Time-resolved analytical profiles for spots 56 (left) and 60 (right) of unpolished grains showing the variation in $^{206}Pb/^{238}U$, $^{238}U$ and $^{232}Th/^{238}U$ with beam penetration depth. The red squares on the $^{206}Pb/^{238}U$ profile show the windows taken for averaging low Th/U sections.

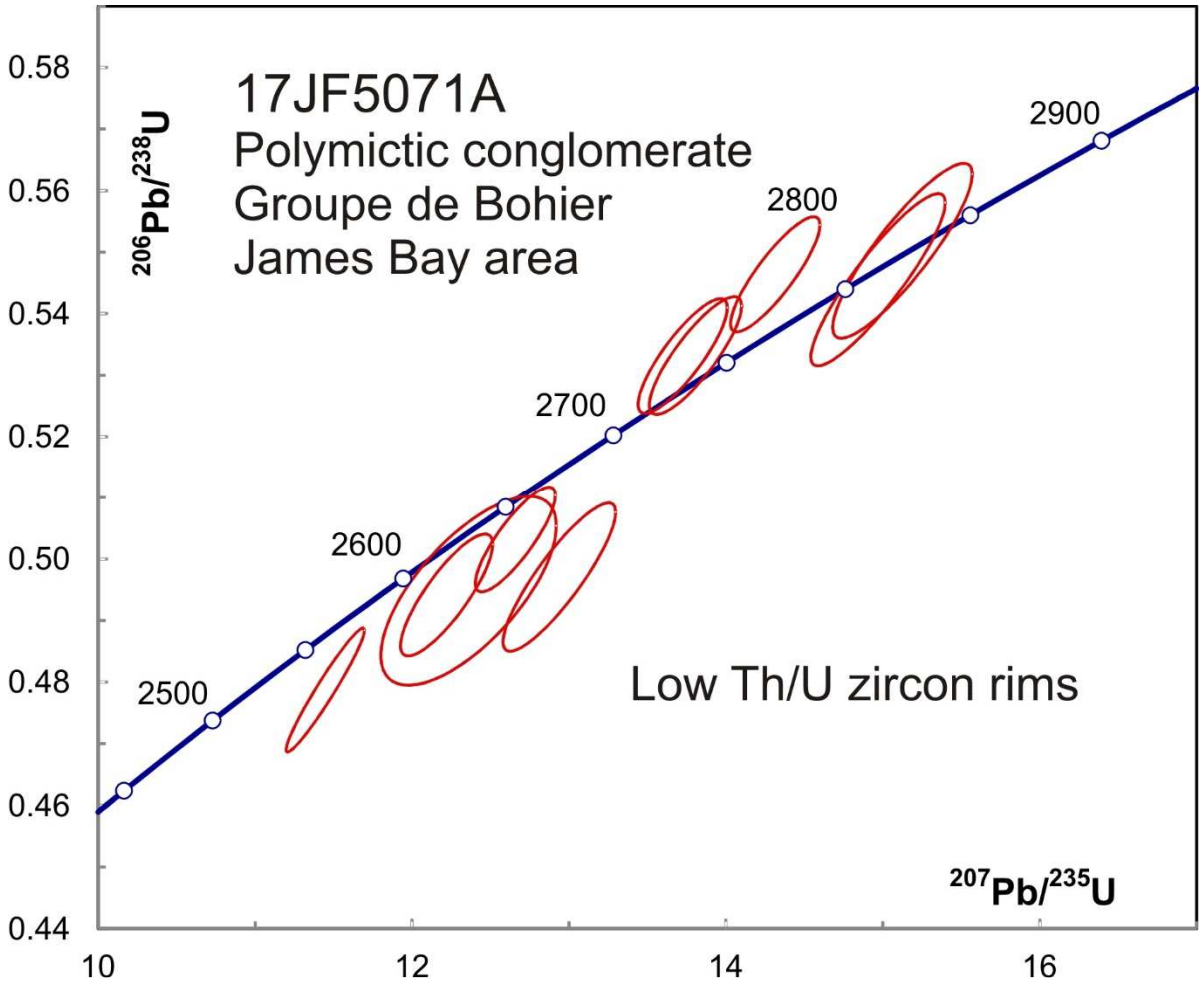


Fig 2-8. Concordia plot showing U-Pb isotopic data from low Th/U rims on whole grain (unpolished) zircon from conglomerate sample 17JF5071A.

### *3-3 17JM6010A Felsic lapilli tuff, Formation d'Érasme, Groupe de René, James Bay area*

This sample yielded abundant brownish to colourless zircon crystals many of which are well rounded (Fig 3-1). BSE images show diverse zoning patterns from oscillatory to patchy (Fig 3-2). U-Pb analyses on 29 spots scatter slightly outside of error with an average age of 2800 ± 6 Ma (MSWD – 2.3) after omitting the youngest analysis (Fig 3-3). The rounded shape of many of the zircon crystals suggests that the volcanic unit has been re-deposited and could thus contain detrital components having diverse ages. The diverse zoning patterns also suggest multiple sources. A relative probability distribution of $^{207}Pb/^{206}Pb$ ages shows a slight shoulder on the left side, which suggests that there might be two unresolved distributions. Dividing the age-ranked distribution into two equal parts gives two averages of 2791 ± 5 Ma and 2813 ± 5 Ma that may more accurately described the distribution. There does not seem to be a consistent relationship between morphology or zoning patterns and age. Therefore, it is possible that the unit sampled a proximal volcanic source characterized by these ages. In this case, a maximum age for deposition of the unit should be given by the youngest concordant analysis at 2766 +/- 22 Ma (grain 3), which appears slightly younger than the others. However, without multiple analyses of the younger age this interpretation remains speculative.

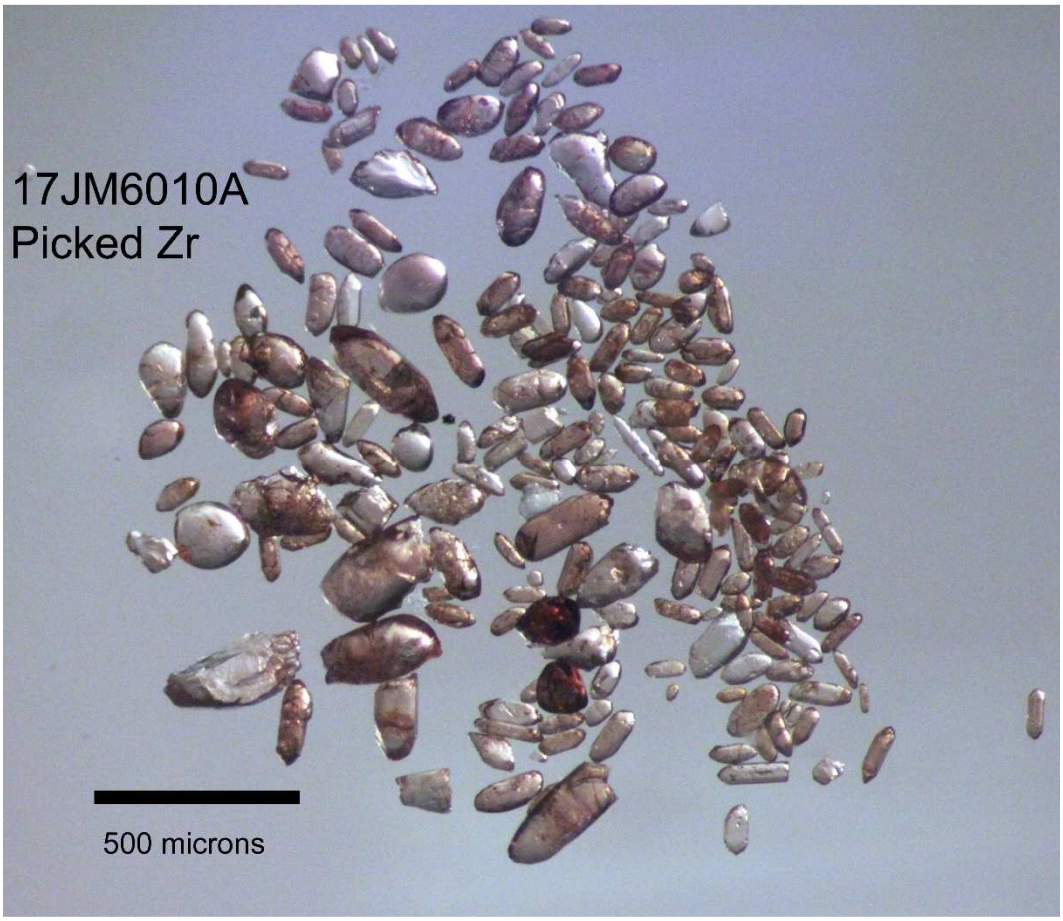

Fig 3-1. Picked zircon from tuff sample 17JM6010A.

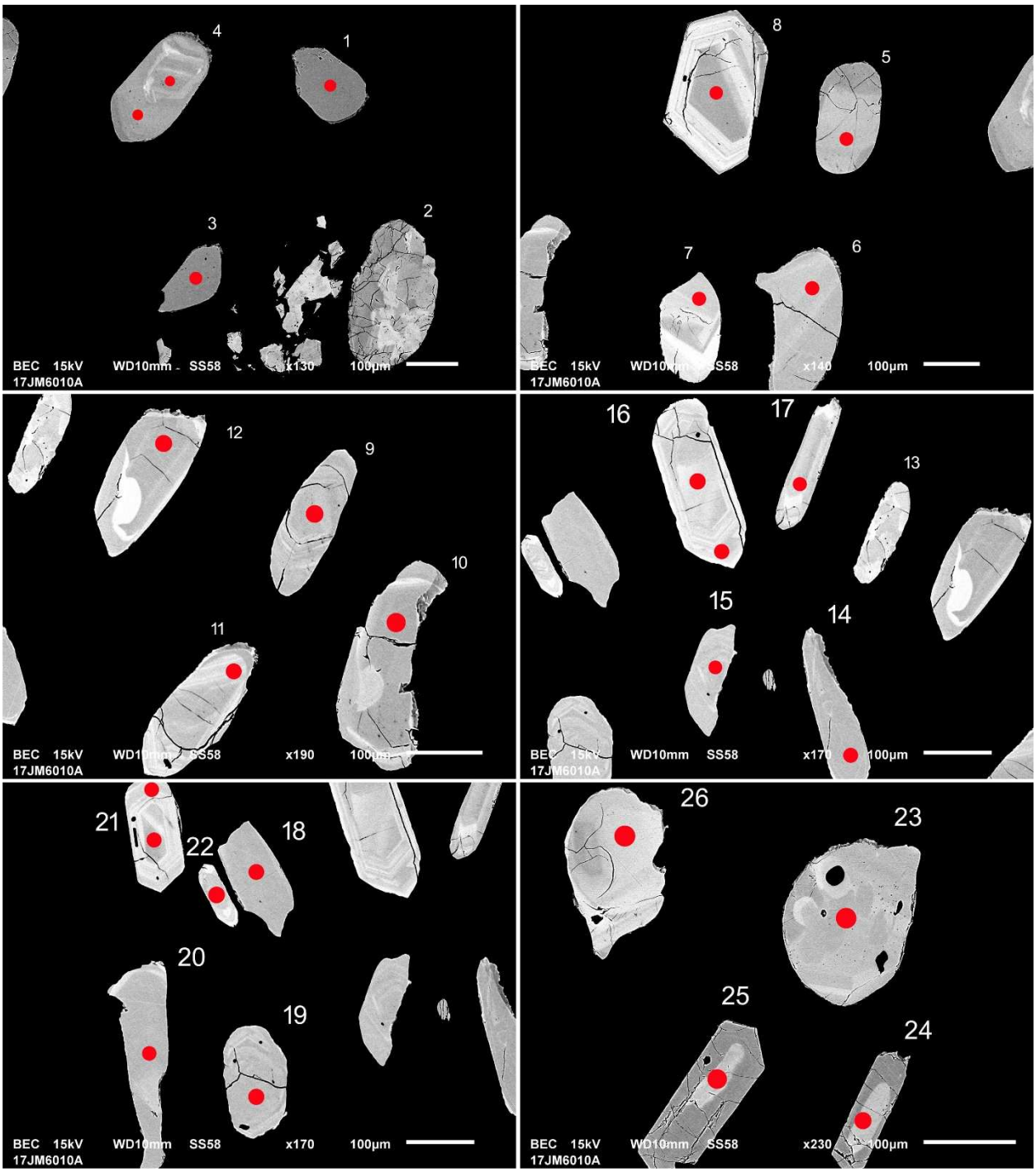


Fig 3-2-1. BSE images of selected grains from tuff sample 17JM6010A. The red spots represent the approximate locations of 20 micron diameter laser ablation pits.

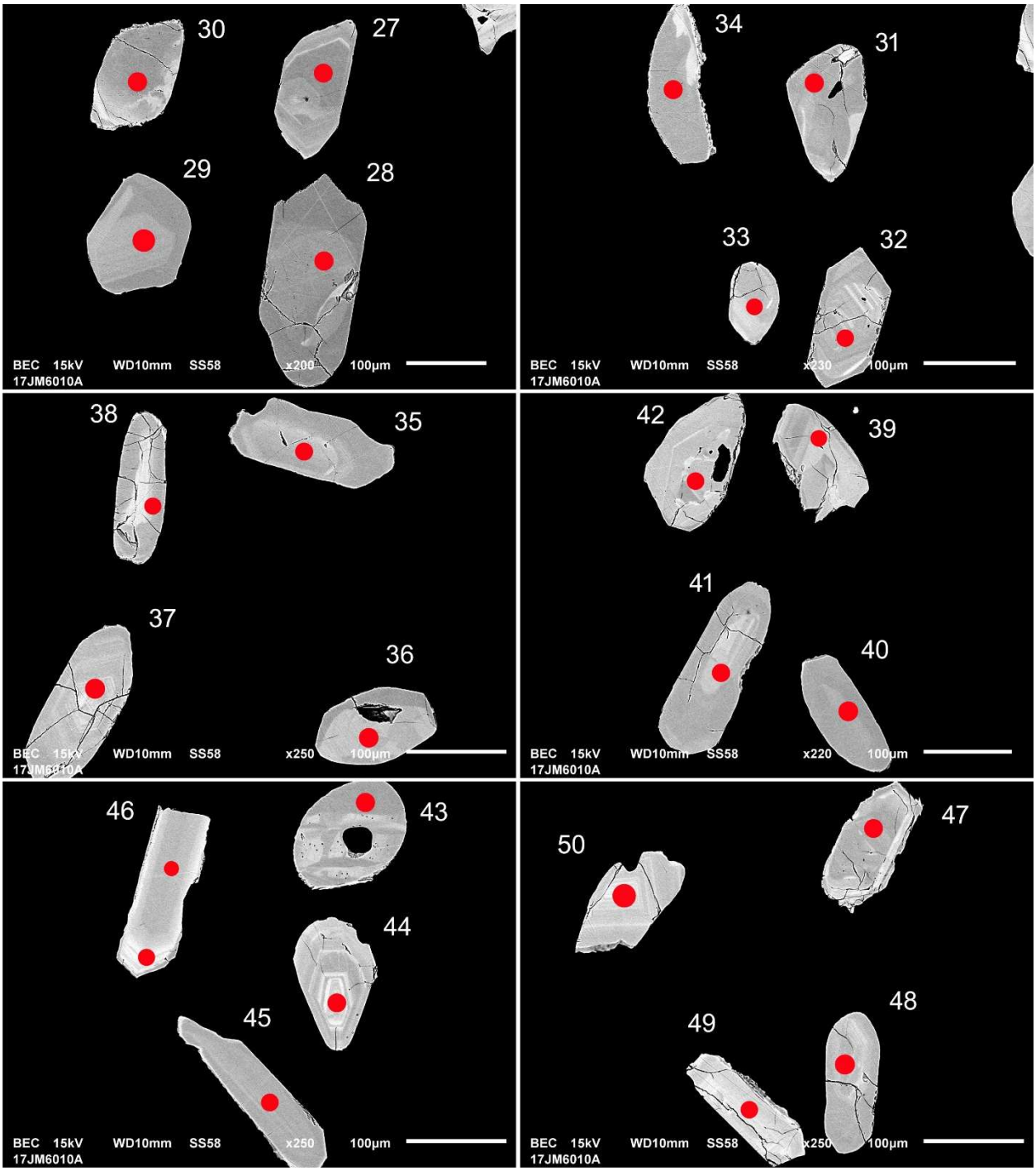


Fig 3-2-2. BSE images of selected grains from tuff sample 17JM6010A. The red spots represent the approximate locations of 20 micron diameter laser ablation pits.

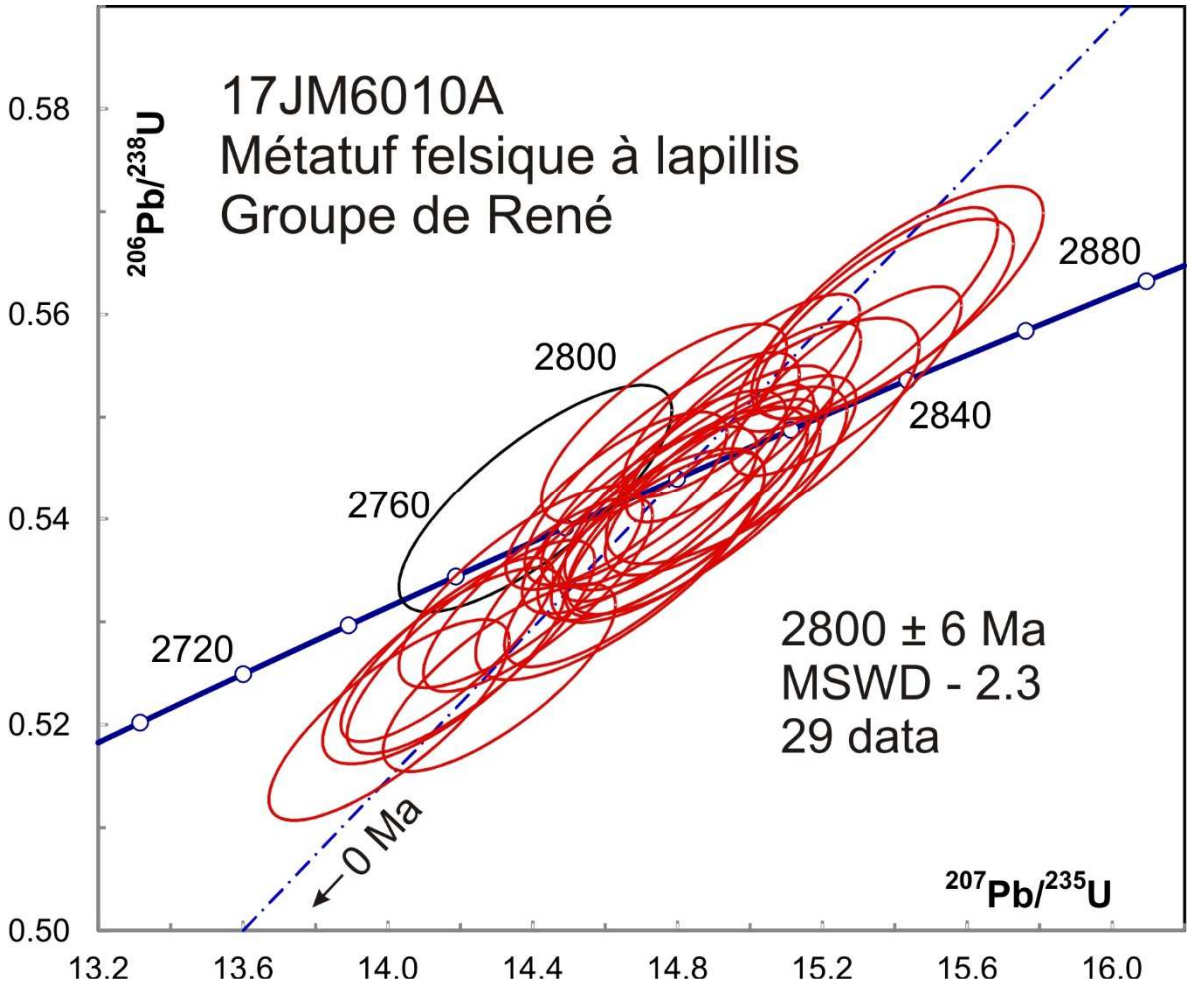


Fig 3-3. Concordia plot showing U-Pb isotopic data on polished zircon from tuff sample 17JM6010A. Ellipse in black is omitted from the distributions.

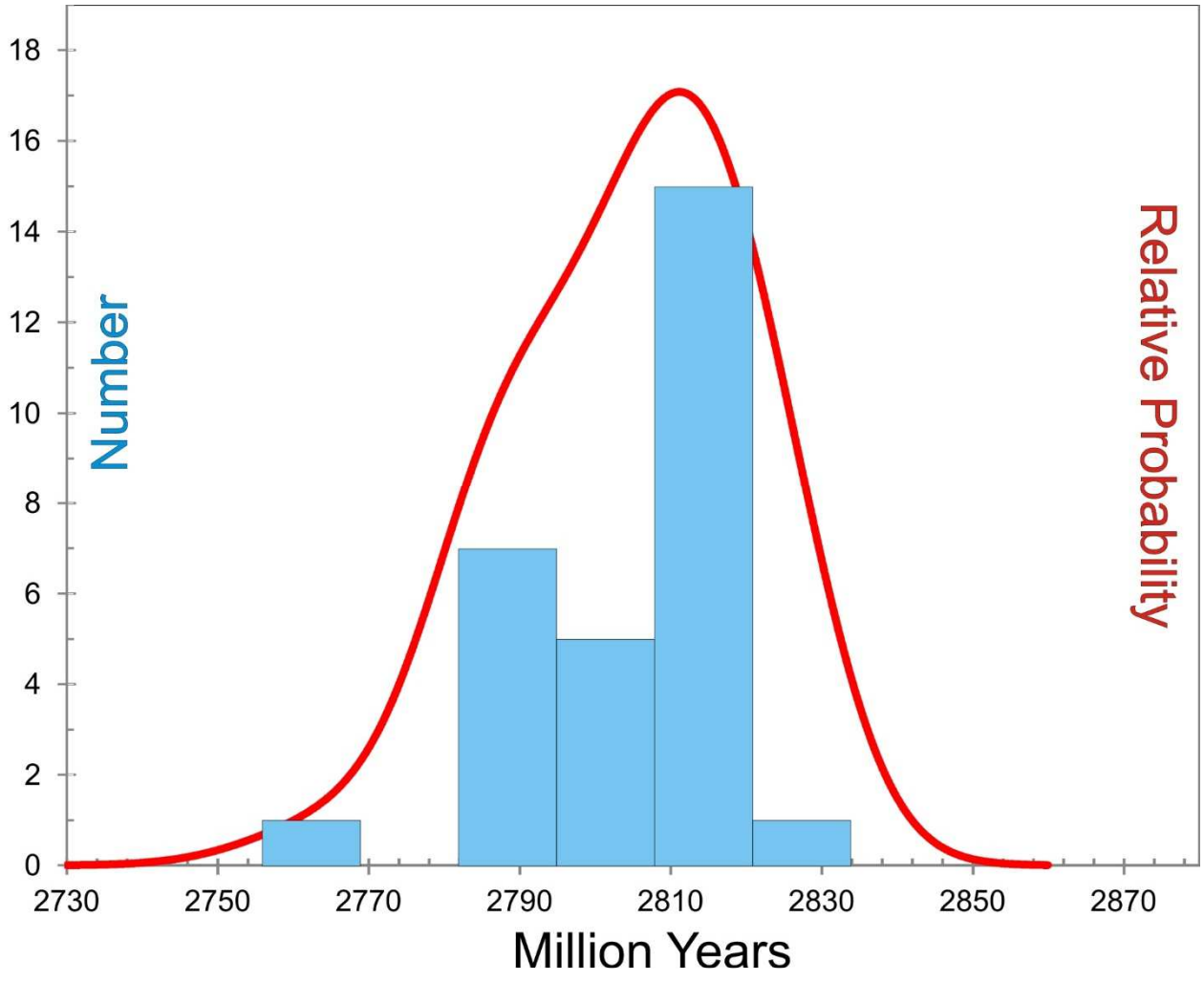


Fig 3-4. Relative probability density distribution and histogram showing U-Pb isotopic data on polished zircon from tuff sample 17JM6010A. The shoulder on the left side suggests the there are two unresolved distributions.

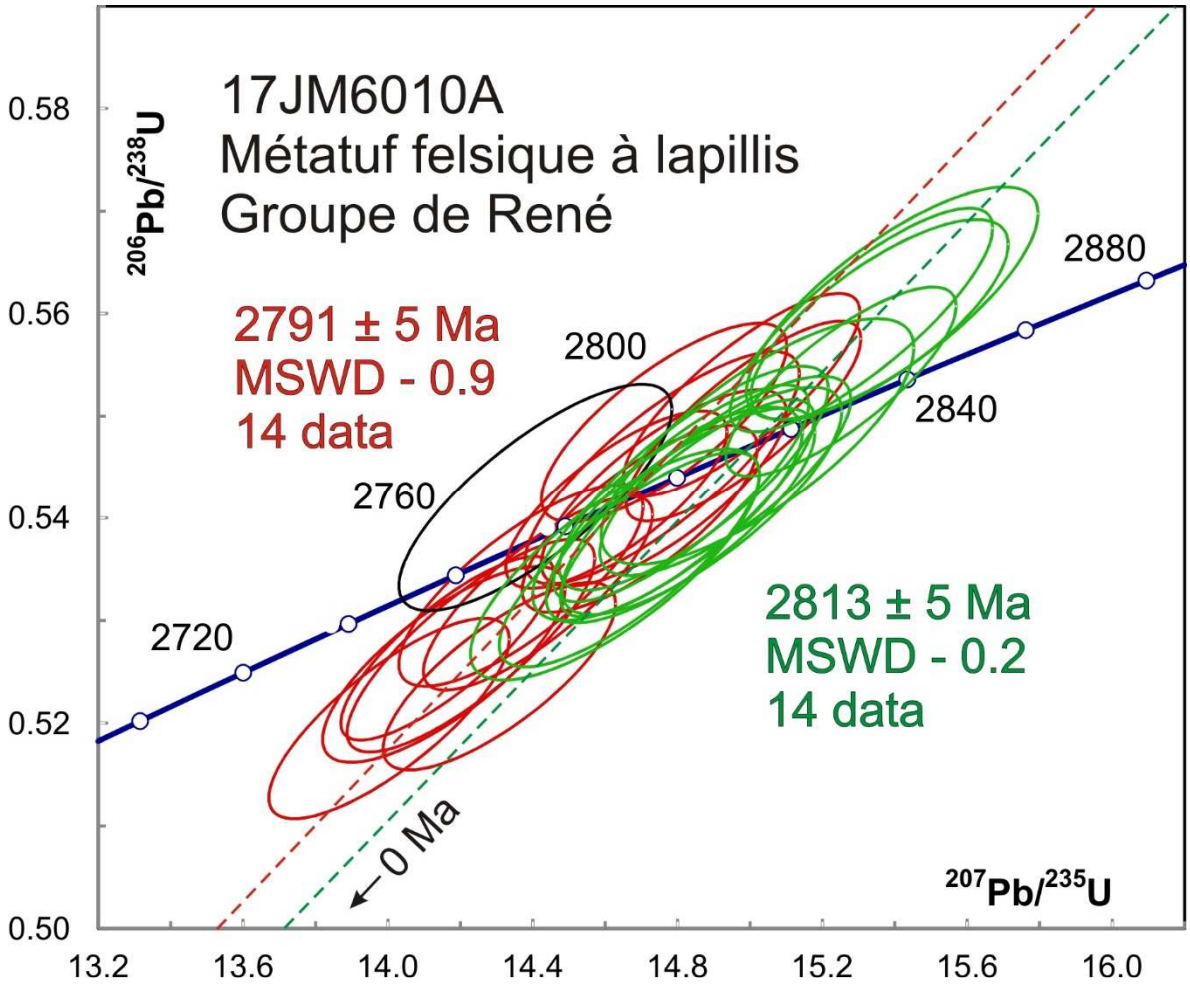


Fig 3-5. Concordia plot showing U-Pb isotopic data on polished zircon from tuff sample 17JM6010A. Hypothetical members of two possible distributions are distinguished by red and green. Ellipse in black is omitted from the distributions.

### *3-4 17JM6017A Île Bohier tonalite, James Bay area*

This sample yielded abundant euhedral short-prismatic zircon (Fig 4-1). BSE images show a uniform pattern of subdued broad or patchy zonation (Fig 4-2). A first round of U-Pb analyses was carried out on the Plasmaquad LA-ICPMS, which is relatively less sensitive, and uses a 213 nm laser. This produced mostly concordant data with an average age of 2766 ± 8 Ma (Fig 4-3) but data scatter slightly outside of error (MSWD – 2.2). The relative probability distribution shows no good evidence for a mixed population so the sample was re-run on a more sensitive Agilent 8800 LA-ICPMS with a 193 nm laser. After removing two slightly older data, which may be affected by inheritance, this data set gives a similar age of 2771 ± 6 Ma (Fig 4-4) and the scatter is within error (MSWD – 0.8). Therefore this is likely the age of crystallization of the tonalite.


Fig 4-1. Picked zircon from tonalite sample 17JM6017A.

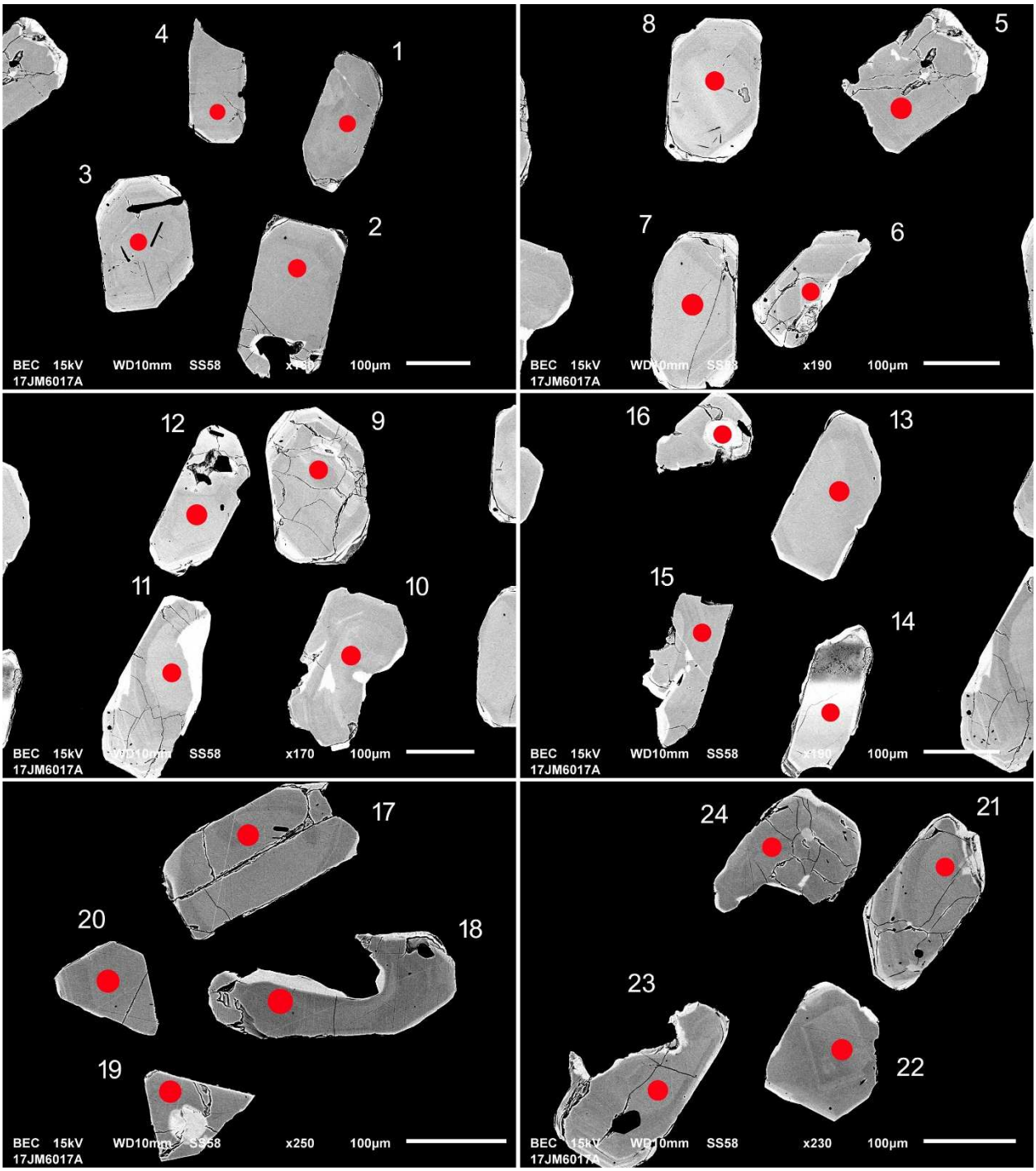


Fig 4-2-1. BSE images of selected grains from tonalite sample 17JM6017A. The red spots represent the approximate locations of laser ablation pits.

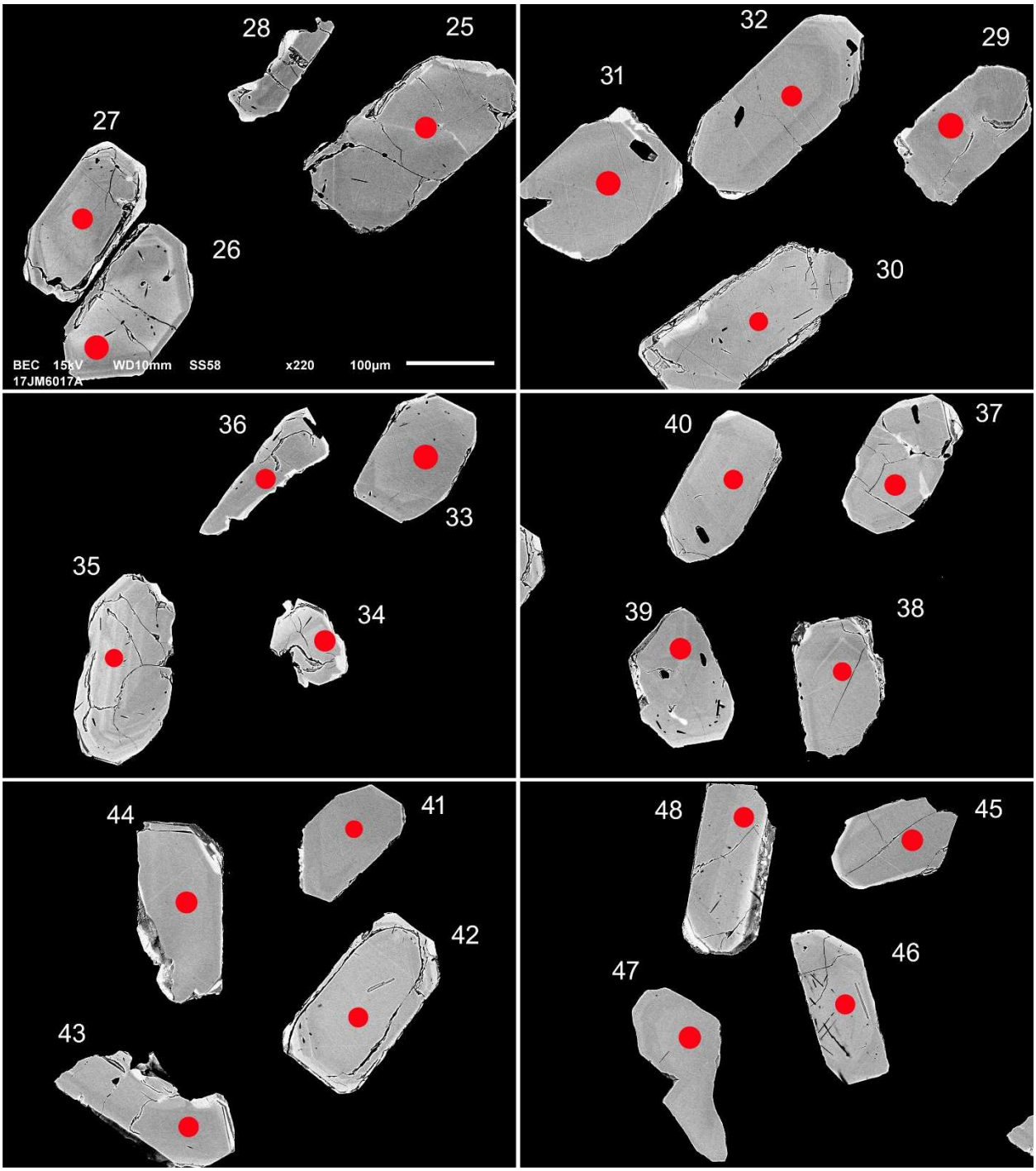


Fig 4-2-2. BSE images of selected grains from tonalite sample 17JM6017A. The red spots represent the approximate locations of laser ablation pits.

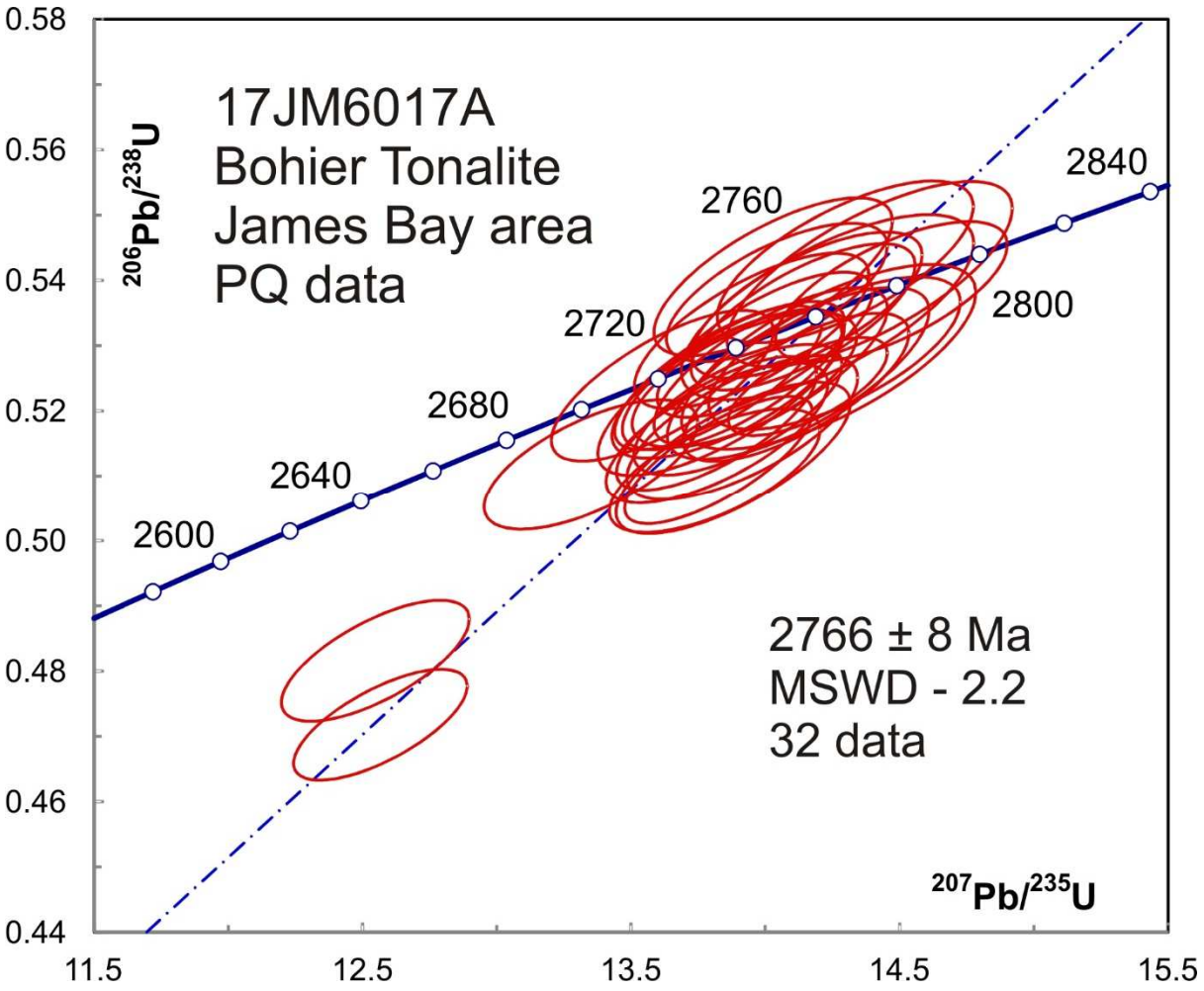


Fig 4-3. Concordia plot showing U-Pb isotopic data on zircon from tonalite sample 17JM6017A obtained on the Plasmaquad LA-ICPMS.

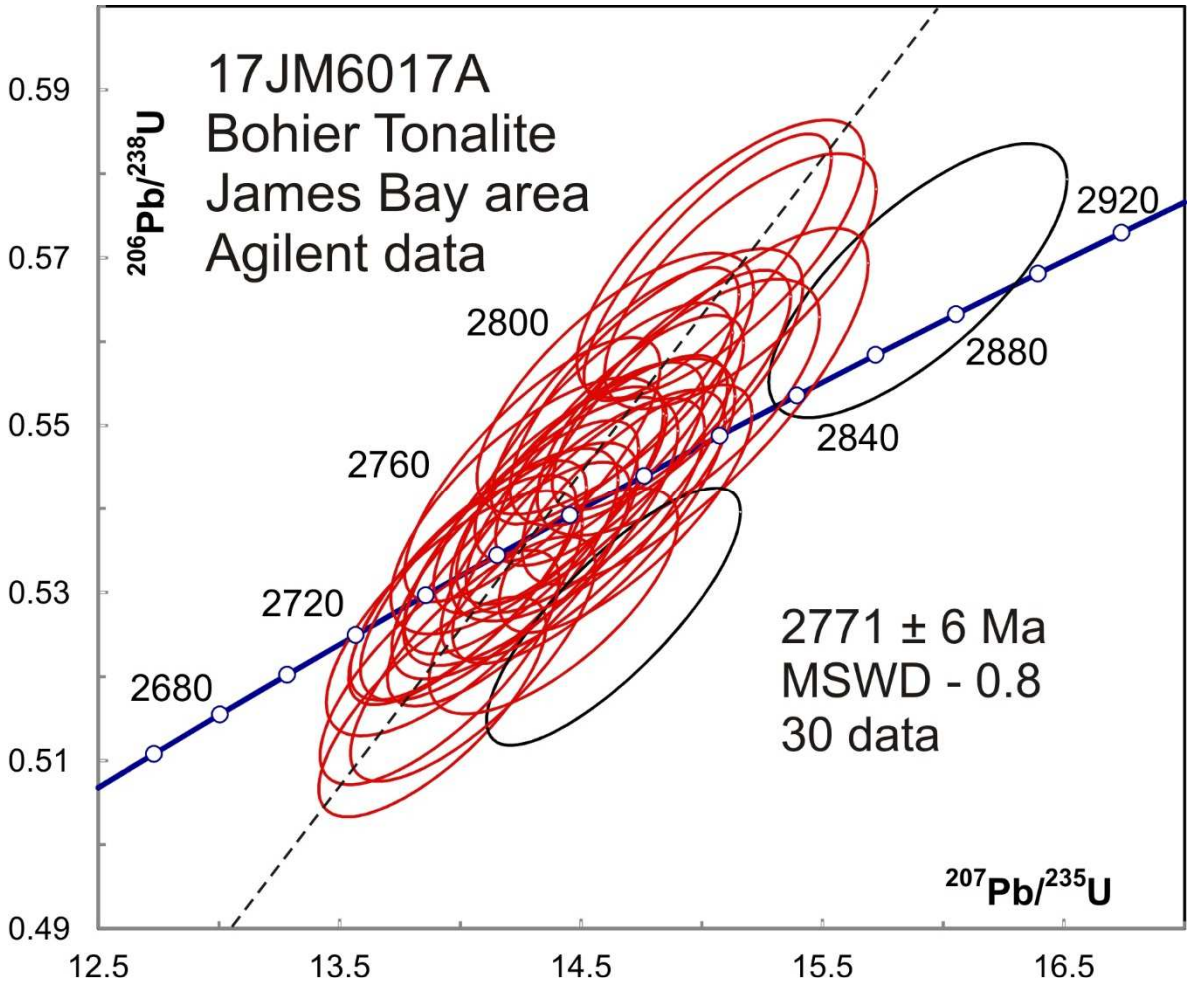


Fig 4-4. Concordia plot showing a second group of U-Pb isotopic data on zircon from tonalite sample 17JM6017A obtained on the Agilent LA-ICPMS.

### *3-5 17JM6027A Clast supported polymict conglomerate, Bohier Group, James Bay area*

This sample yielded generally cracked euhedral to subrounded zircon that varies from brown to colourless (Fig 5-1). BSE images show oscillatory or patchy zoning in many of the grains (Fig 5-2). Despite the diversity of colour, $^{207}Pb/^{206}Pb$ ages on 76 spots scatter only slightly outside of error around an average of 2768 ± 3 Ma (Fig 5-3, MSWD – 2.0). The population age appears to be unimodal (Fig 5-4) suggesting that the sediment was locally sourced from a single short-lived igneous complex.

The best estimate for an older age limit on deposition is the average age of 2768 ± 3 Ma, not the youngest analysis at 2737 ± 16 Ma. Although this would be an older limit if it represented a different source from the main population, and one would take the youngest measured age for an apparently uncorrelated data set, where there is a good chance that all data have the same age, the youngest datum will be biased downward by the statistical distribution. It is therefore better to take the average age of what is considered to be a uniform population.

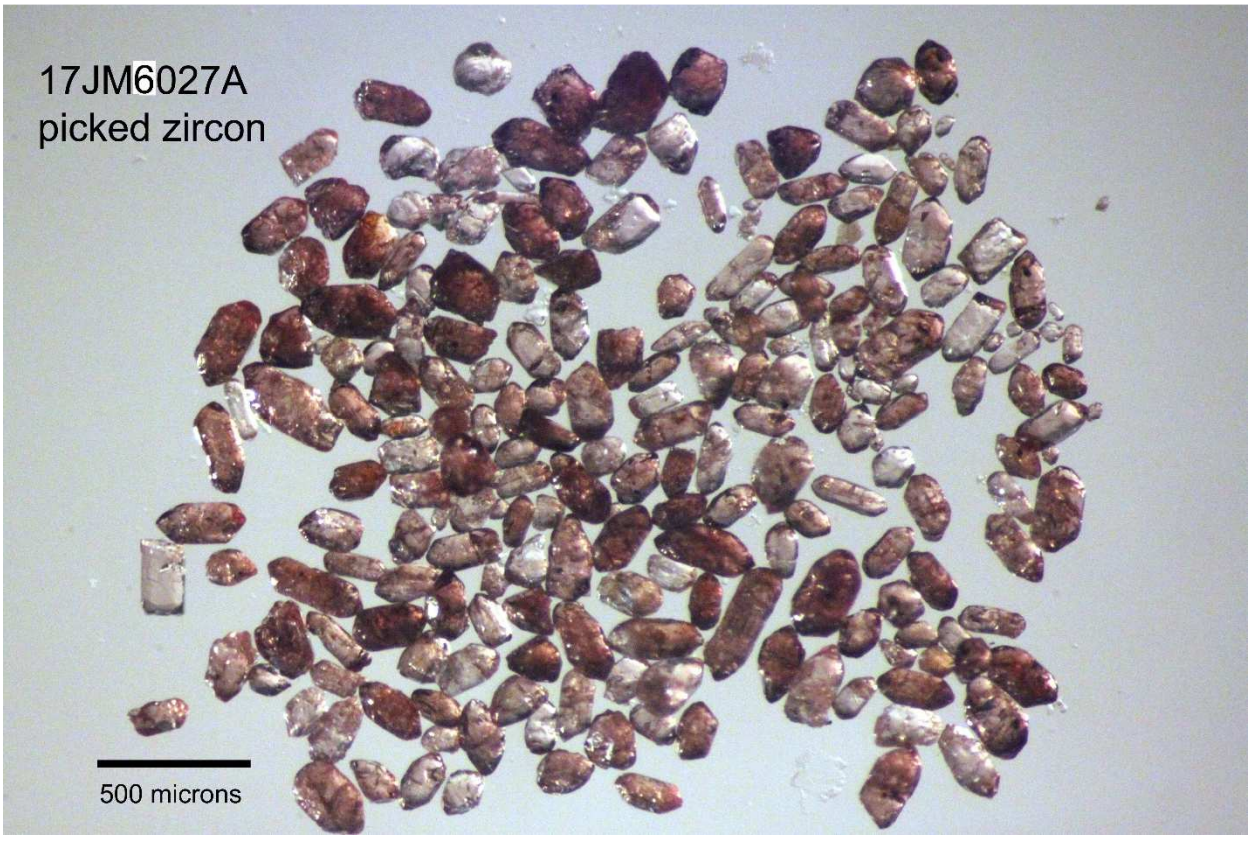


Fig 5-1. Picked zircon from conglomerate sample 17JM6027A.

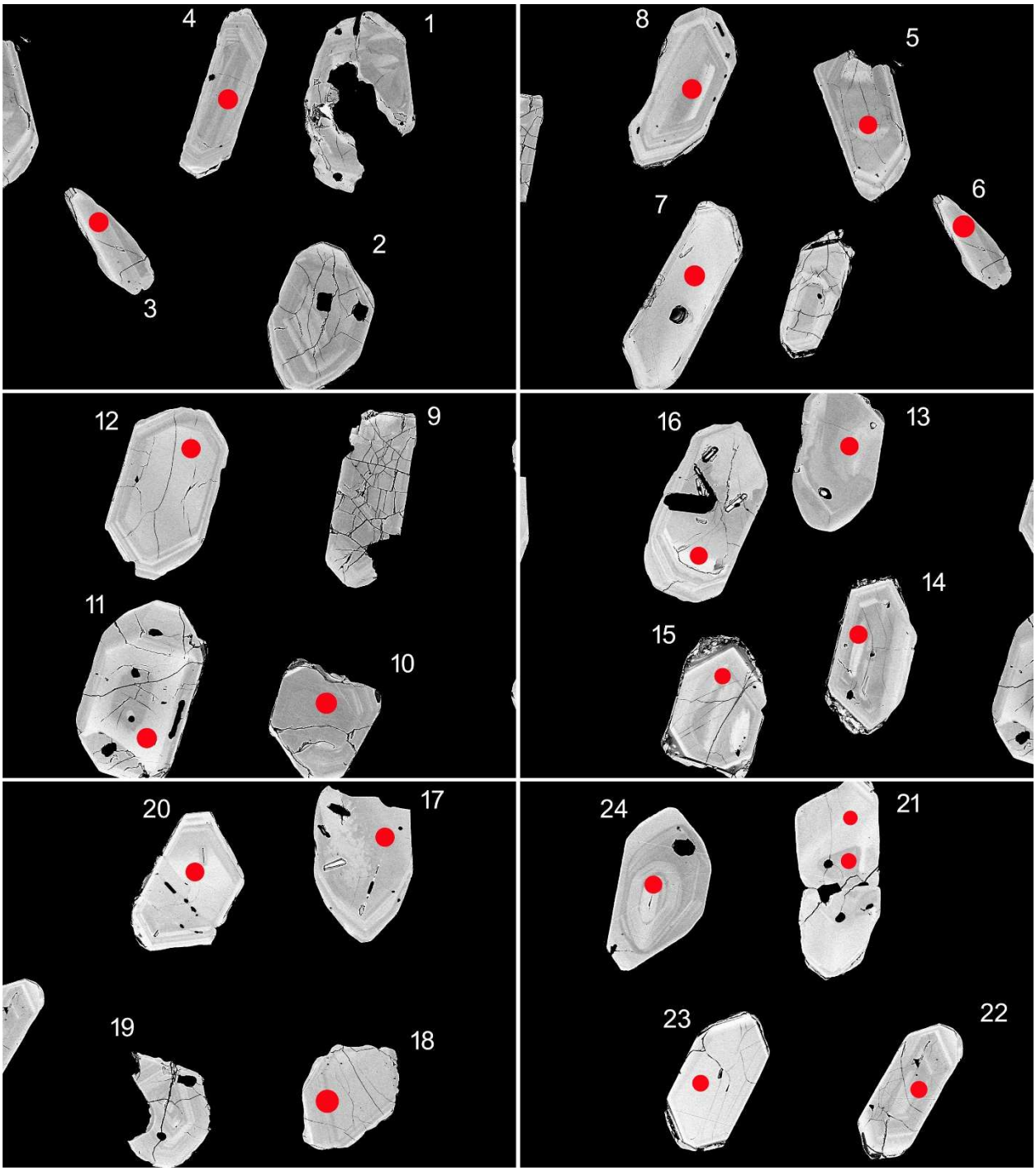


Fig 5-2-1. BSE images of selected grains from conglomerate sample 17JM6017A. The red spots represent the approximate locations of laser ablation pits.

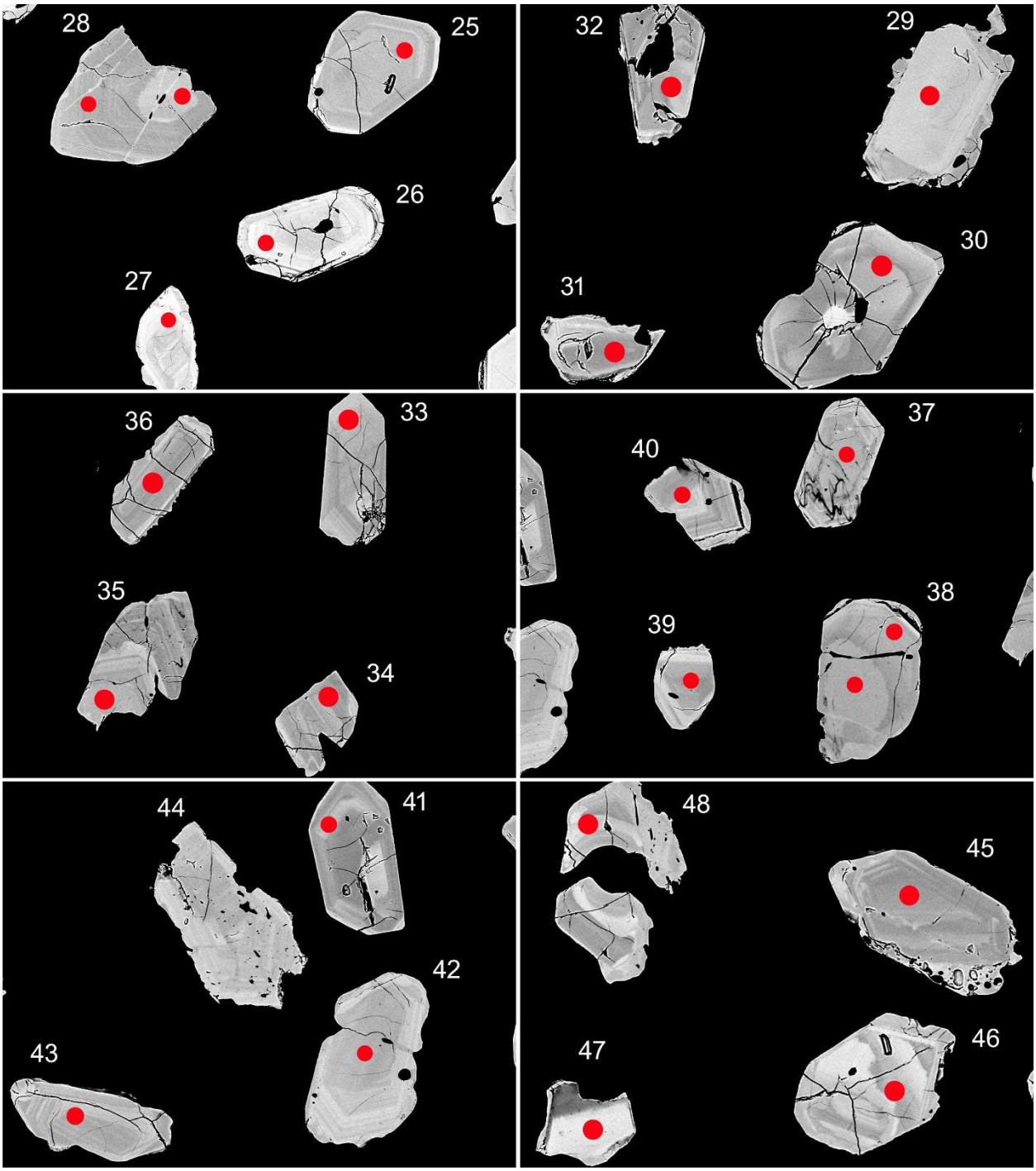


Fig 5-2-2. BSE images of selected grains from conglomerate sample 17JM6017A. The red spots represent the approximate locations of laser ablation pits.

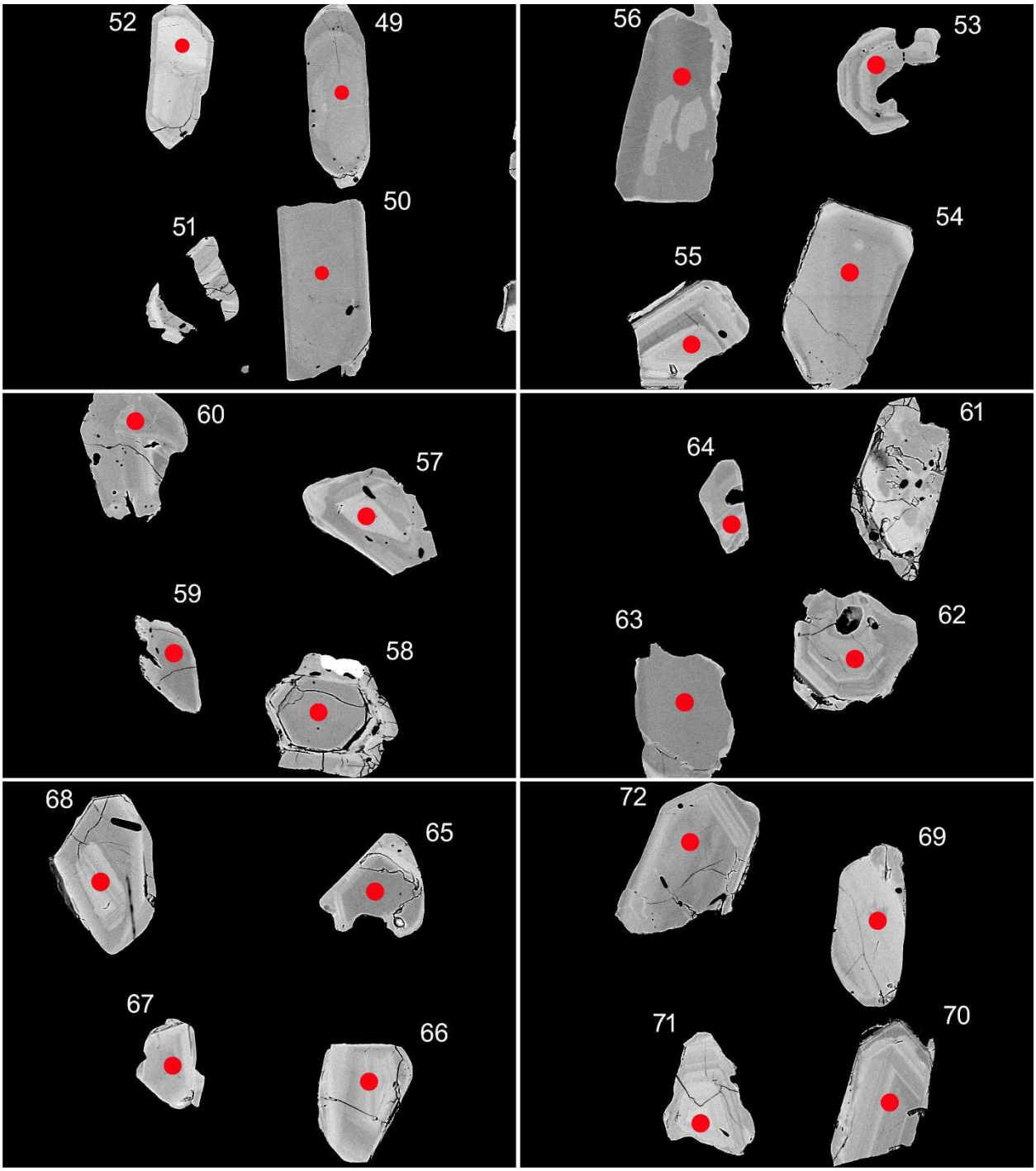


Fig 5-2-3. BSE images of selected grains from conglomerate sample 17JM6017A. The red spots represent the approximate locations of laser ablation pits.

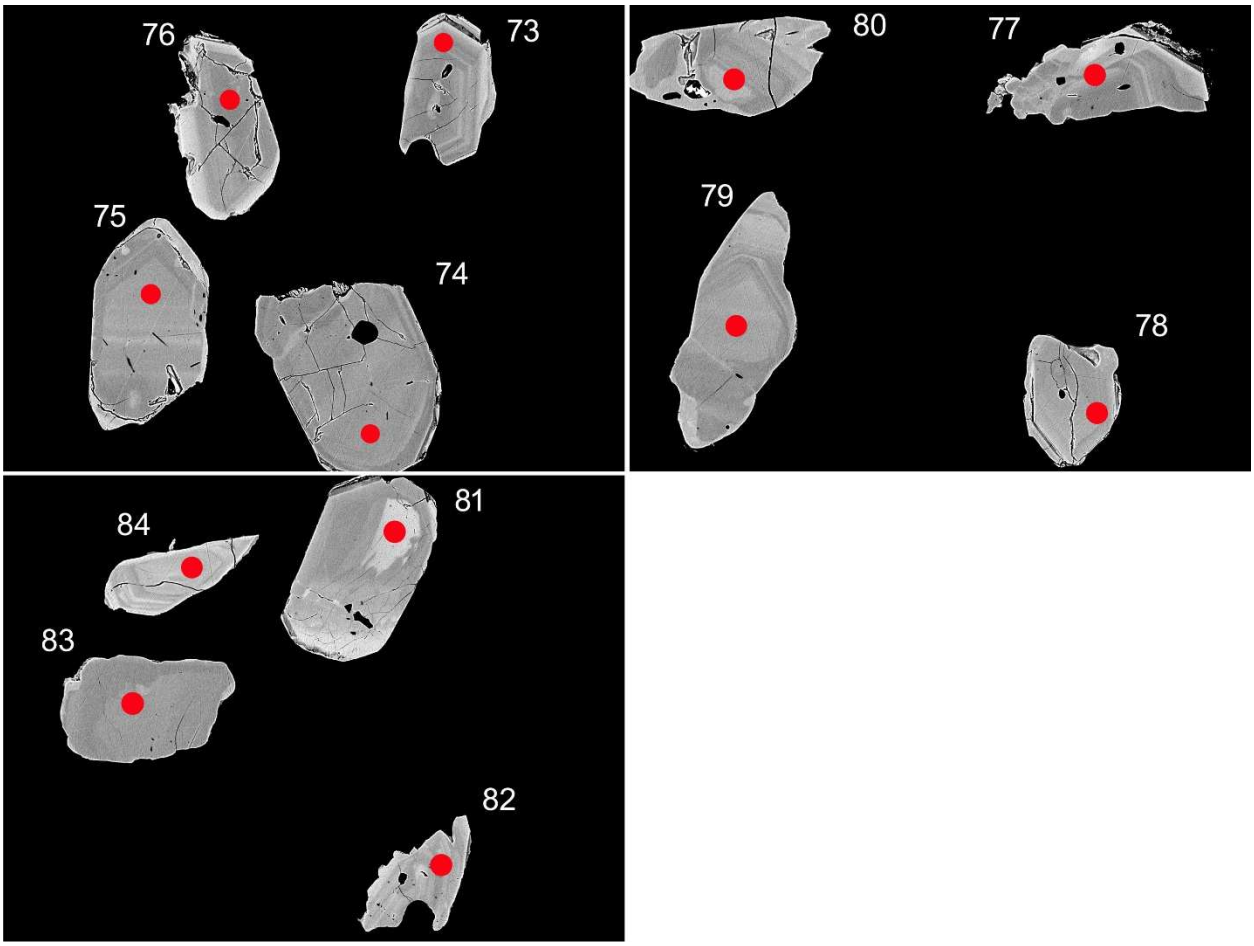


Fig 5-2-4. BSE images of selected grains from conglomerate sample 17JM6017A. The red spots represent the approximate locations of laser ablation pits.

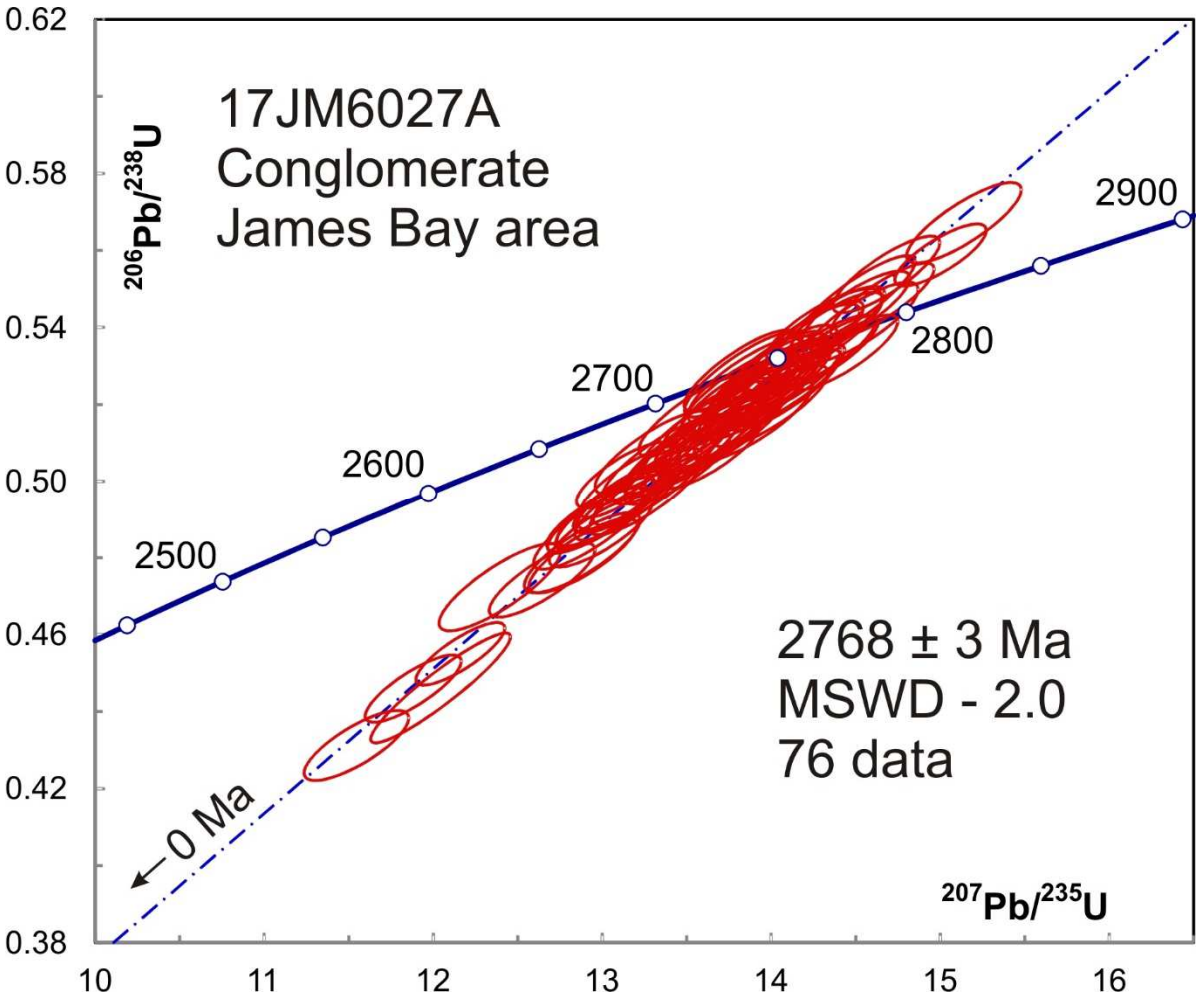


Fig 5-3. Concordia plot showing U-Pb isotopic data on zircon from conglomerate sample 17JM6027A.

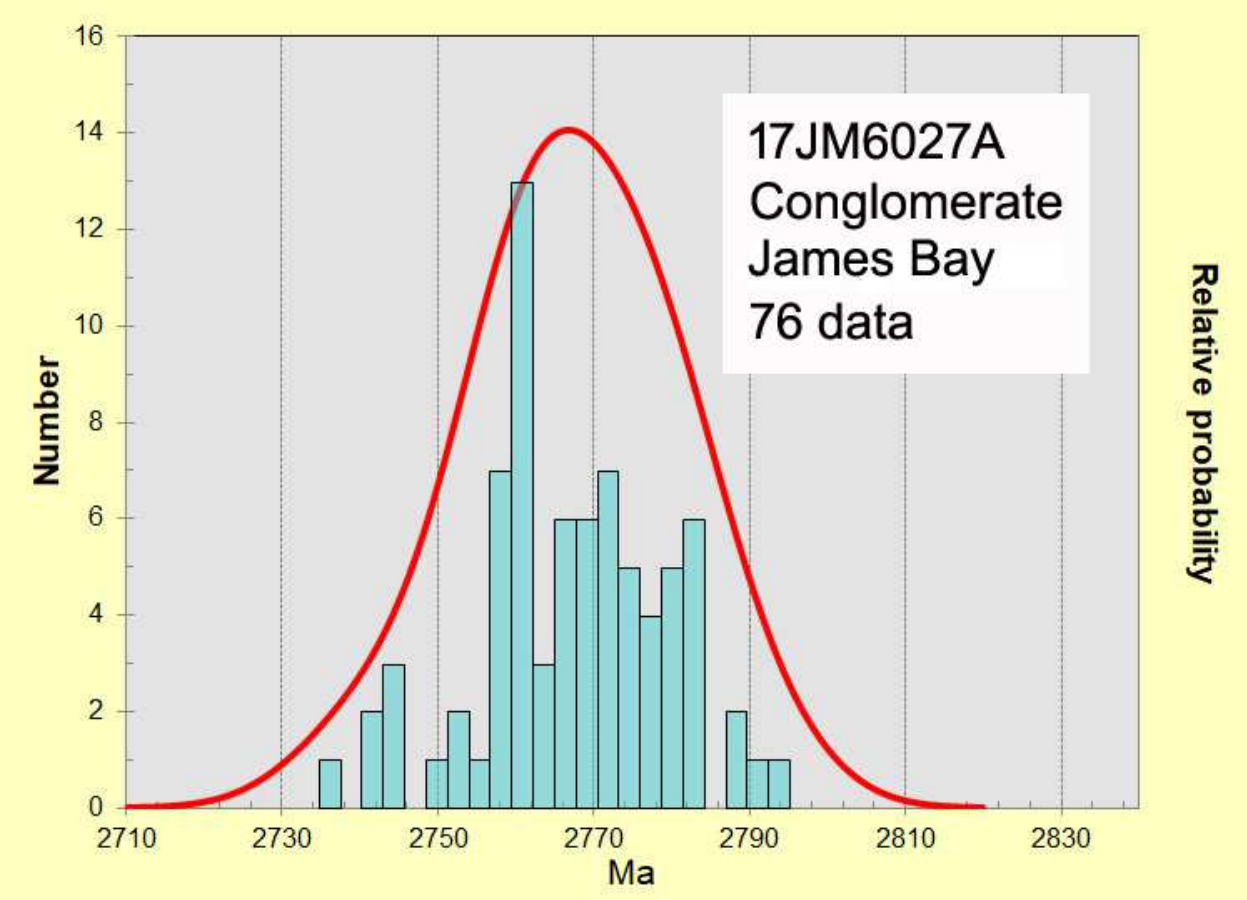


Fig 5-4. Relative probability density distribution and histogram showing U-Pb isotopic data on polished zircon from conglomerate sample 17JM6027A.

### *3-6 17JM6059A Granodiorite, Lac Cadieux Suite, James Bay area*

The zircon recovered from this sample is mostly highly damaged and altered (Fig 6-1). Larger grains were polished and imaged by BSE but alteration is pervasive (Fig 6-2). Penetration of dark alteration along high-U micron-sized zones can be seen near the margins of grains where the polishing plane intersects the zoning planes at a steep angle (e.g. grain 4, Fig 6-2). Gray to bright patchy areas in the central region of grains probably represent differential exposure of thin altered zones, where the plane of polishing intersects the zoning at a shallow angle. It is probably not possible to ablate for U-Pb dating without intersecting altered zones. Some of the smaller zircon grains appear to be less damaged so these were mounted unpolished for analysis (Fig 6-3). Grains were photographed under a black background and areas showing no evidence of turbidity were ablated.

U-Pb data show a complex pattern of inheritance, which is not unusual for chemically evolved felsic rocks, which probably formed from crustal melting. Many of the analyses had to be rejected because of high Sr signals and irregular profiles, which may indicate alteration (Table 1). Alteration not only leads to discordance, which may give too young an age, but can also be associated with high levels of common Pb, which biases the analysis toward too old an age. This is most likely the case with the six oldest analyses, which were rejected (Table 1). The accepted analyses spread between $^{207}Pb/^{206}Pb$ ages of 2654 Ma to 2776 Ma (Fig 6-4). The youngest overlapping group consists of only two near-concordant data with an average age of 2658 ± 10 Ma. An older group of 12 data overlap with an age of 2699 ± 5 Ma. A further complication is that some grains show a short profile at the beginning of the analysis with low Th/U and high U (see raw data profiles in data repository). This probably represents a metamorphic zircon overgrowth but it could be a magmatic overgrowth if the Th/U ratio of the magma were low. The age of the overgrowth is difficult to determine. Efforts to average over short windows where Sr and Th/U are low gave $^{207}Pb/^{206}Pb$ ages that scatter over 100 Ma. The best analysis, from grain 25, gives an age of 2591 ± 18 Ma. The best available estimate for emplacement of the pluton is 2658 ± 10 Ma.


Fig 6-1. Picked zircon from granodiorite sample 17JM6059A.

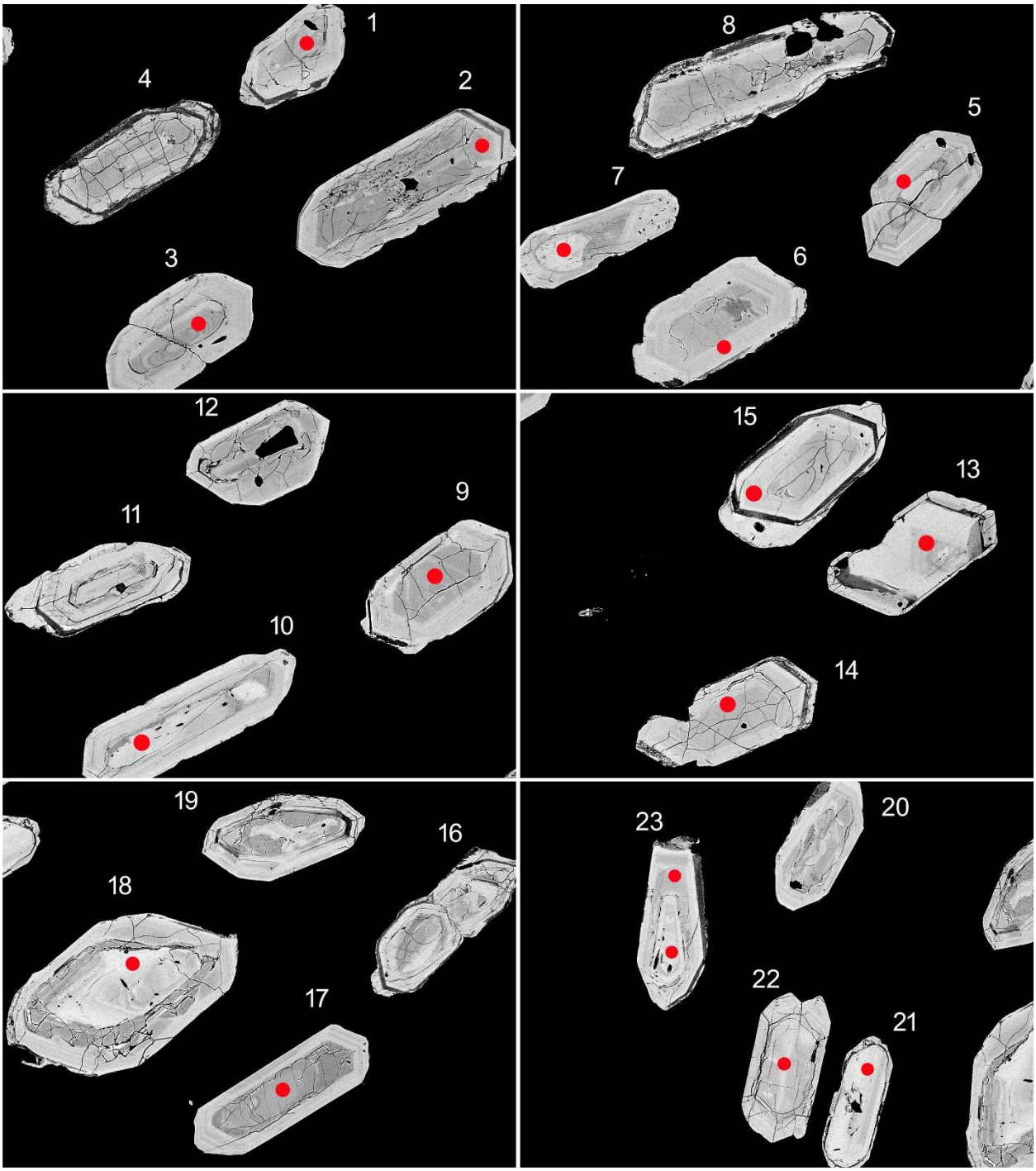


Fig 6-2 BSE images of selected grains from granodiorite sample 17JM6059A. Dark grey areas show alteration, which tends to penetrate along high-U zones. Greyish patchy areas around the center of grains probably represent differential exposure of thin altered zones, which cannot be avoided during ablation below surface. Hence there grains were not analyzed.

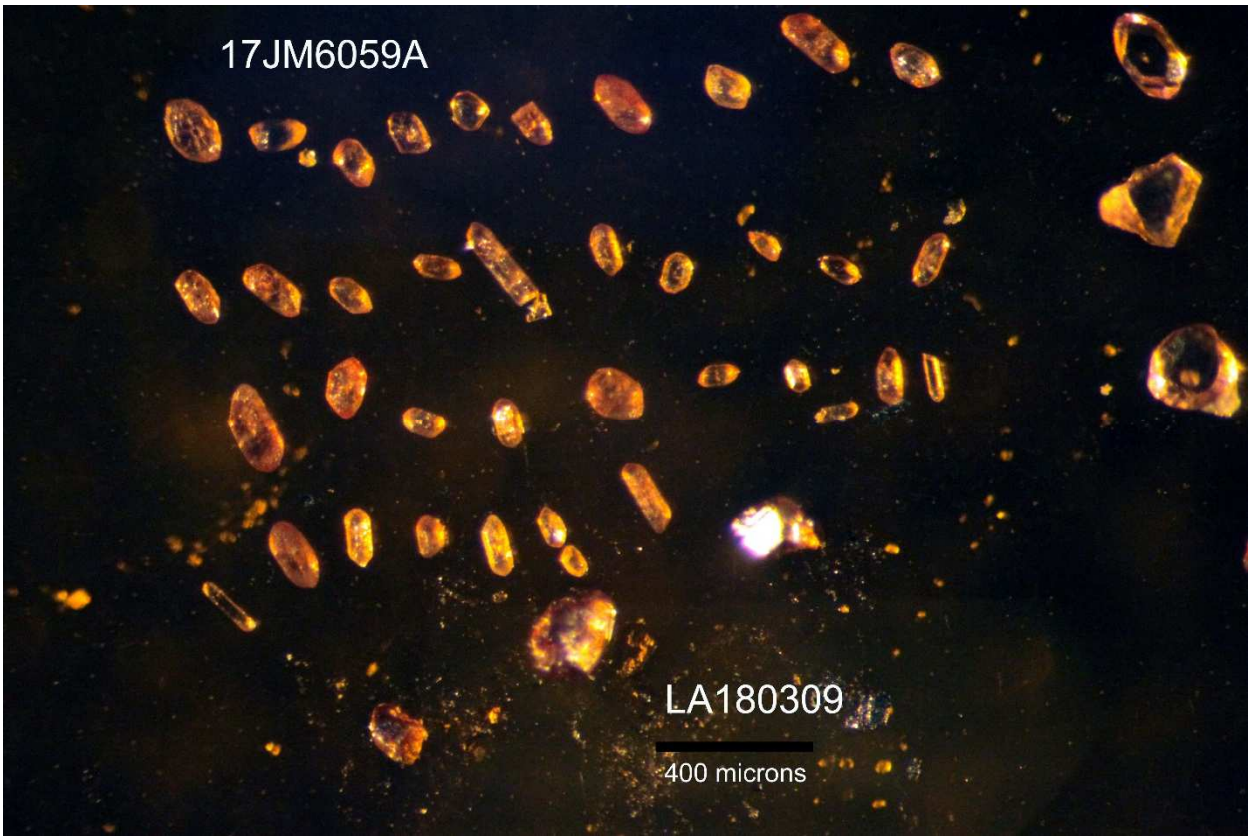


Fig 6-3. Mounted zircon from granodiorite sample 17JM6059A.

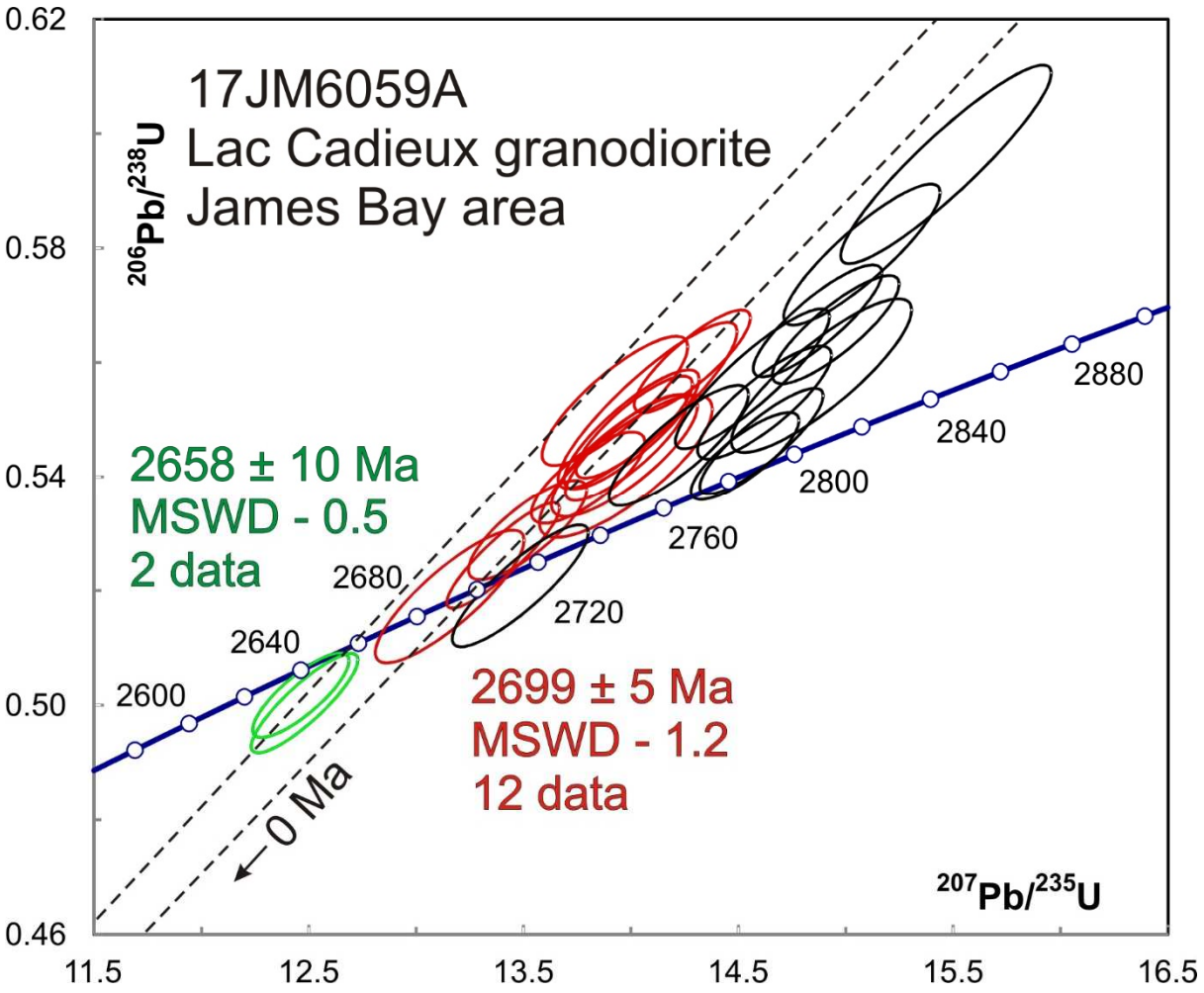


Fig 6-4. Concordia plot showing a U-Pb isotopic data on unpolished zircon from granodiorite sample 17JM6059A. Ellipses in black were not included in the averages.

### *3-7 17CB1073B Pegmatitic granite, Aveneau Suite, Labrador Trough*

This sample yielded a small amount of generally damaged zircon grains, many of which have visible cores (Fig 7-1). This is typical of S-type magmas, which are thought to be produced from partial melting of sedimentary rocks containing detrital zircon, which forms refractory cores inside the high-U magmatic zircon phase. The magmatic zircon can be difficult to date because of alteration that affects damaged domains but such rocks also typically contain magmatic monazite, which is more resistant to alteration and Pb loss.

BSE images of zircon (Fig 7-2) show altered (dark) domains localized within high-U (bright) overgrowths around unaltered cores. Analyses of overgrowths showed variable Sr contents but low-Sr (unaltered) sections of time-resolved profiles gave clustered data that average to a $^{207}Pb/^{206}Pb$ age of 1782 ± 8 Ma (Fig 7-3). Th/U ratios of this zircon phase are low (<0.1), which can be an indication of metamorphic zircon but is also characteristic of zircon that crystallized from partial melts of sedimentary rocks. Analyses of cores give ages that range from about 2750 Ma to 2920 Ma (Fig 7-4) but the majority cluster only slightly outside of error around an age of 2834 ± 5 Ma, which is likely the main age of provenance if there is a sedimentary protolith.

S-type magmas typically crystallize monazite, which is present in the magnetic mineral fractions. It occurs as variably altered fragments that are not immediately recognizable because of the absence of whole crystals (Fig 7-5) These were mounted and polished along with a group of darker, less translucent grains (last four grains in Fig 7-6). BSE images show only rare zoning (e.g. grain 11, Fig 7-7). There is no obvious difference in the images of the darker grains (17-20, Fig 7-7) but these proved to be older than the others (Table 1, Fig 7-8). The clearer monazite grains give overlapping ages with an average of 1785 ± 7 Ma, while the four darker ones appear to lie on a mixing line with an upper intercept age of 2548 ± 60 Ma, when anchored at the age of the younger monazite. Since this is significantly younger than the age of the zircon cores, it suggests that the protolith may have grown metamorphic monazite around this time.


Fig 7-1. Picked zircon from pegmatite sample 17CB1073B.

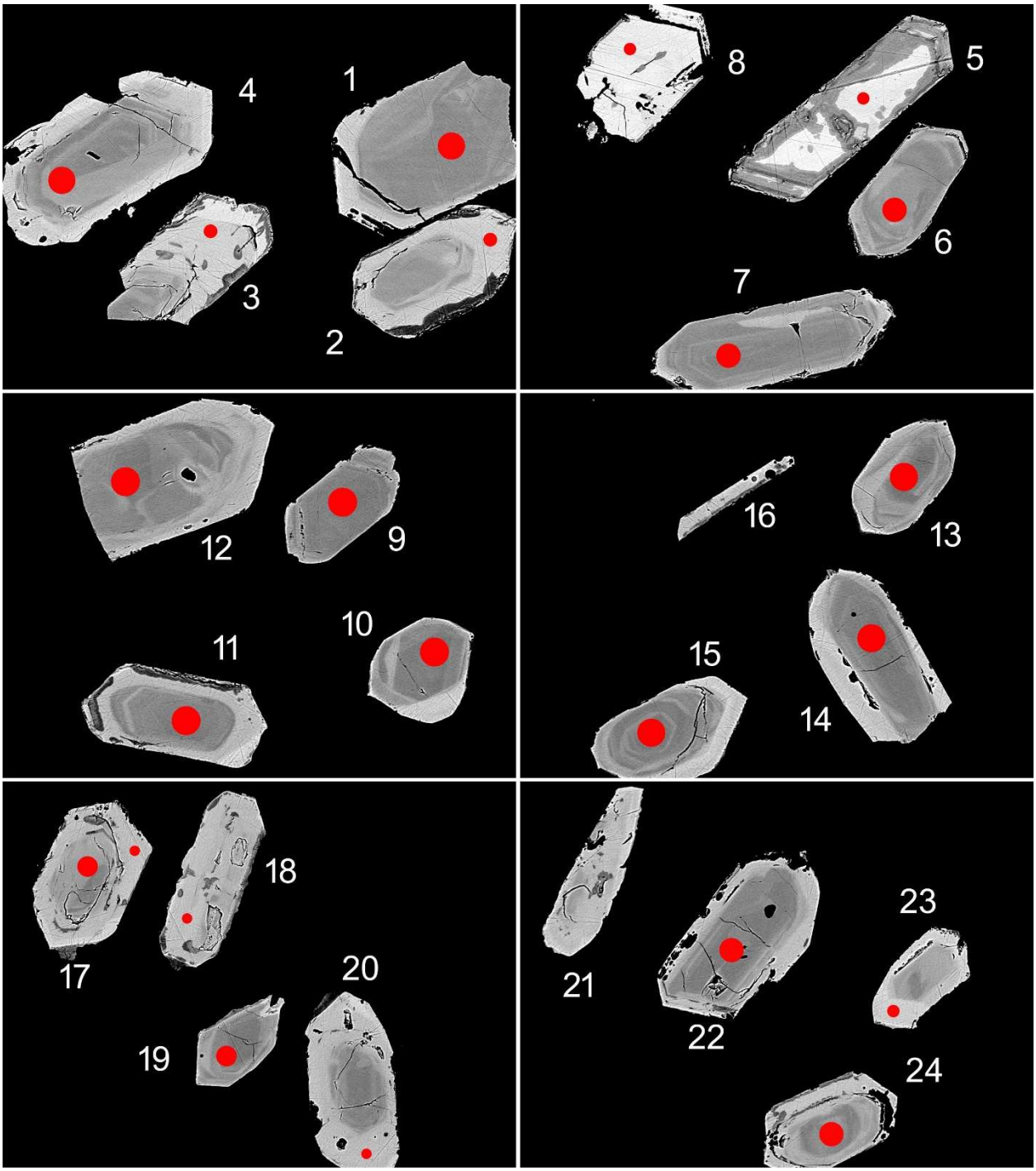


Fig 7-2-1 BSE images of selected grains from pegmatite sample 17CB1073B. Dark grey areas show alteration, which tends to penetrate along high-U zones. The red spots represent the approximate locations of laser ablation pits.

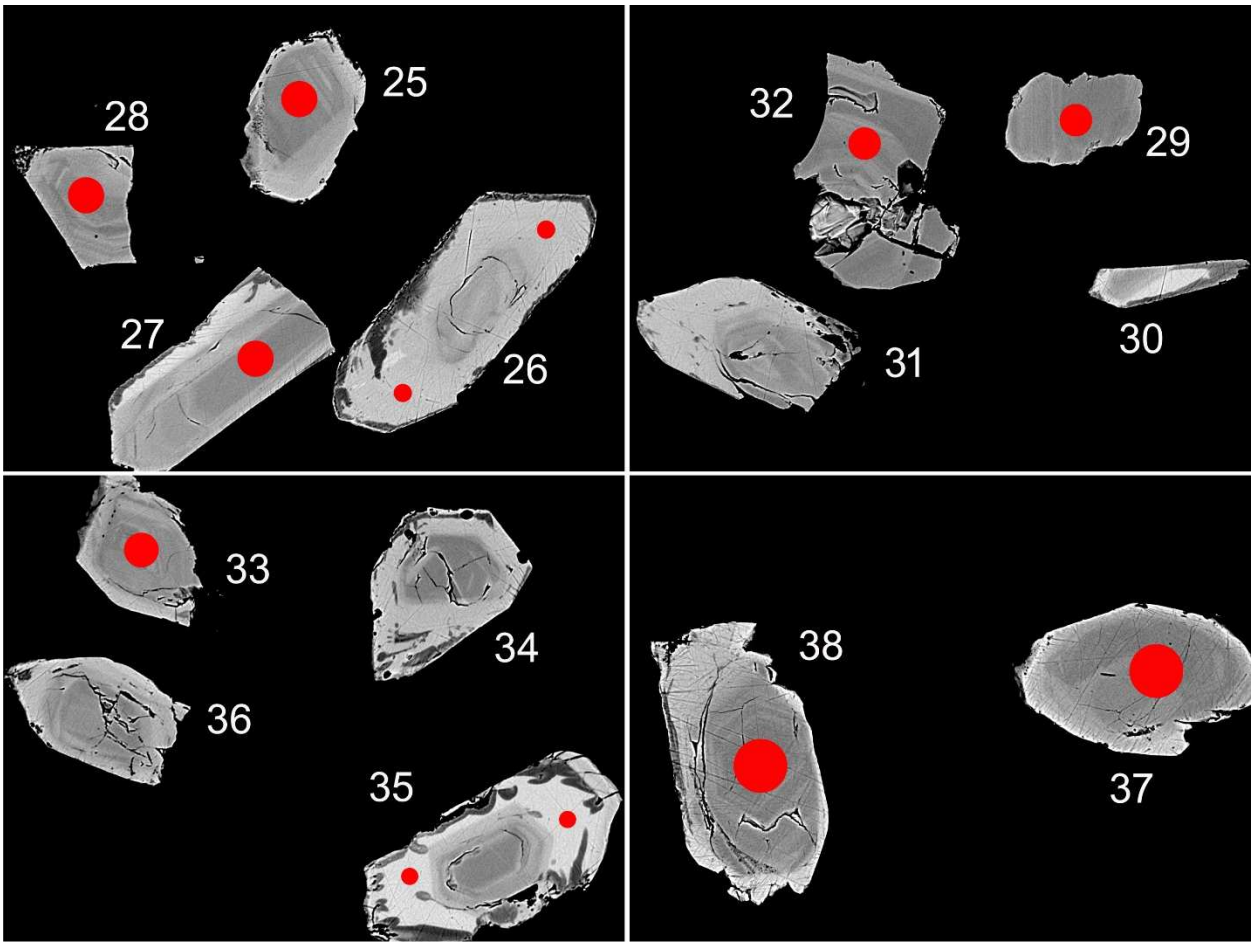


Fig 7-2-2 BSE images of selected grains from pegmatite sample 17CB1073B. Dark grey areas show alteration, which tends to penetrate along high-U zones. The red spots represent the approximate locations of laser ablation pits.

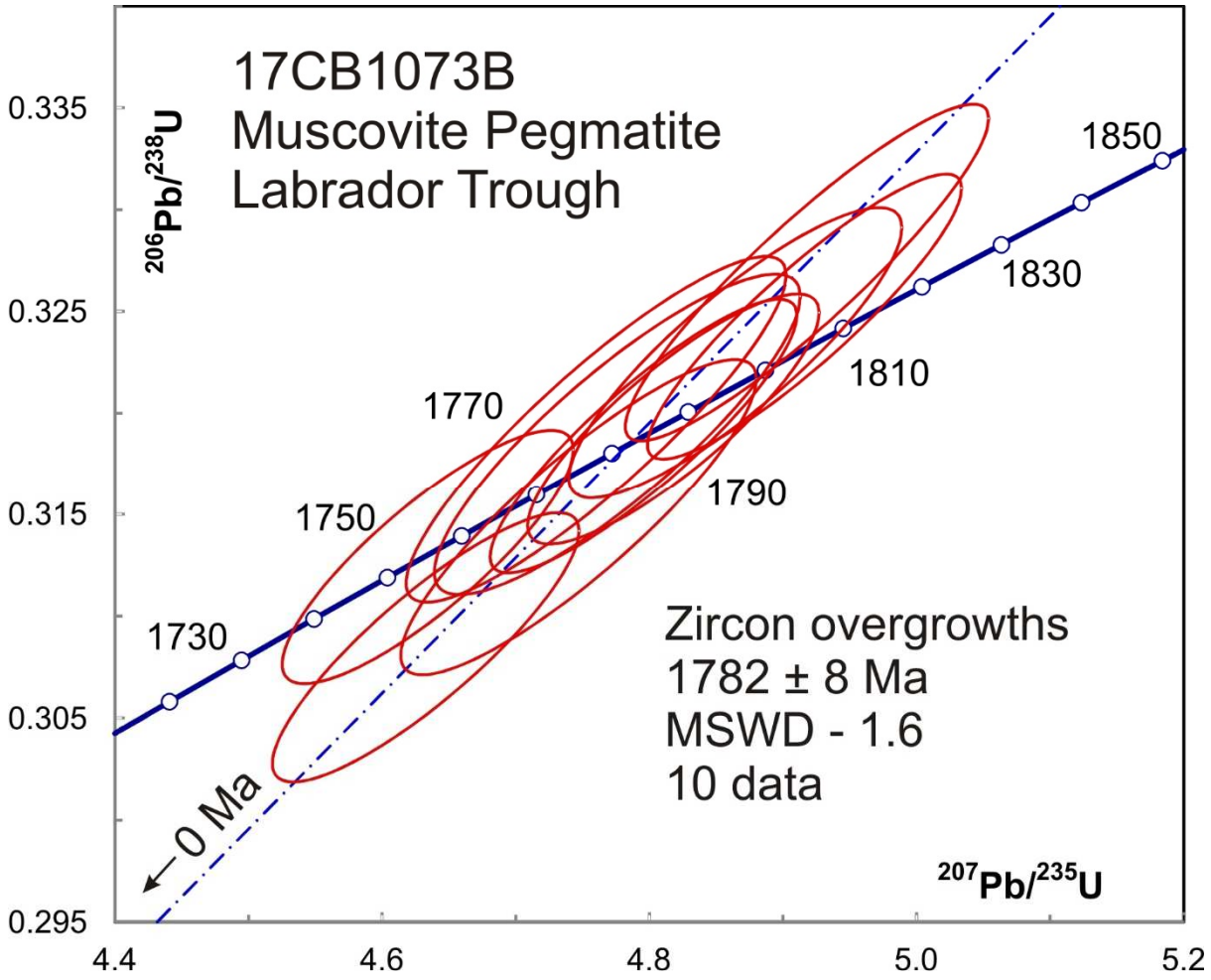


Fig 7-3. Concordia plot showing U-Pb isotopic data on zircon overgrowths from pegmatite sample 17CB1073B.

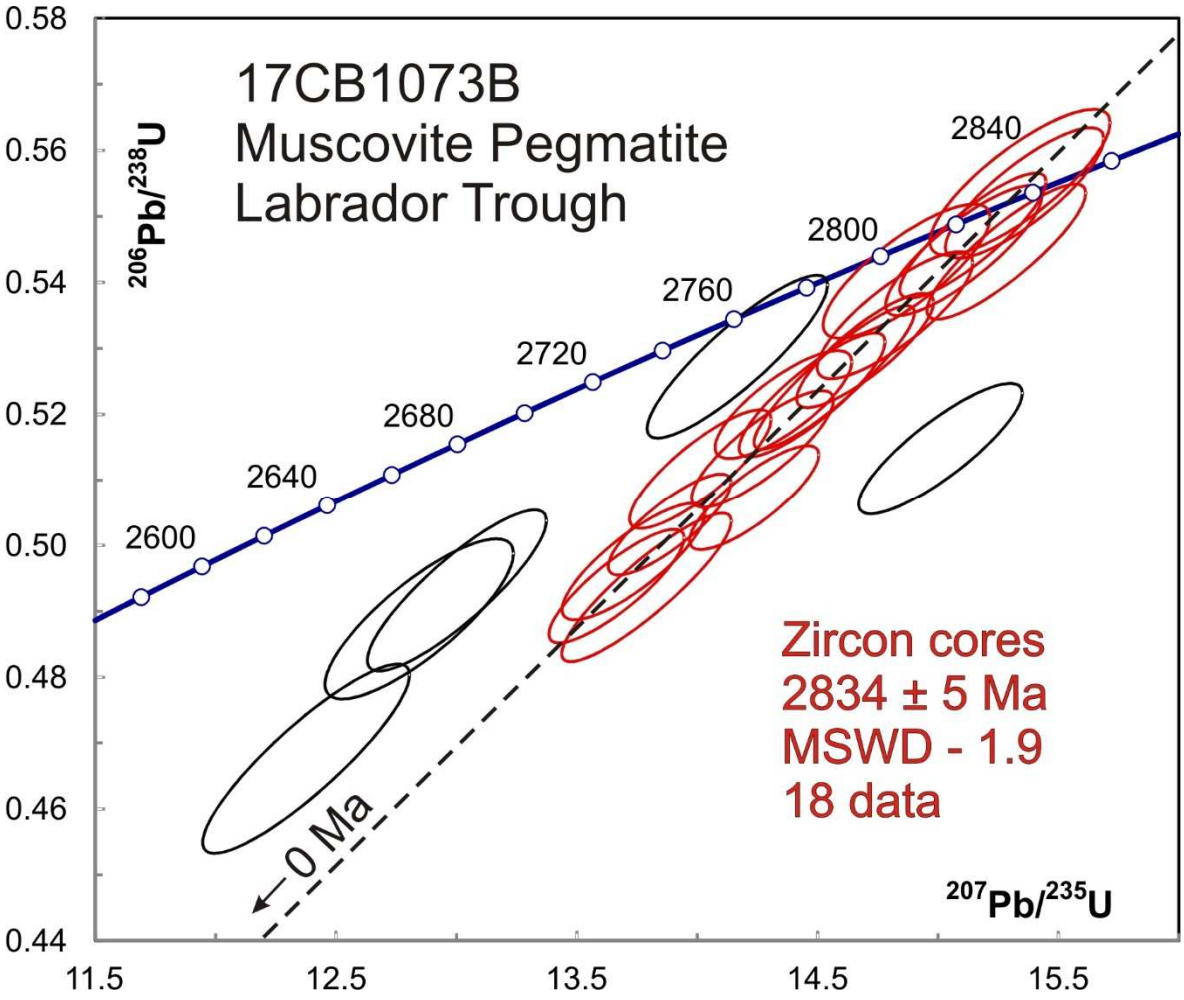


Fig 7-4. Concordia plot showing U-Pb isotopic data on zircon cores from pegmatite sample 17CB1073B. Black ellipses are not included in the average age.


Fig 7-5. Picked monazite from pegmatite sample 17CB1073B.


Fig 7-6. Polished monazite from pegmatite sample 17CB1073B.

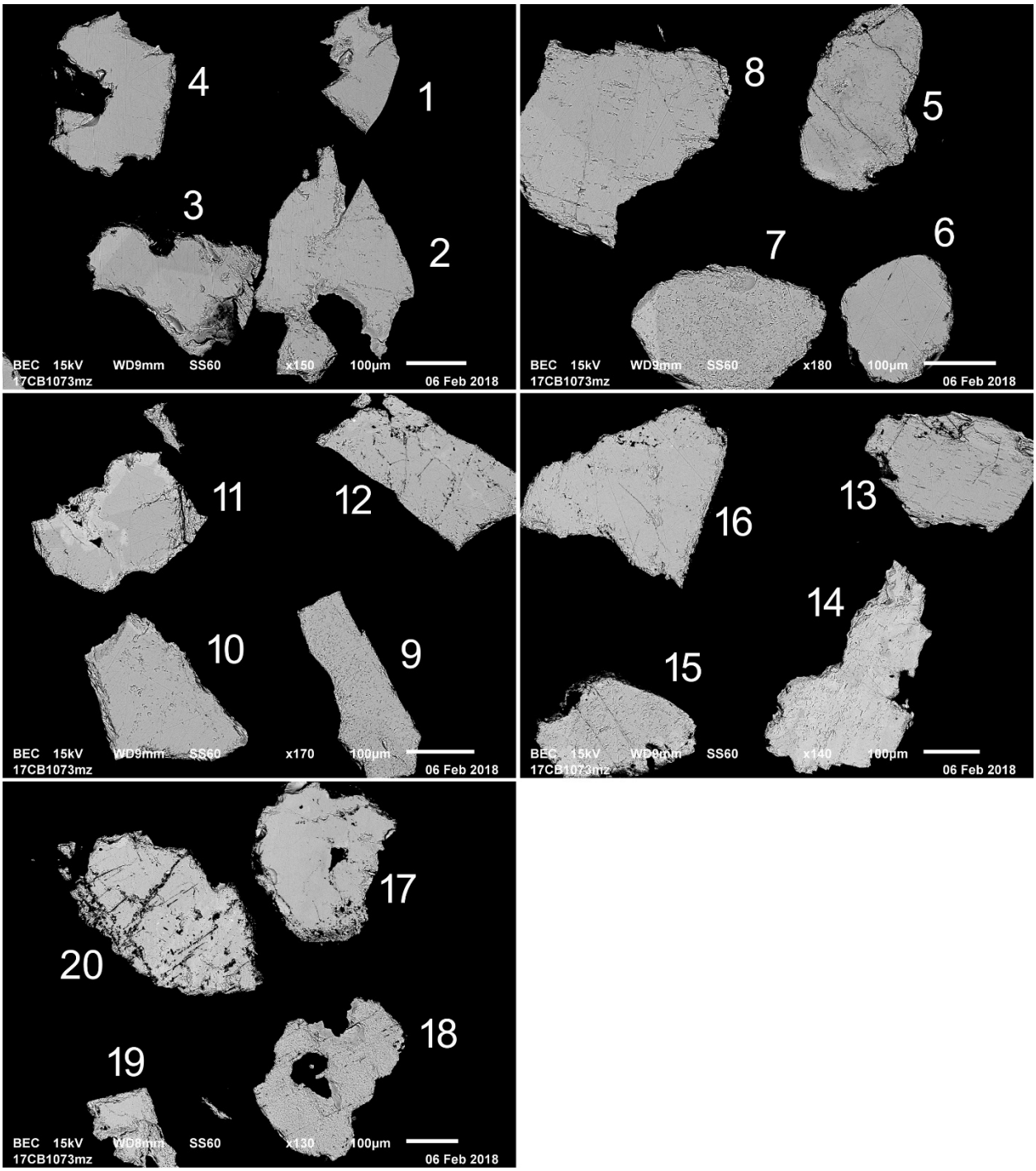


Fig 7-7 BSE images of polished monazite grains from pegmatite sample 17CB1073B.

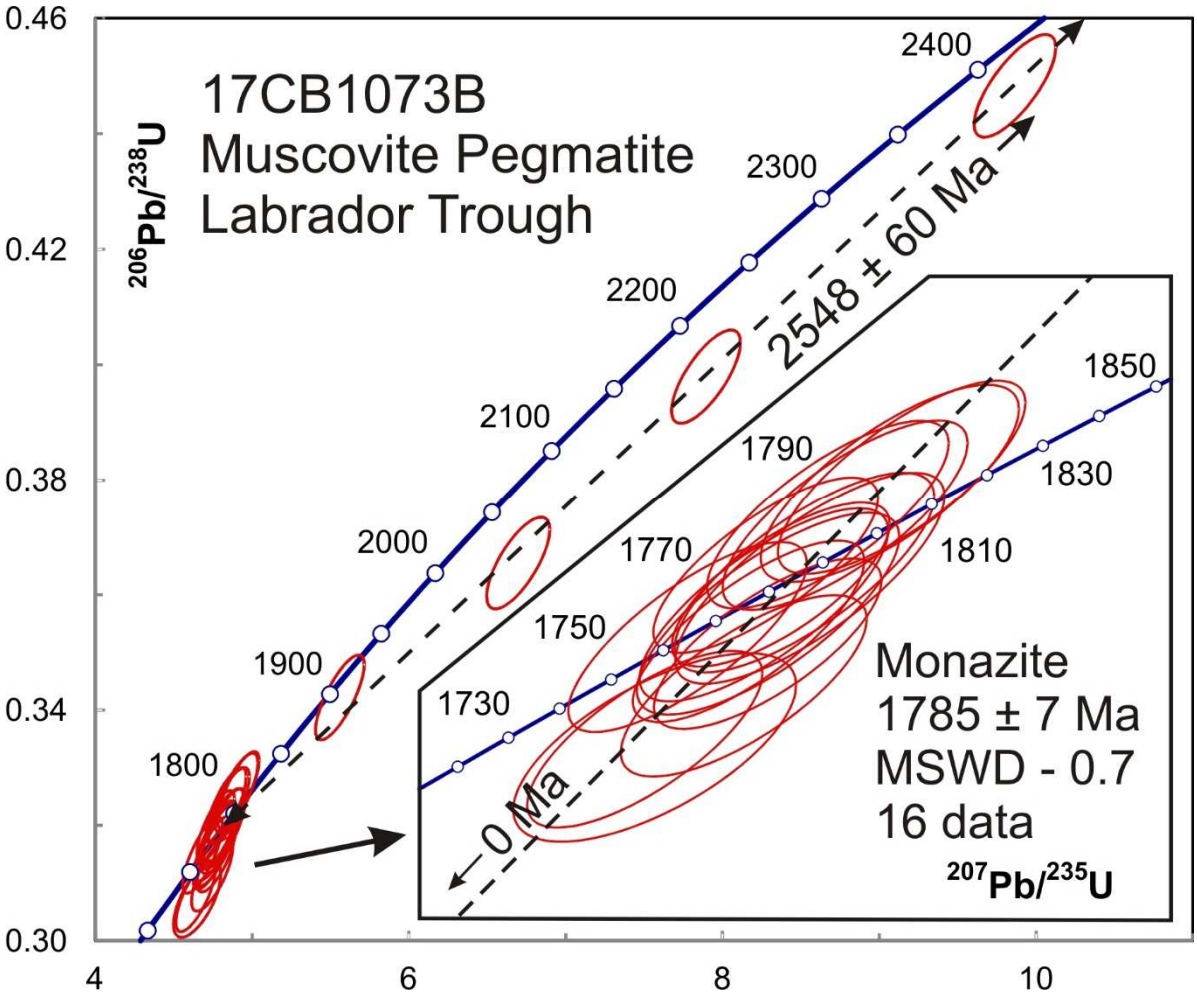


Fig 7-8. Concordia plot showing U-Pb isotopic data on monazite from pegmatite sample 17CB1073B.

### *3-8 17CB1099B Quartzite, Arnaud Complex, Labrador Trough*

This sample yielded generally rounded, brown to colourless, variably cracked zircon (Fig 8-1). BSE images show a variety of textures (Fig 8-2), including one monazite crystal (grain 60). Some analyses from high U phases had to be rejected because the signal overloaded the detector. The successful analyses produced Archean $^{207}Pb/^{206}Pb$ ages that scatter over the range 2748-2998 Ma (Fig 8-3). A relative probability density plot shows a number of peaks (Fig 8-4). The predominant cluster defines an age of 2882 ± 6 Ma (28 spots, MSWD – 1.5), based on the largest group of data that scatter within error.

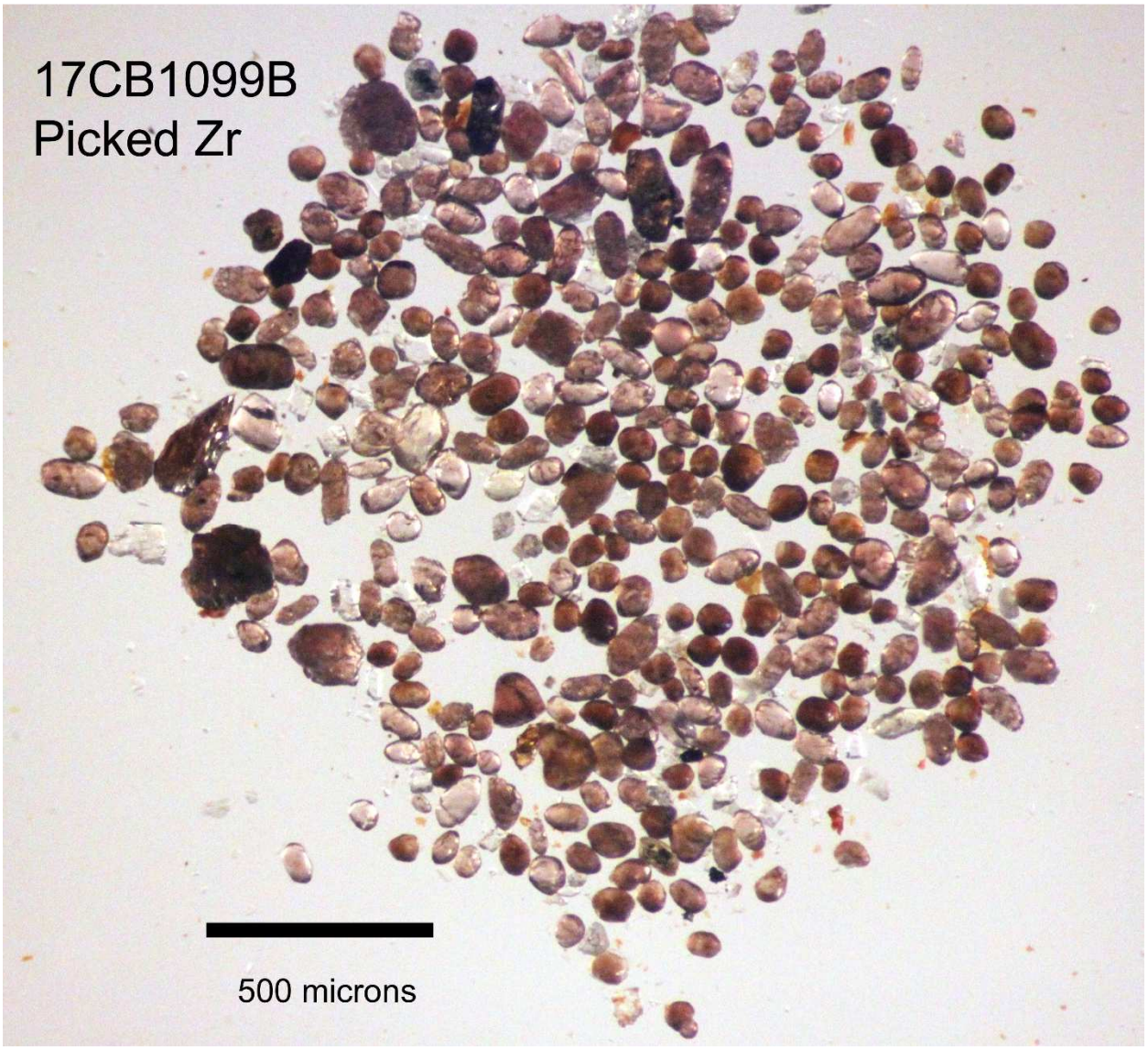


Fig 8-1. Picked zircon from quartzite sample 17CB1099B.

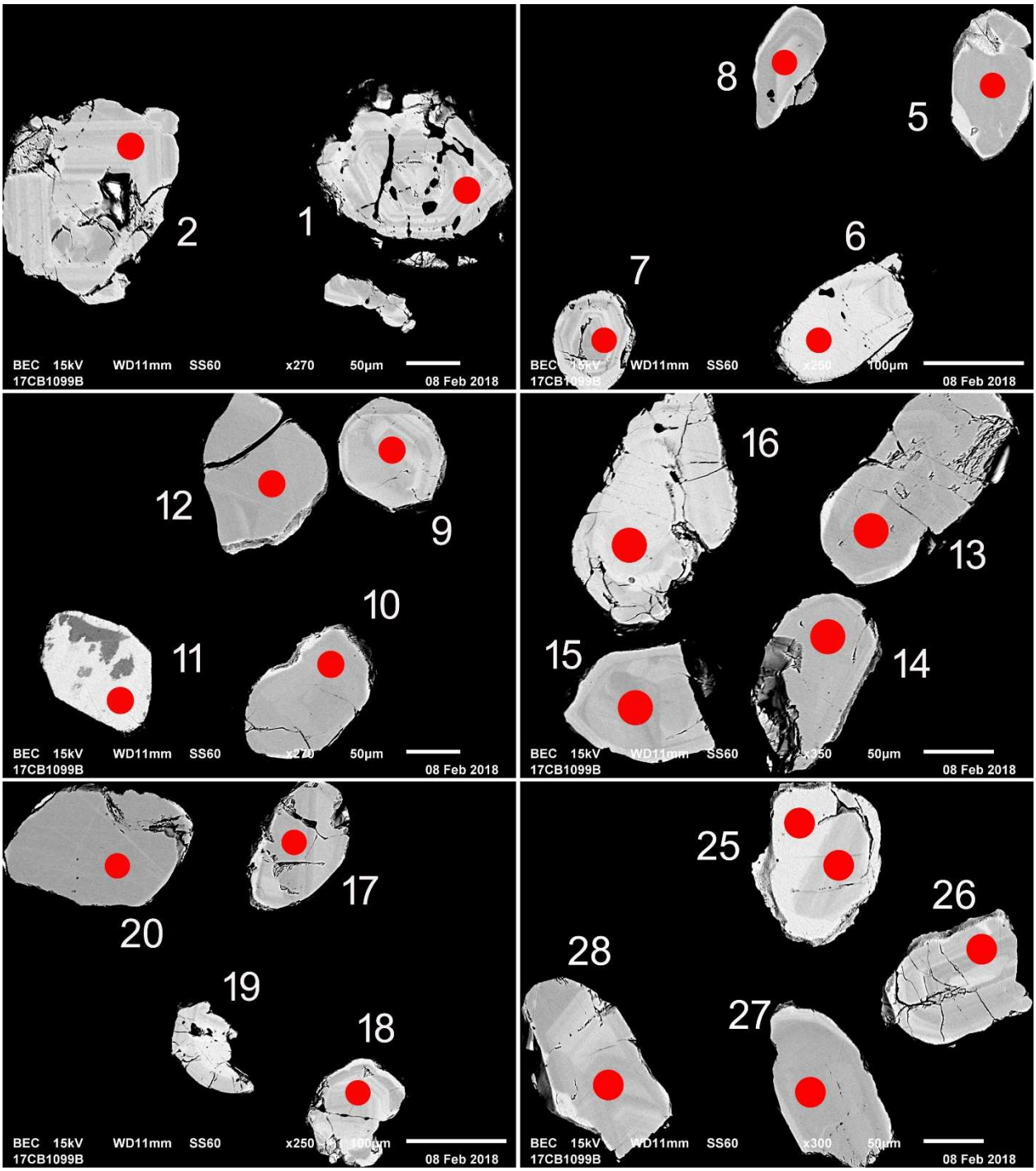


Fig 8-2-1 BSE images of selected grains from quartzite sample 17CB1099B. The red spots represent the approximate locations of laser ablation pits.

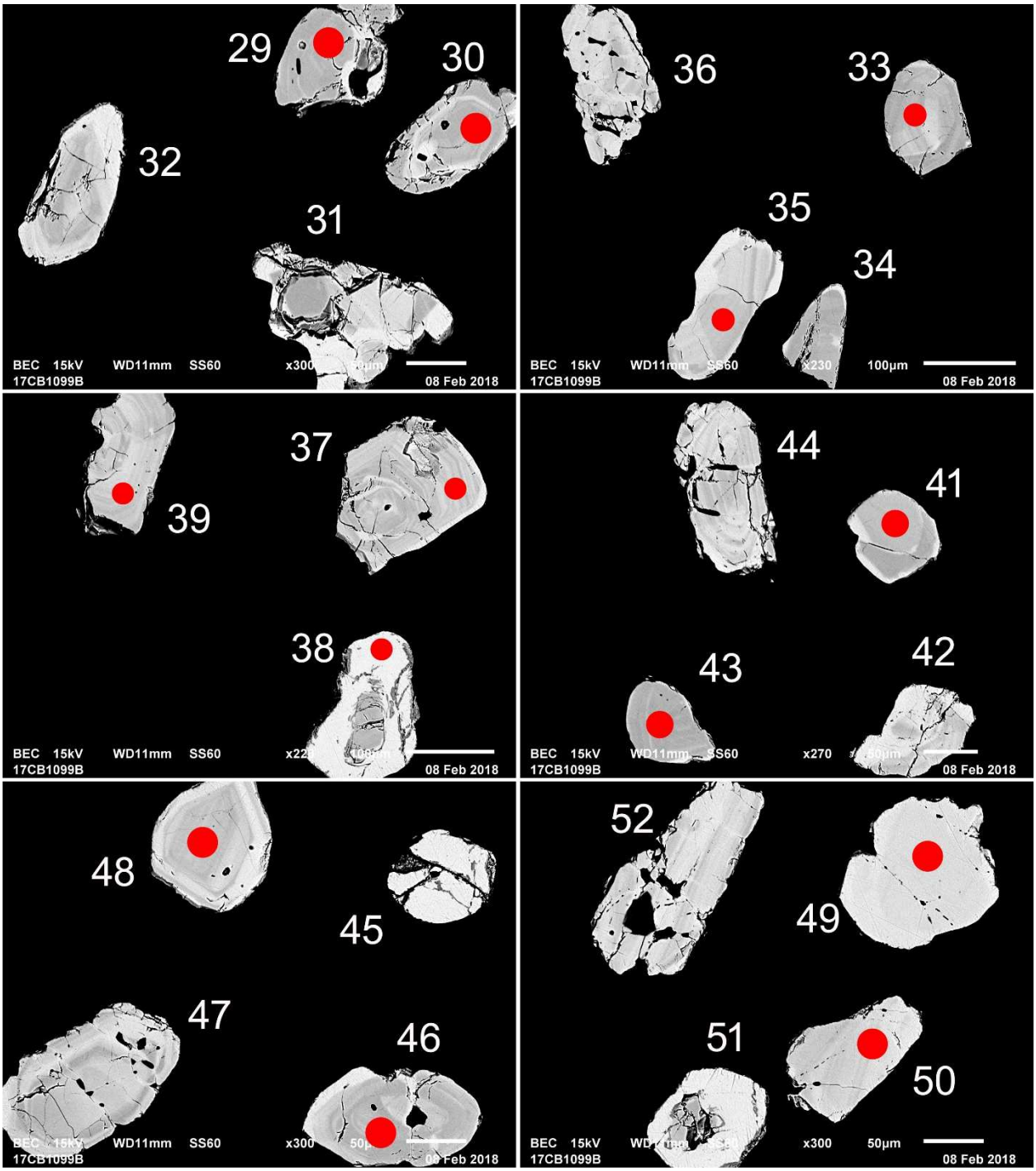


Fig 8-2-2 BSE images of selected grains from quartzite sample 17CB1099B. The red spots represent the approximate locations of laser ablation pits.

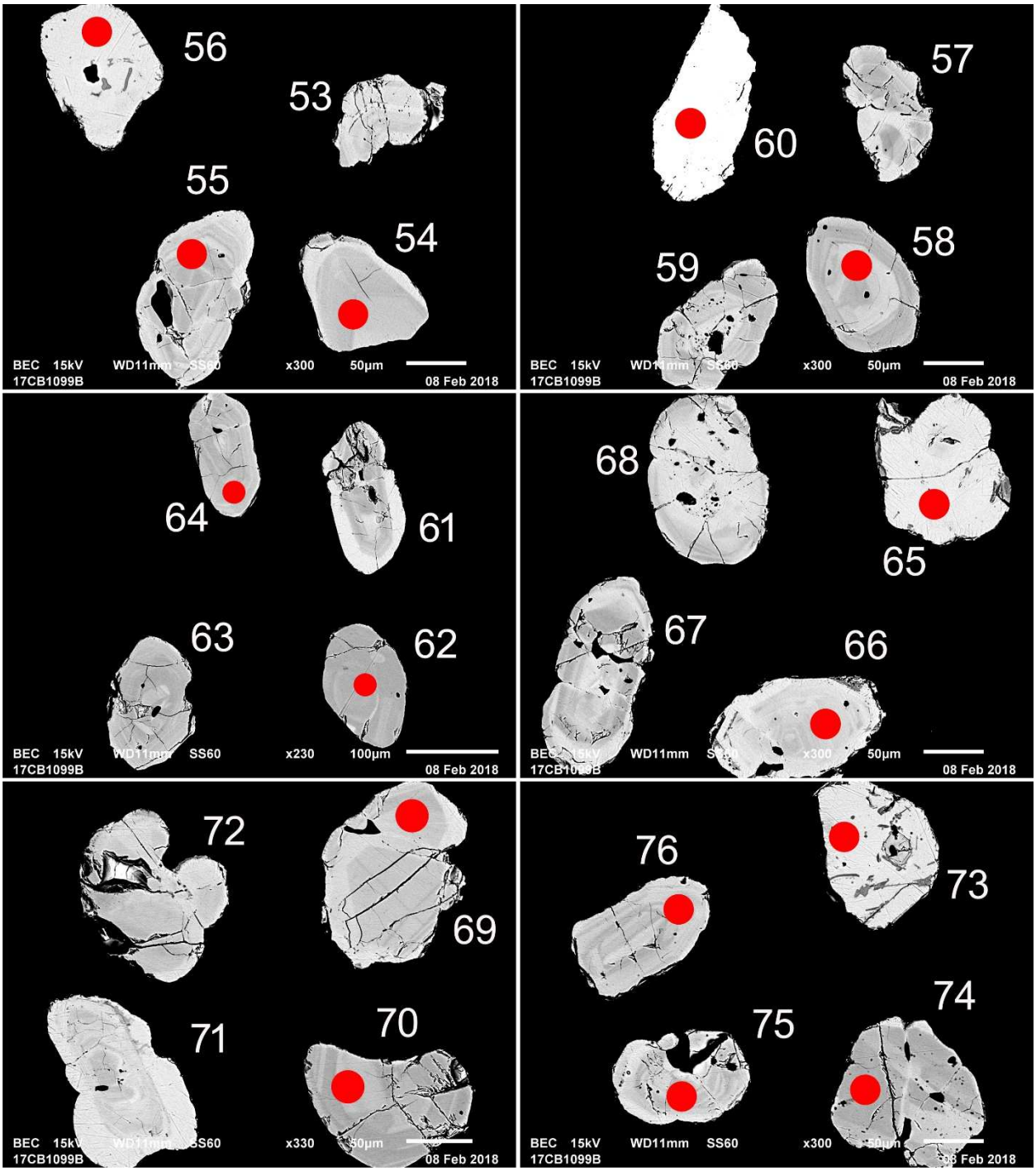


Fig 8-2-3 BSE images of selected grains from quartzite sample 17CB1099B. The red spots represent the approximate locations of laser ablation pits.

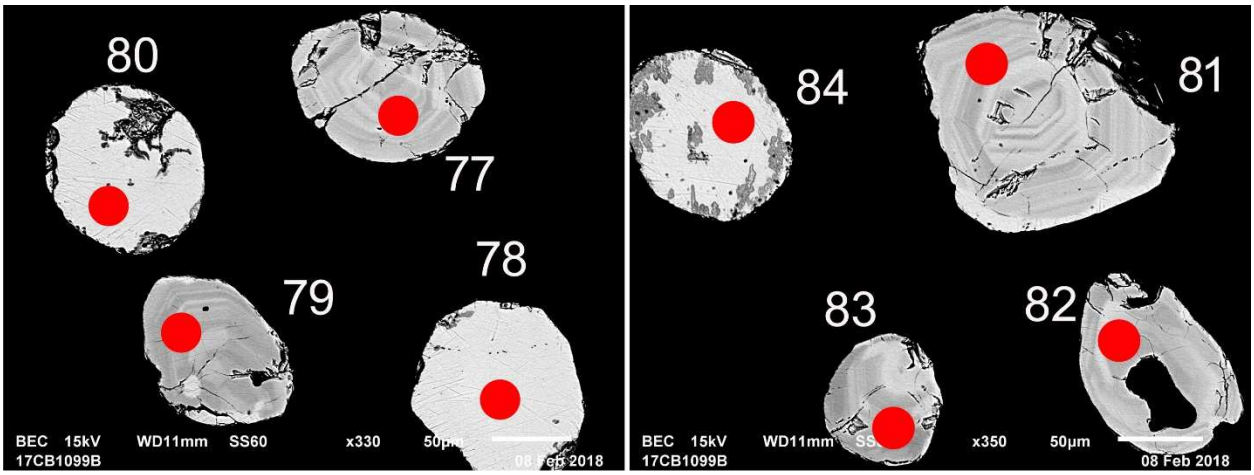


Fig 8-2-4 BSE images of selected grains from quartzite sample 17CB1099B. The red spots represent the approximate locations of laser ablation pits.

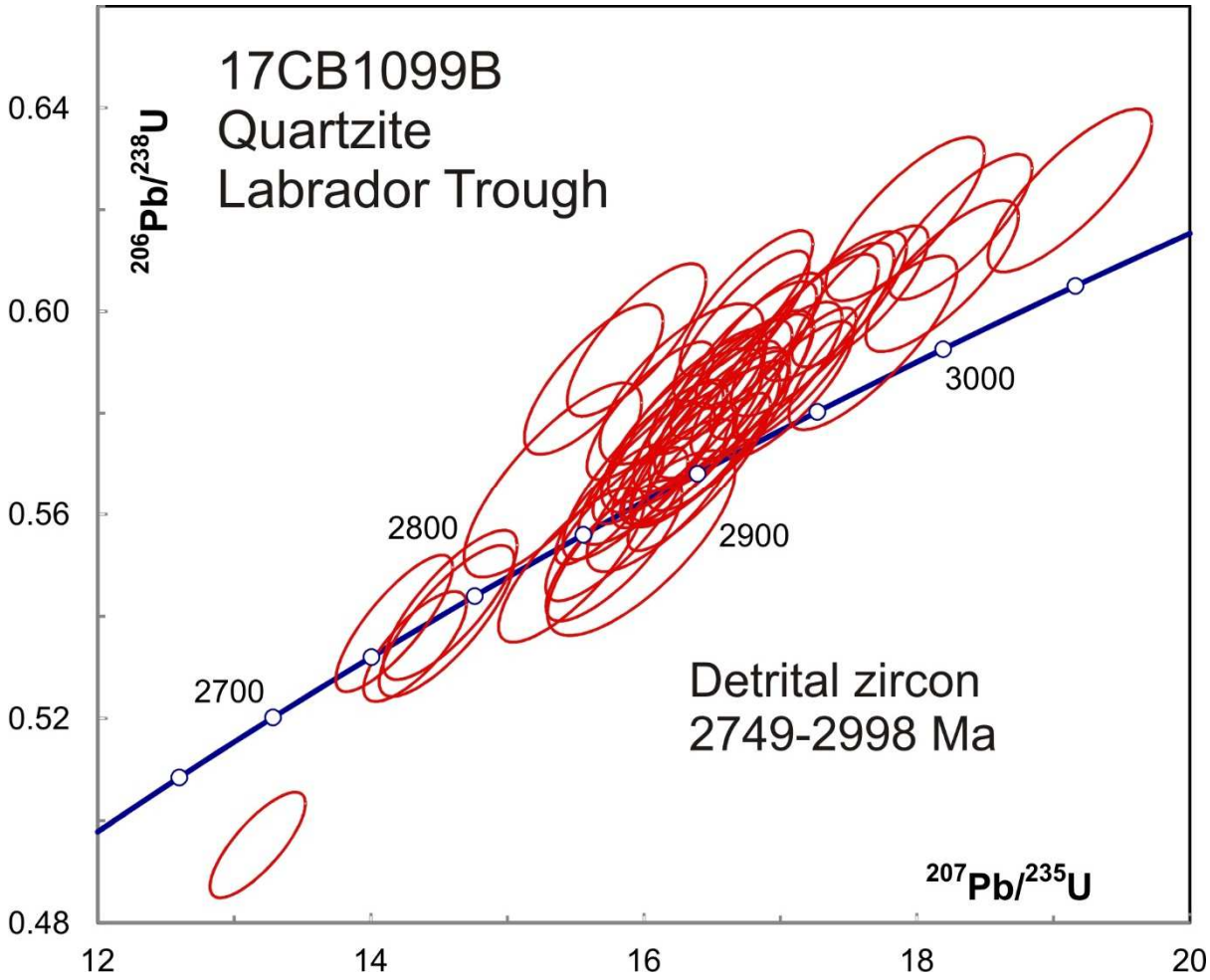


Fig 8-3. Concordia plot showing U-Pb isotopic data on zircon from quartzite sample 17CB1099B.

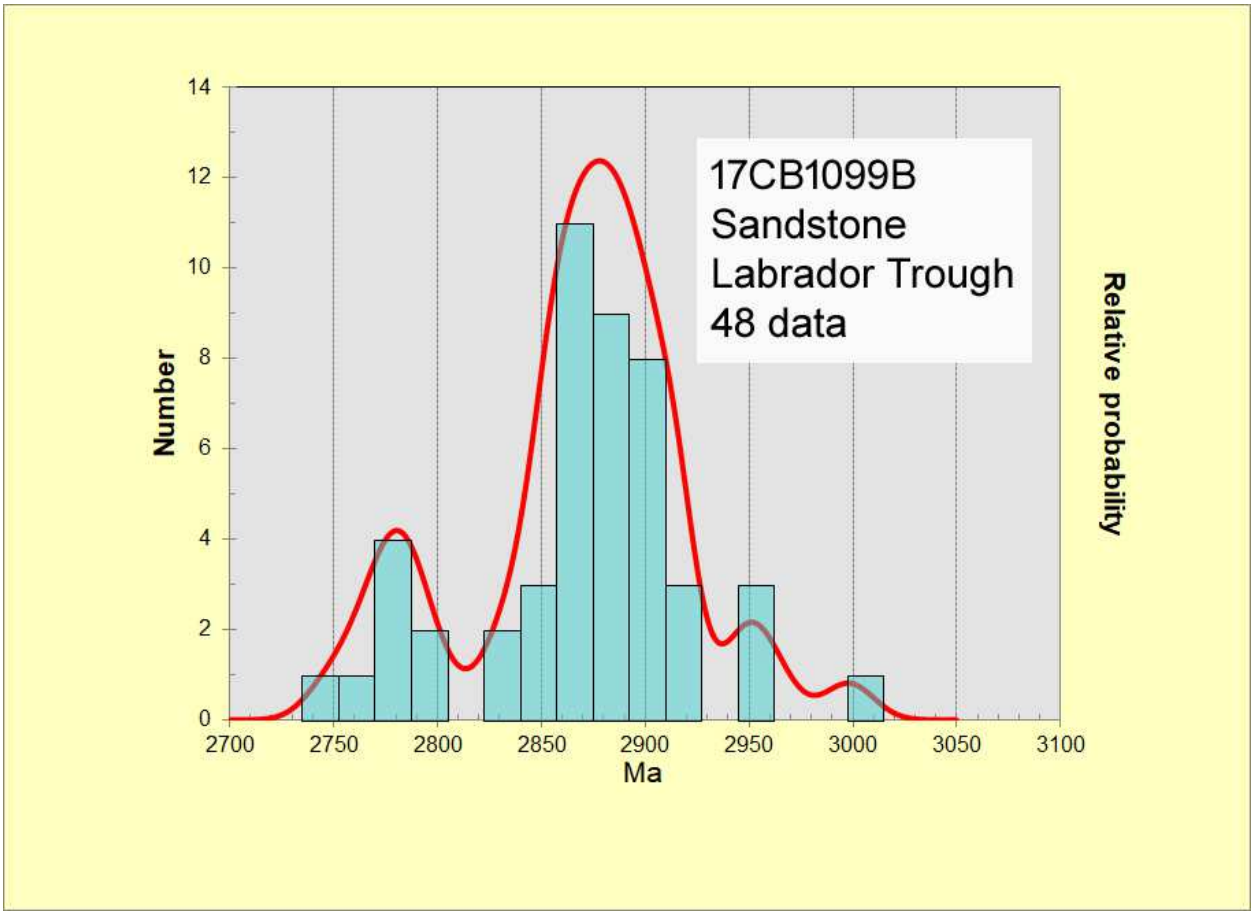


Fig 8-4. Relative probability density distribution and histogram showing U-Pb isotopic data on polished zircon from quartzite sample 17CB1099B.

### *3-9 17WC4222A Tonalite gneiss with felsic injections, Ungava Complex, Labrador Trough*

This sample yielded abundant subrounded, generally cracked zircon (Fig 9-1). BSE images on polished grains show a fairly consistent pattern of oscillatory zoning with no evidence of overgrowths (Fig 9-2). U-Pb analyses on 25 spots scatter outside of error and the distribution appears to be skewed toward younger ages, or else there are two unresolved groups (Fig 9-3). Averaging an older group of 18 data gives 2843 ± 7 Ma, while the remaining 7 data give 2773 ± 7 Ma. There is no apparent difference between younger and older spots and no textural evidence for magmatic overgrowths. If the region was affected by Proterozoic metamorphism, the younger grains may have been slightly reset, or the younger age may represent the age of the felsic veins.


Fig 9-1. Picked zircon from tonalite sample 17WC4222A.

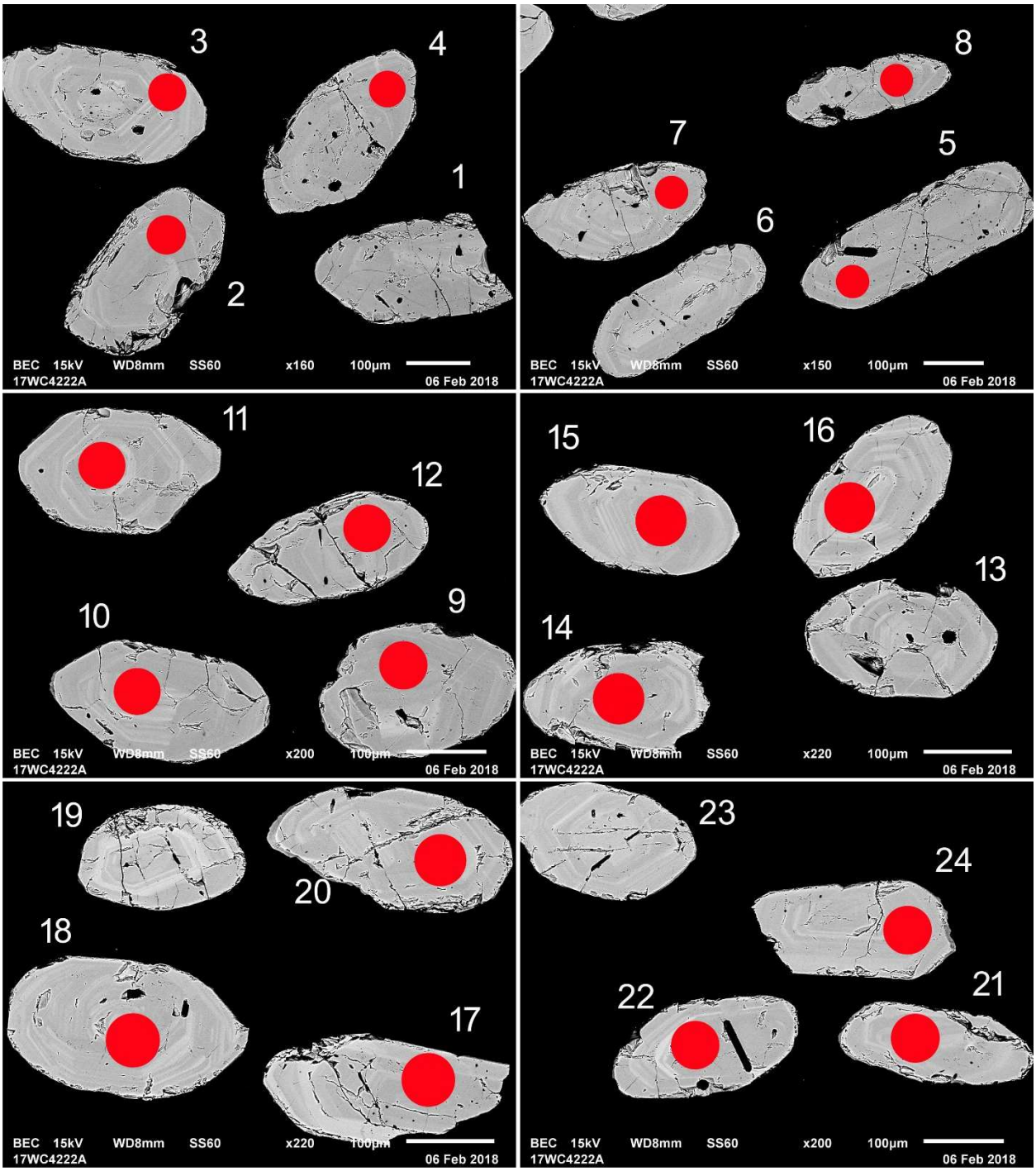


Fig 9-2-1 BSE images of selected grains from tonalite sample 17WC4222A. The red spots represent the approximate locations of laser ablation pits.

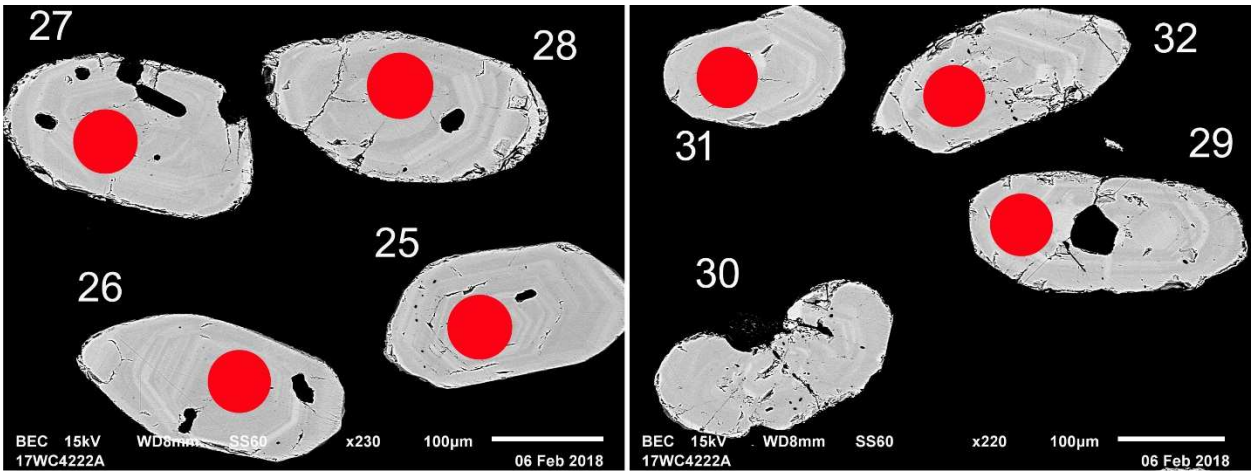


Fig 9-2-2 BSE images of selected grains from tonalite sample 17WC4222A. The red spots represent the approximate locations of laser ablation pits.

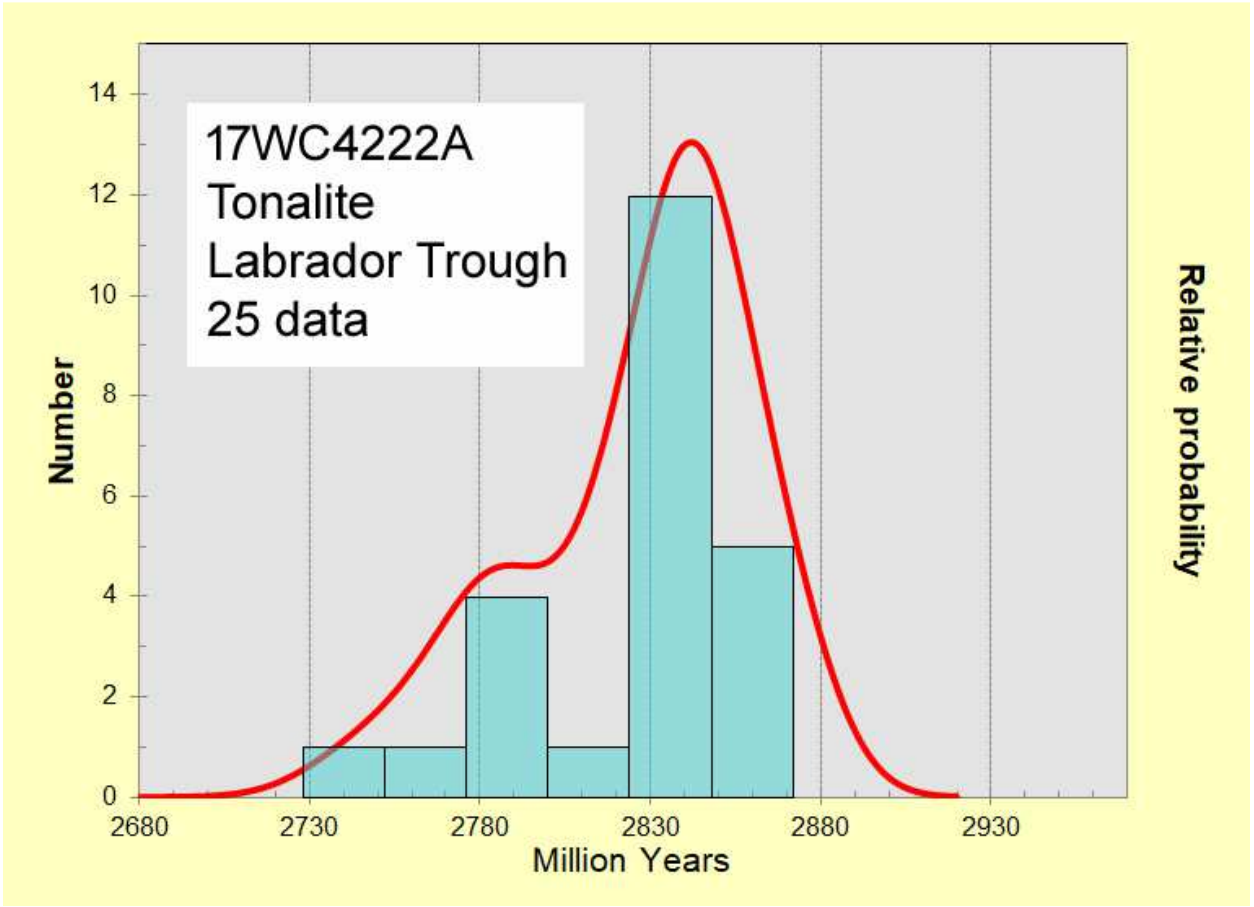


Fig 9-3. Relative probability density plot showing $^{207}Pb/^{206}Pb$ ages on zircon from tonalite sample 17WC4222A.

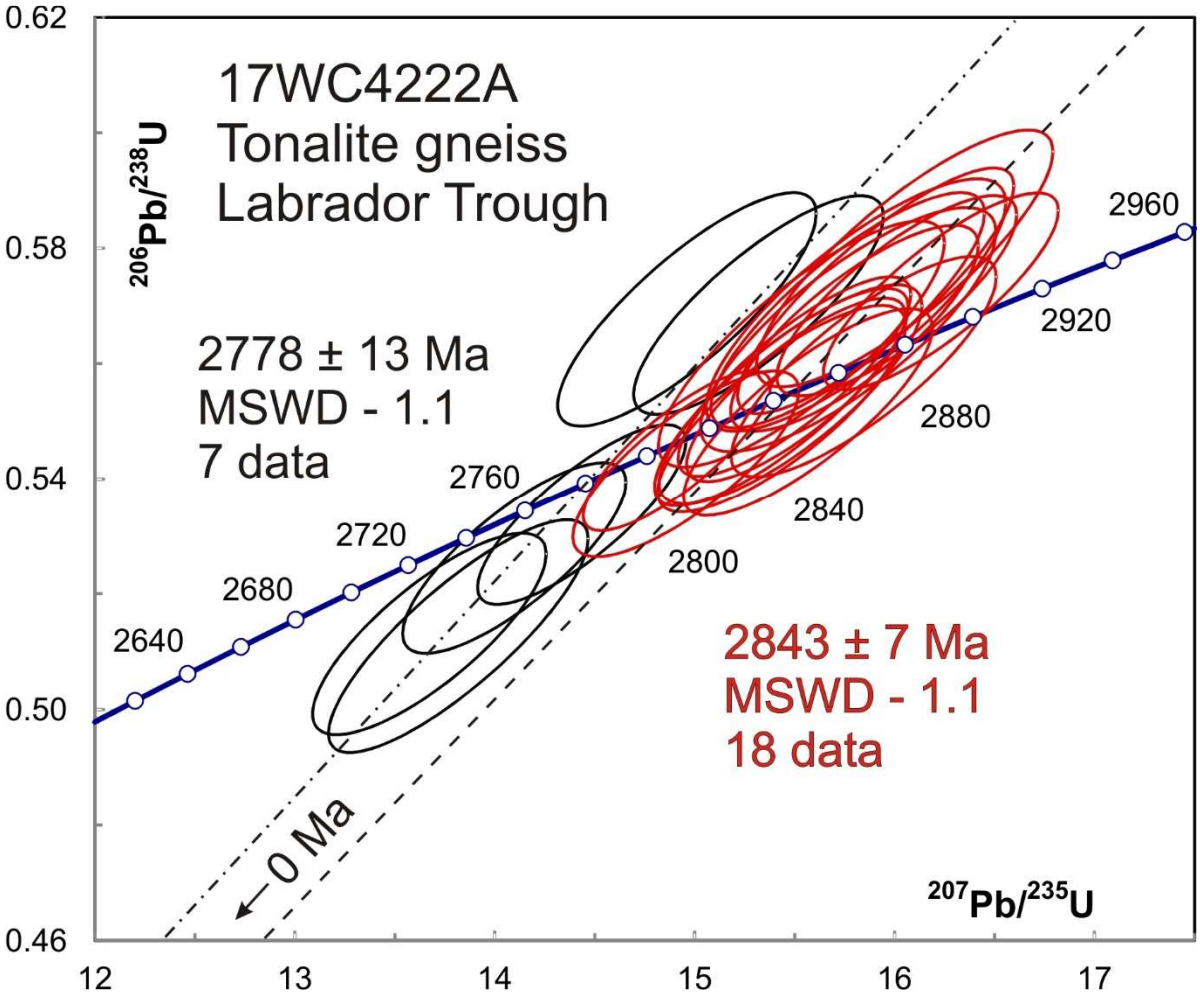


Fig 9-4. Concordia plot showing U-Pb isotopic data on zircon from tonalite sample 17WC4222A. Possible younger zircon is distinguished by black ellipses.

### *3-10 17BC6068A Monzodiorite, Sainte-Hélène Complex, Ungava Area*

This sample yielded abundant, generally cracked and partly altered, subrounded zircon (Fig 10-1). BSE images show zoning but also the possible presence of cores (Fig 10-2). U-Pb analyses on 24 spots cluster around Paleoproterozoic ages with a few older data (Fig 10-3). The youngest data scatter outside of error and may form two unresolved clusters (Fig 10-4). The 11 youngest data define an average age of 1901 ± 8 Ma (Fig 10-5), which is probably the best estimate for final crystallization of the pluton. A slightly older cluster of 9 data define an average age of 1957 ± 9 Ma. There is no clear distinction between older and younger spots. Either the older age represents residual inheritance or an early phase of melting and crystallization in a long-lived system


Fig 10-1. Picked zircon from monzodiorite sample 17BC6068A.

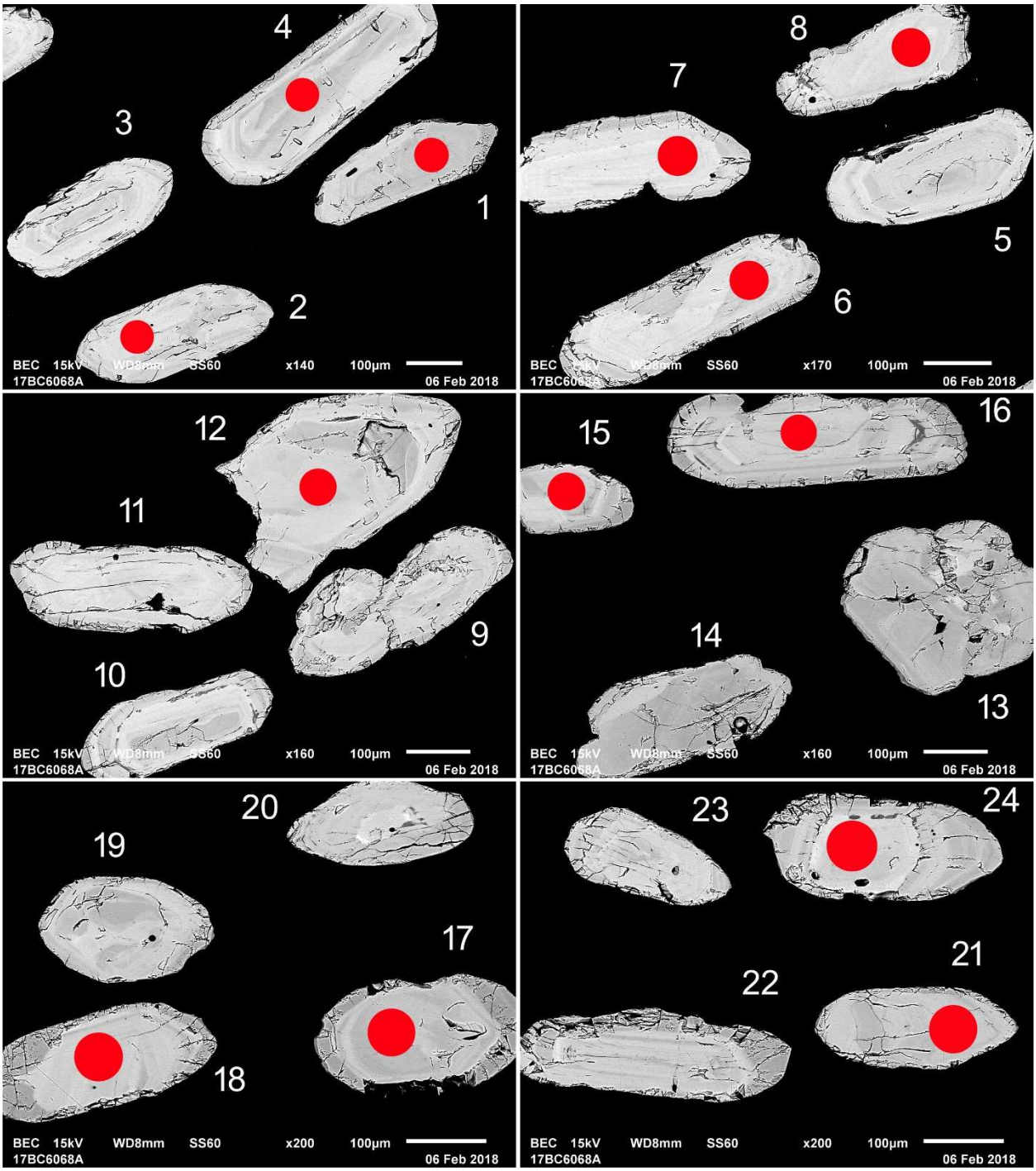


Fig 10-2-1 BSE images of selected grains from monzodiorite sample 17BC6068A. The red spots represent the approximate locations of laser ablation pits.

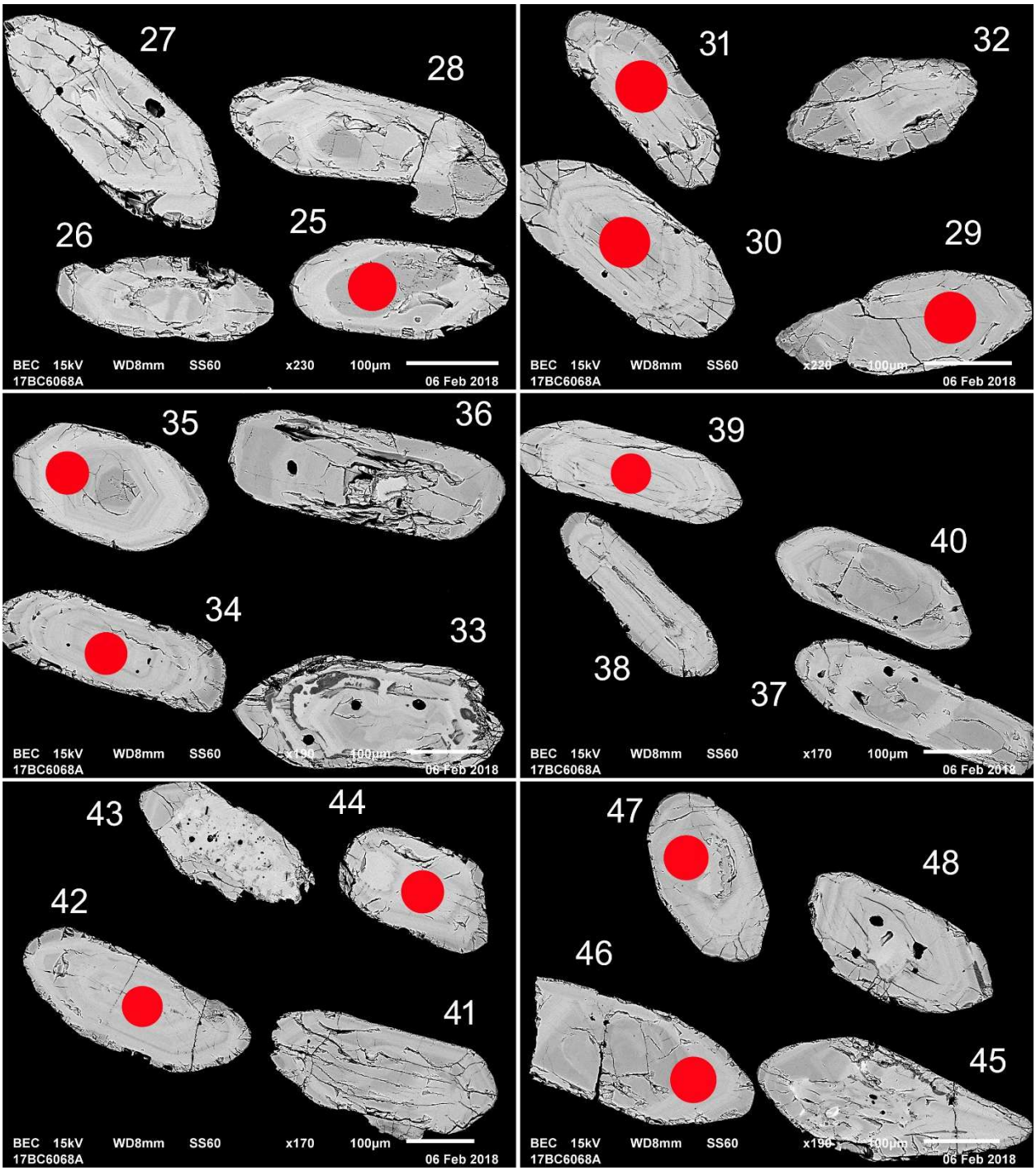


Fig 10-2-2 BSE images of selected grains from monzodiorite sample 17BC6068A. The red spots represent the approximate locations of laser ablation pits.

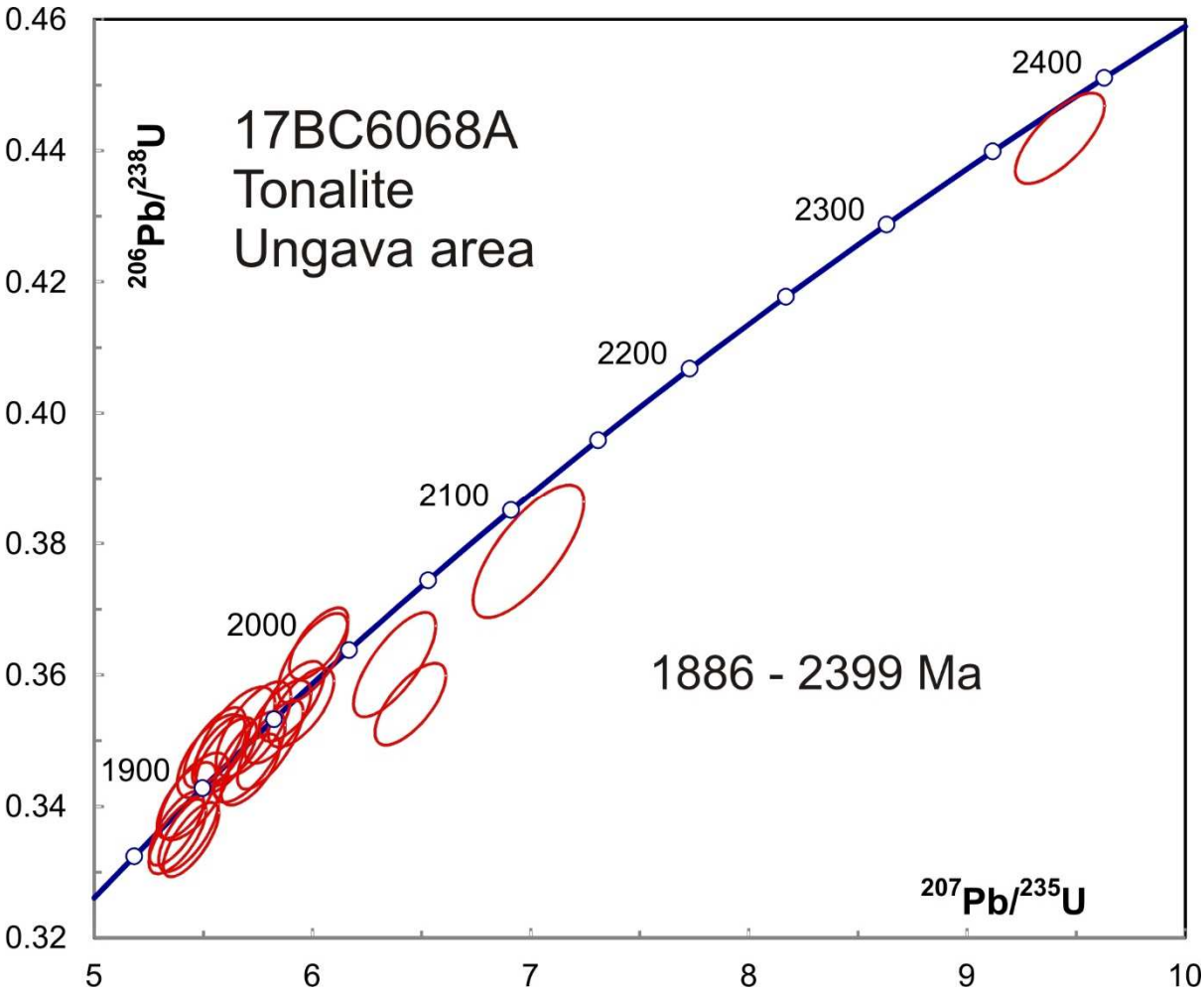


Fig 10-3. Concordia plot showing all U-Pb isotopic data on zircon from monzodiorite sample 17BC6069A.

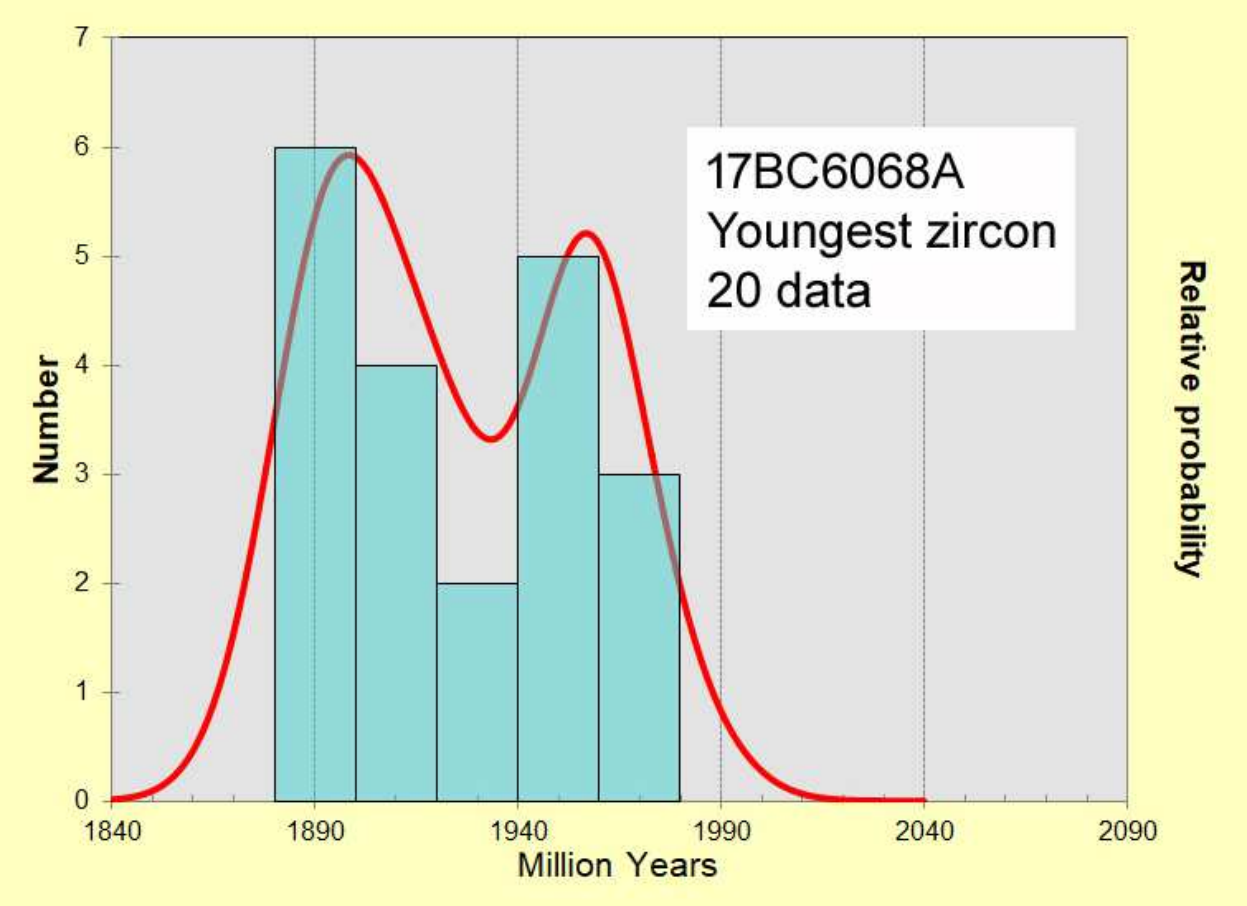


Fig 10-4. Relative probability density plot showing $^{207}Pb/^{206}Pb$ ages on zircon from monzodiorite sample 17BC6068A.

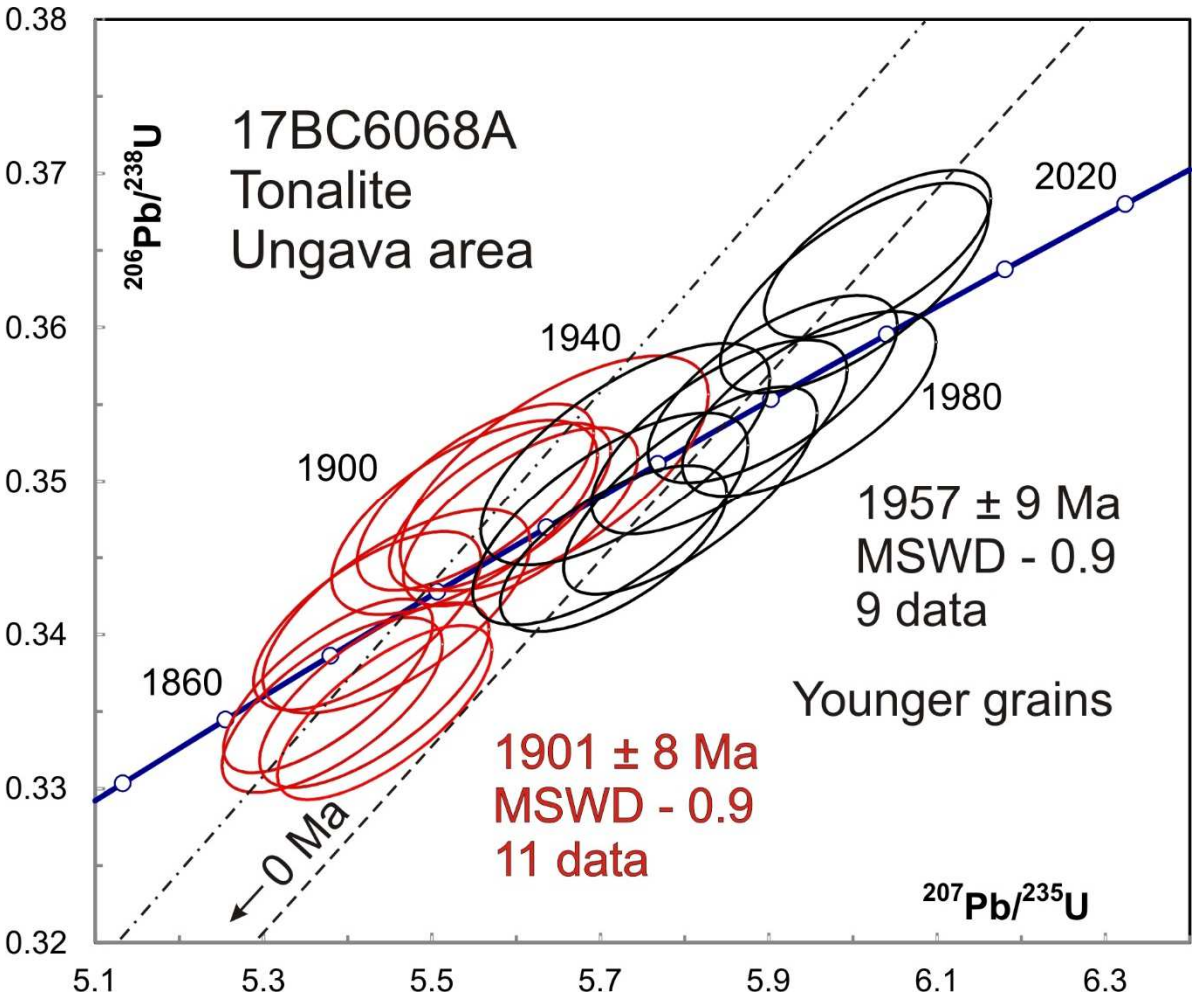


Fig 10-5. Concordia plot showing the youngest U-Pb isotopic data on zircon from monzodiorite sample 17BC6069A.

### *3-11 17LP2065A Tonalite, Kovic Complex, Ungava Area*

Zircon recovered from this sample is subrounded and cracked but somewhat fresher than that from the previous tonalite sample (Fig 11-1). BSE images show oscillatory zoning in most grains with rare cores (grain 4) and overgrowths (grain 8) in some (Fig 11-2). Most of the U-Pb analyses scatter within error around an average of 1852 ± 6 Ma (Fig 11-3). Two are somewhat discordant and gave very slightly older ages (Table 1) so these were omitted from the average. The core in grain 4 gave the oldest age while the well-defined rim in grain 8 gave the youngest but they are not resolvable. Th/U ratios are within the magmatic range, except for the relatively high-U rim around grain 8, which may be a metamorphic overgrowth. If so, crystallization was nearly coeval with metamorphism.


Fig 11-1. Picked zircon from tonalite sample 17LP2065A.

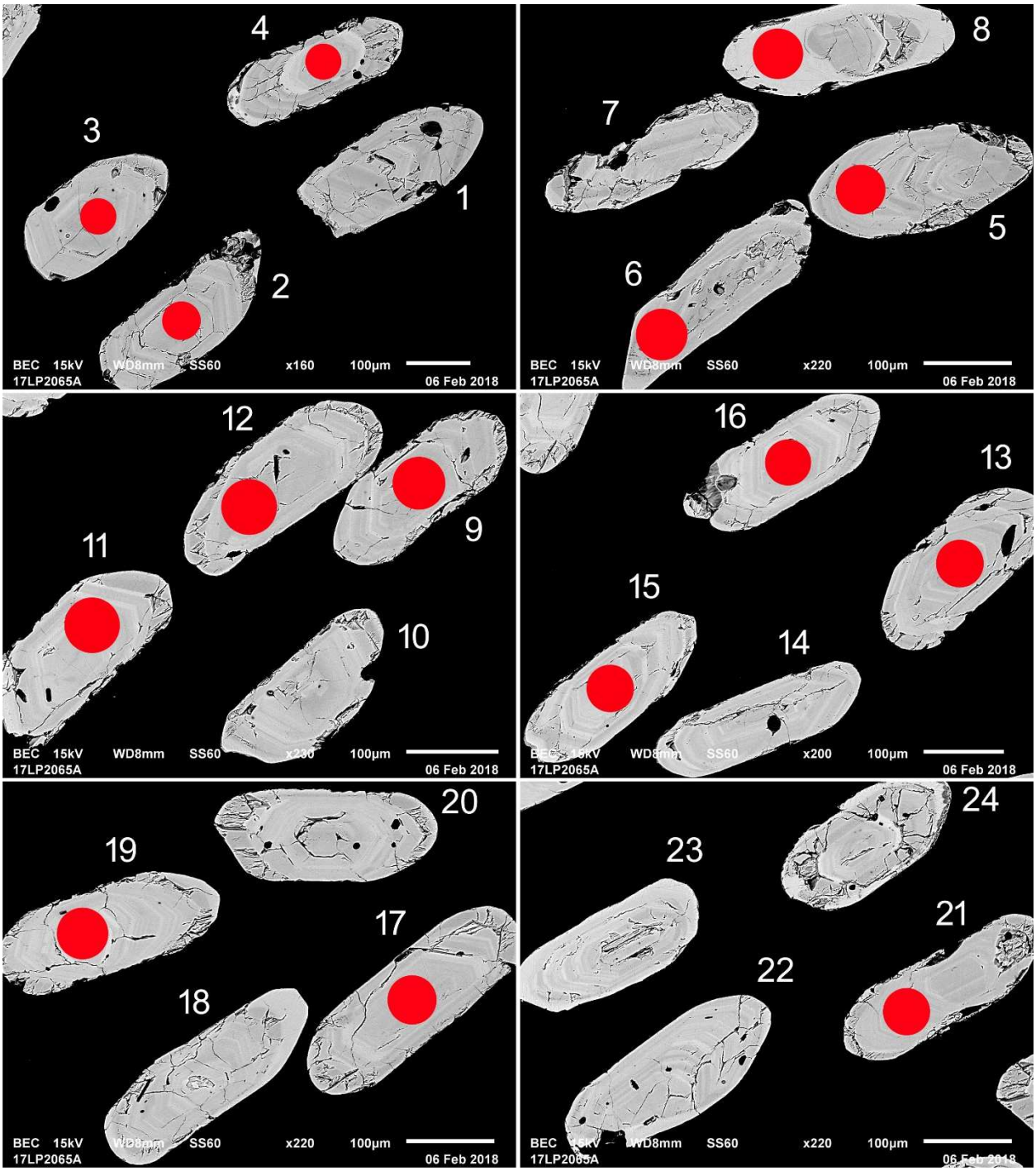


Fig 11-2-1 BSE images of selected grains from tonalite sample 17LP2065A. The red spots represent the approximate locations of laser ablation pits.

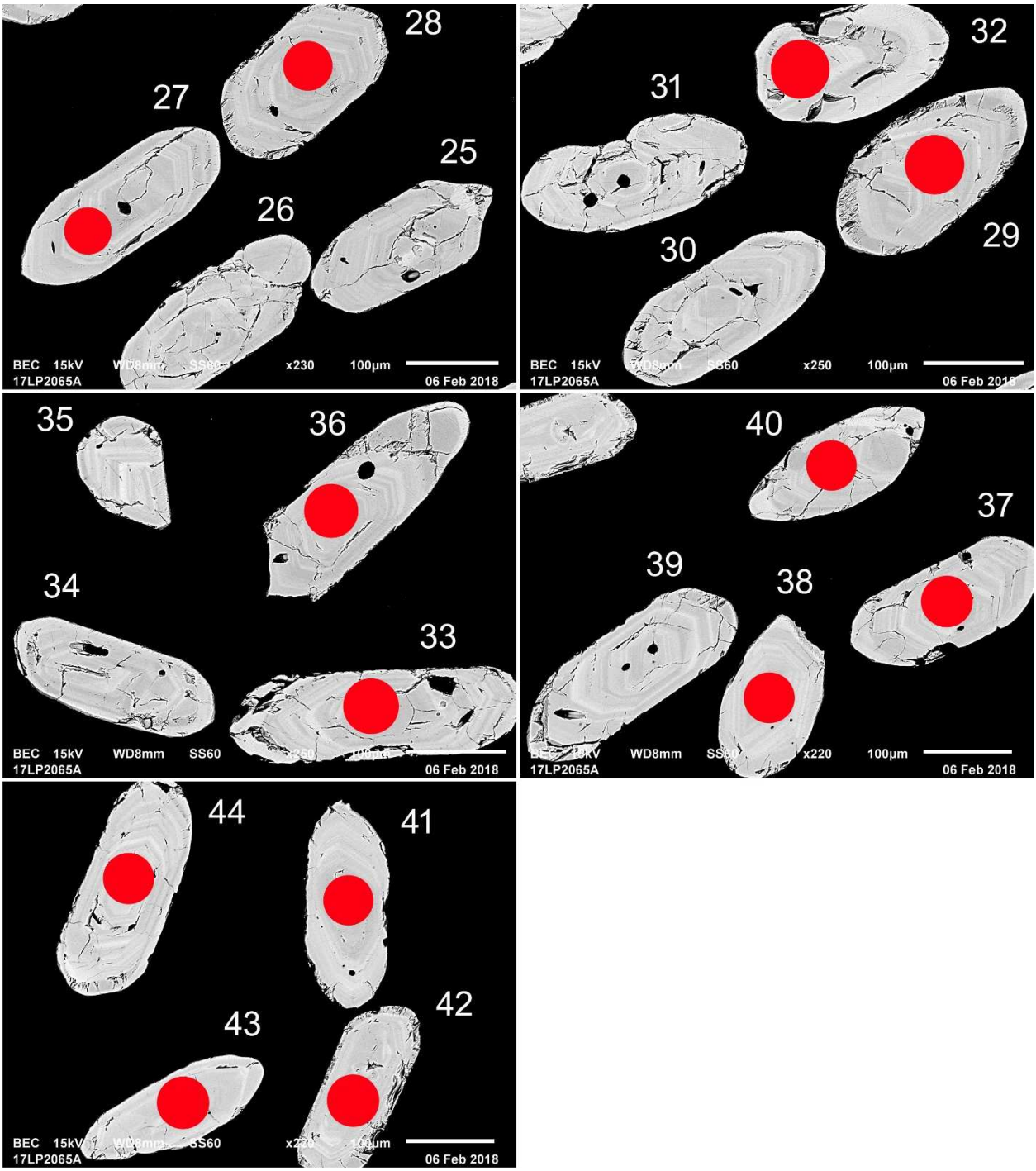


Fig 11-2-2 BSE images of selected grains from tonalite sample 17LP2065A. The red spots represent the approximate locations of laser ablation pits.

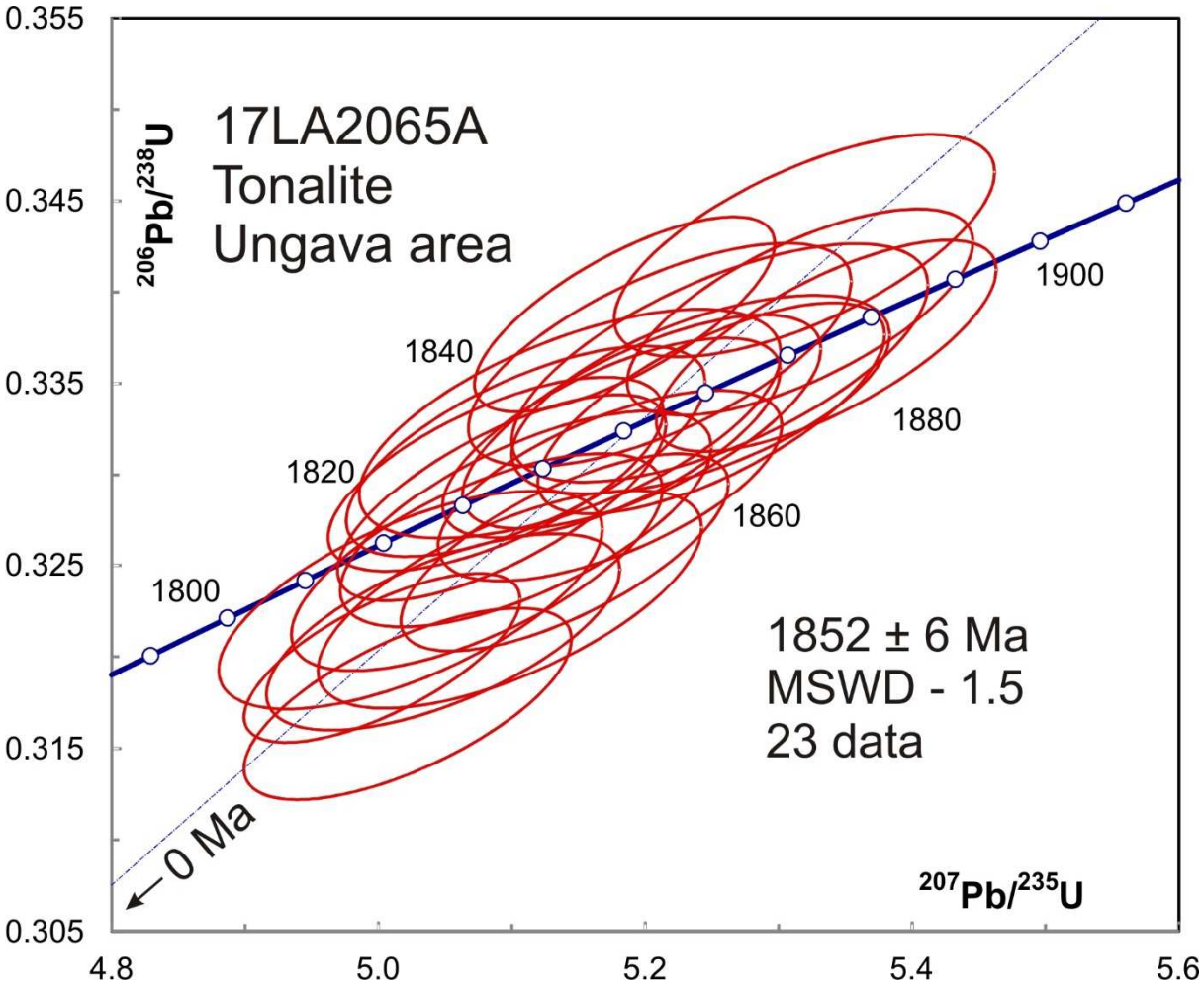


Fig 11-3. Concordia plot showing U-Pb isotopic data on zircon from tonalite sample 17LA2065A. Two discordant data are off scale and not included in the average age.

### *3-12 17SM4102A: Opdalite, Navvaataaq Suite, Ungava Area*

This rock yielded irregularly shaped, fresh zircon (Fig 12-1). BSE images show no or patchy zoning, with possible remnants of oscillatory zoning in a few cases (e.g. grains 29 and 30, Fig 12-2). U-Pb analyses show a range of ages from 2560 Ma to 1806 Ma (Fig 12-3) with most data clustered over the older part of the range from 2560 Ma to about 2400 Ma (Fig 12-4). The spot analyses show somewhat variable U concentrations but consistent Th/U of around 1, which is near the upper range for most magmatic zircon (Table 1). There is therefore no evidence for mixing of two zircon phases. It is likely that the zircon is late Archean and suffered Pb loss due to diffusion during a prolonged high-grade Paleoproterozoic metamorphism. If so, the oldest age of 2560 ± 26 Ma is likely a minimum estimate for original emplacement, while the youngest age of 1806 ± 38 Ma is a maximum age estimate for the end of metamorphism. There is no obvious difference between grains having the youngest spots and the others. Unfortunately, there is insufficient control on Pb/U ratios to define reliable intercept ages from the diffusion line.


Fig 12-1. Picked zircon (irregular, colourless, high relief grains) from opdalite sample 17SM4102A. Fraction includes minerals other than zircon.

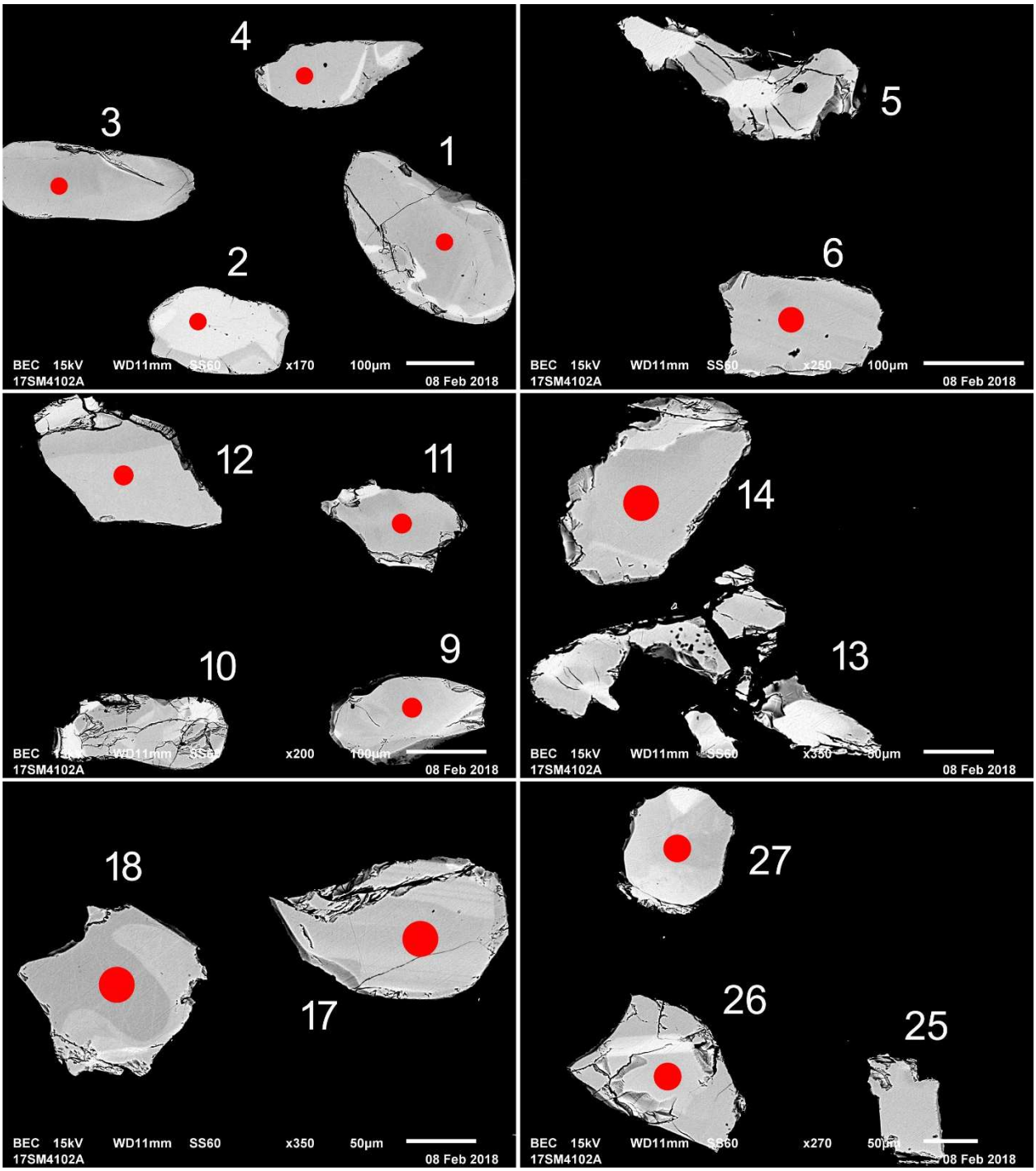


Fig 12-2-1 BSE images of selected grains from opdalite sample 17SM4102A. The red spots represent the approximate locations of laser ablation pits.

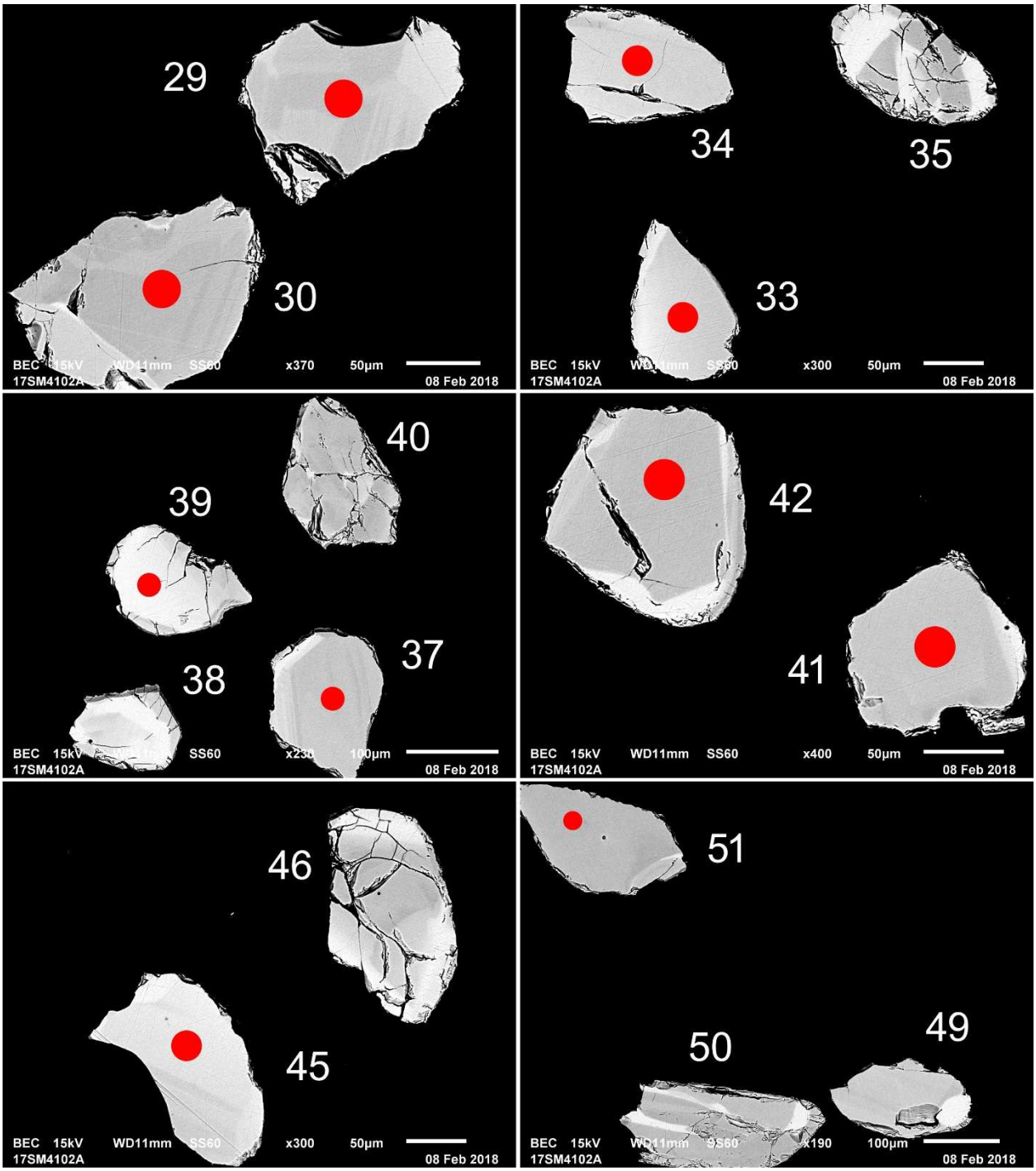


Fig 12-2-2 BSE images of selected grains from opdalite sample 17SM4102A. The red spots represent the approximate locations of laser ablation pits.

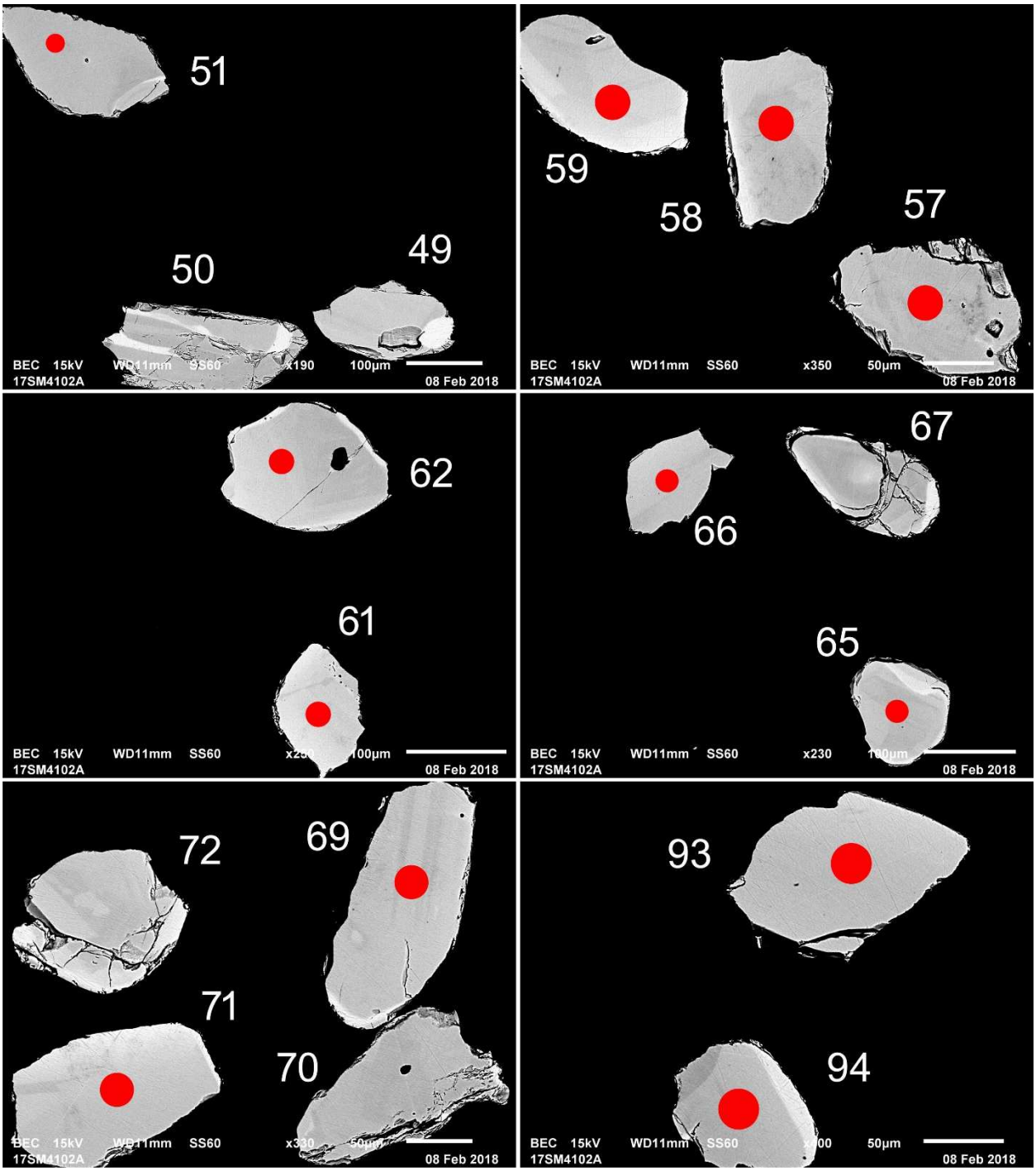


Fig 12-2-3 BSE images of selected grains from opdalite sample 17SM4102A. The red spots represent the approximate locations of laser ablation pits.

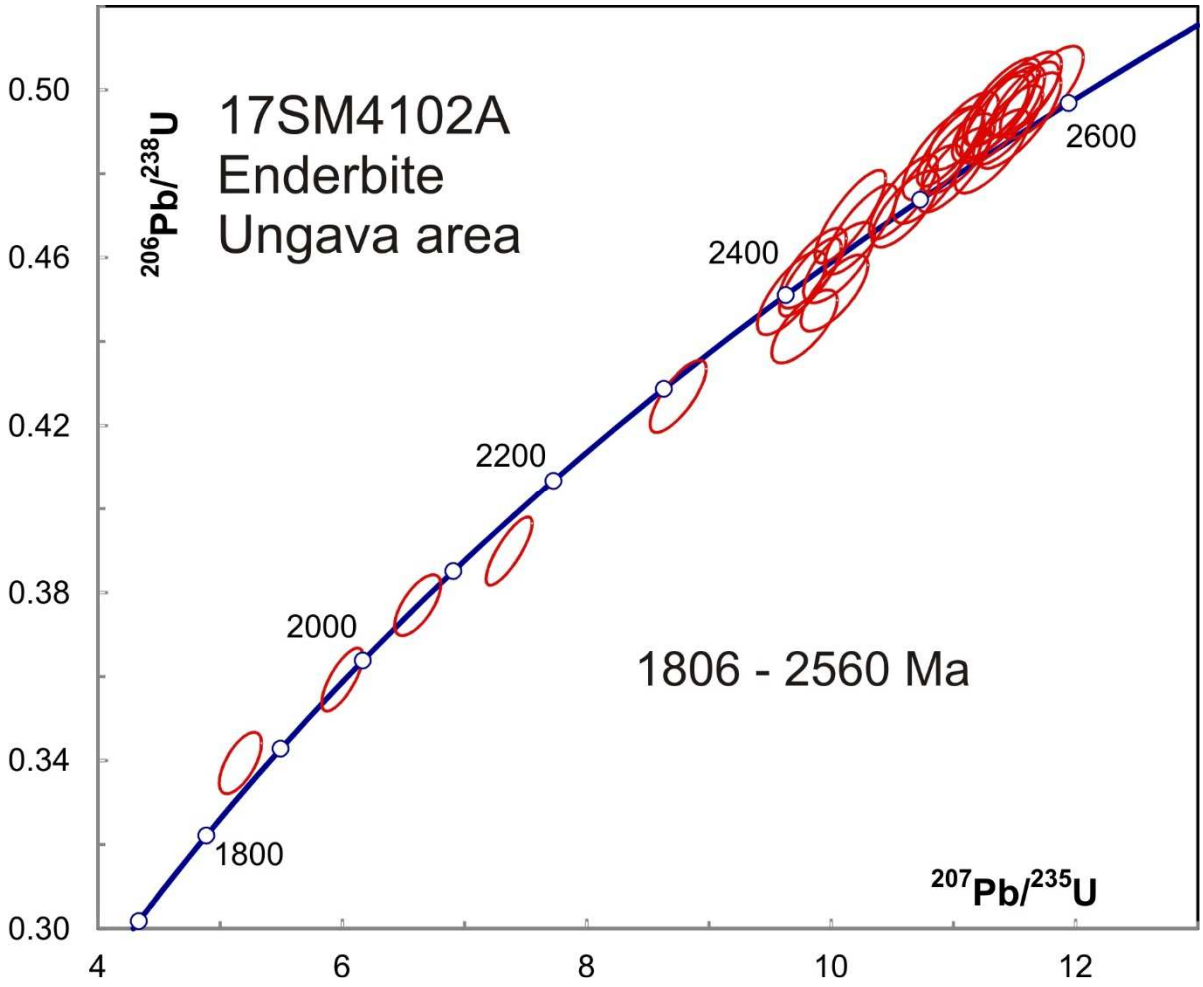


Fig 12-3. Concordia plot showing U-Pb isotopic data on zircon from opdalite sample 17SM4102A.

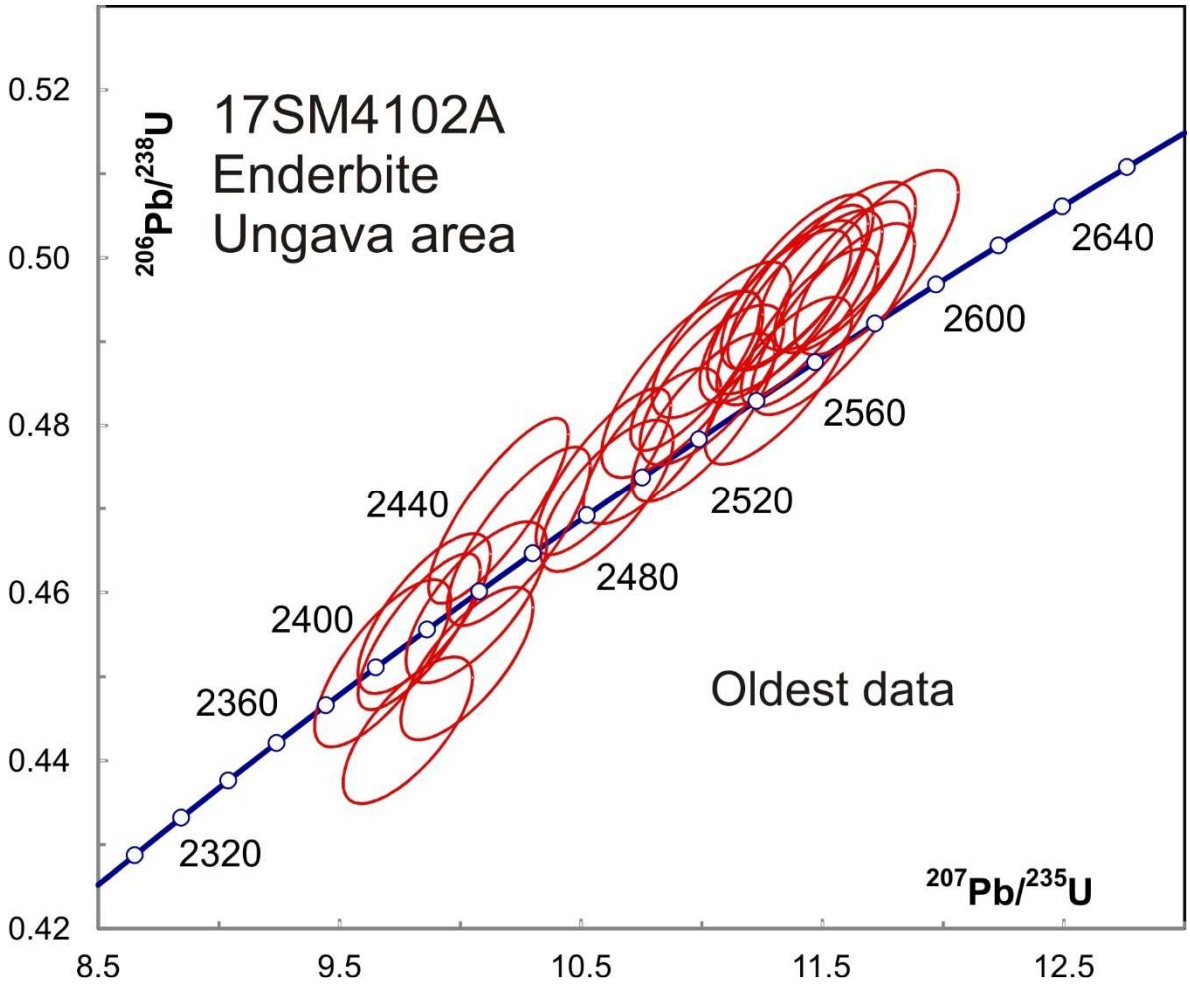


Fig 12-4. Concordia plot showing oldest U-Pb isotopic data on zircon from opdalite sample 17SM4102A.

### *3-13 17MP1013A: Orthopyroxene-bearing quartz diorite, Pingasualuit Complex Ungava Area*

This sample yielded subrounded, fractured zircon (Fig 13-1). BSE images show a general lack of zonation but possible high-U (bright) overgrowths (Fig 13-2). Overgrowths show an irregular contact with darker interiors probably because grinding was not very deep and the polishing plane is sub-parallel to the overgrowth contact. This is intentional so as to preserve a sufficient area of overgrowth material for analysis. U-Pb spot analyses give a range of ages from 2609 Ma to 1869 Ma (Fig 13-3) and can be divided into two groups based on Th/U ratios. Six spots having Th/U < 0.1 cluster at the young end of the range with an average age of 1880 ± 9 Ma (Fig 13-4). These spots appear to be on overgrowths and probably represent a metamorphic phase. Analyses showing magmatic Th/U ratios scatter widely and are probably from magmatic zircon that crystallized before 2609 Ma and suffered partial diffusional Pb loss during Paleoproterozoic metamorphism.


Fig 13-1. Picked zircon from quartz-hypersthene diorite sample 17MP1013A.

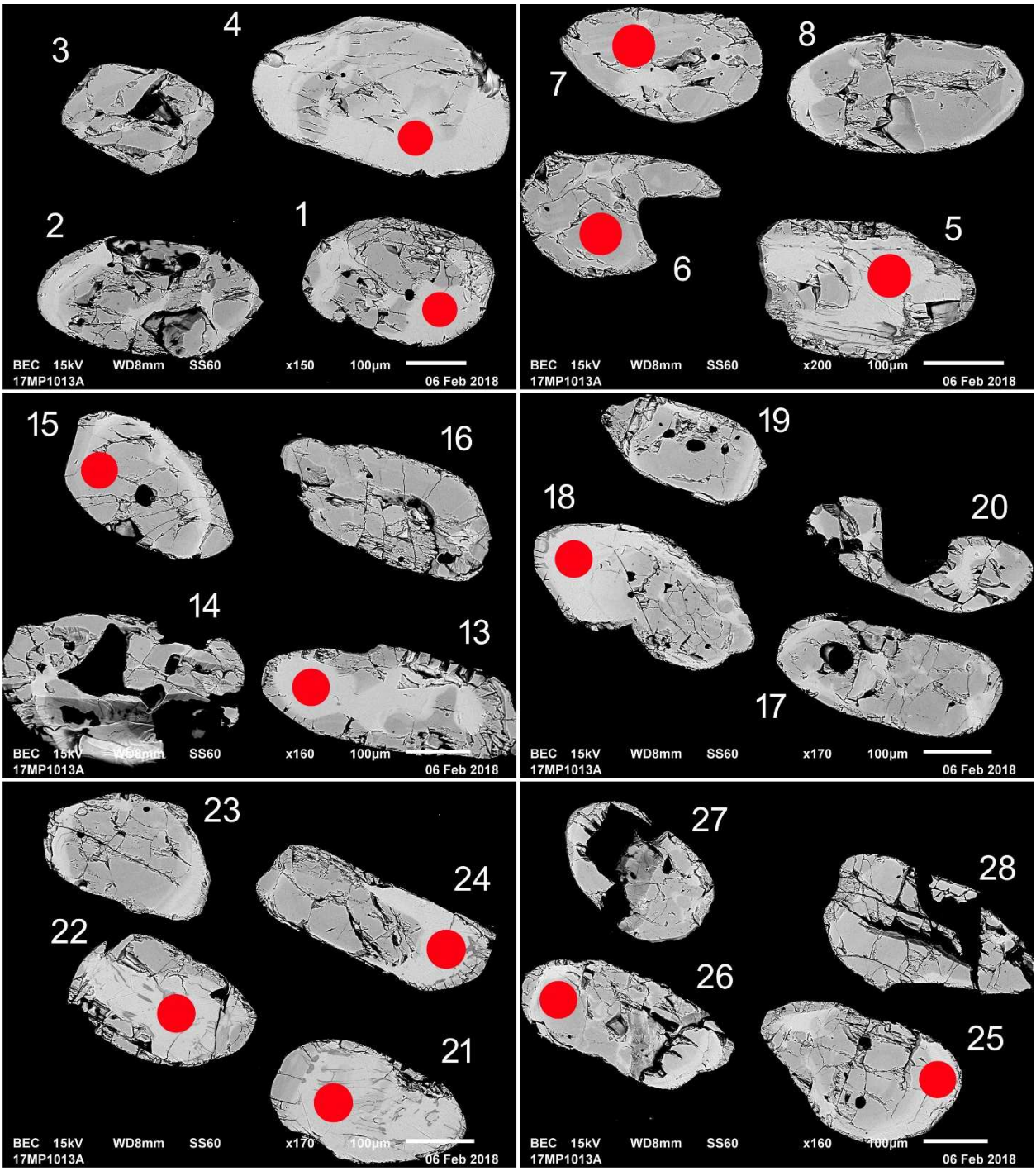


Fig 13-2-1 BSE images of selected grains from quartz-hypersthene diorite sample 17MP1013A. The red spots represent the approximate locations of laser ablation pits.

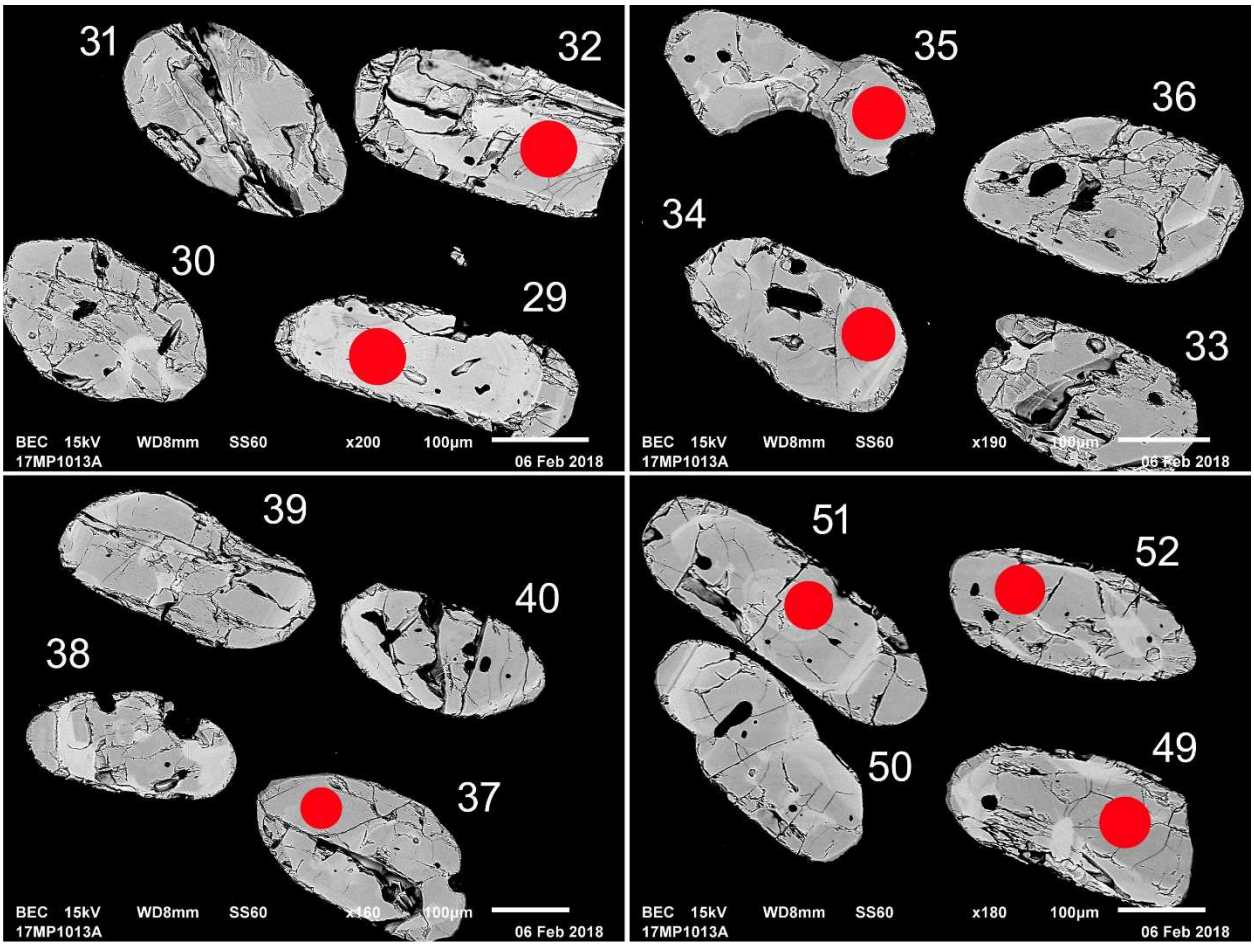


Fig 13-2-2 BSE images of selected grains from quartz-orthopyroxene diorite sample 17MP1013A. The red spots represent the approximate locations of laser ablation pits.

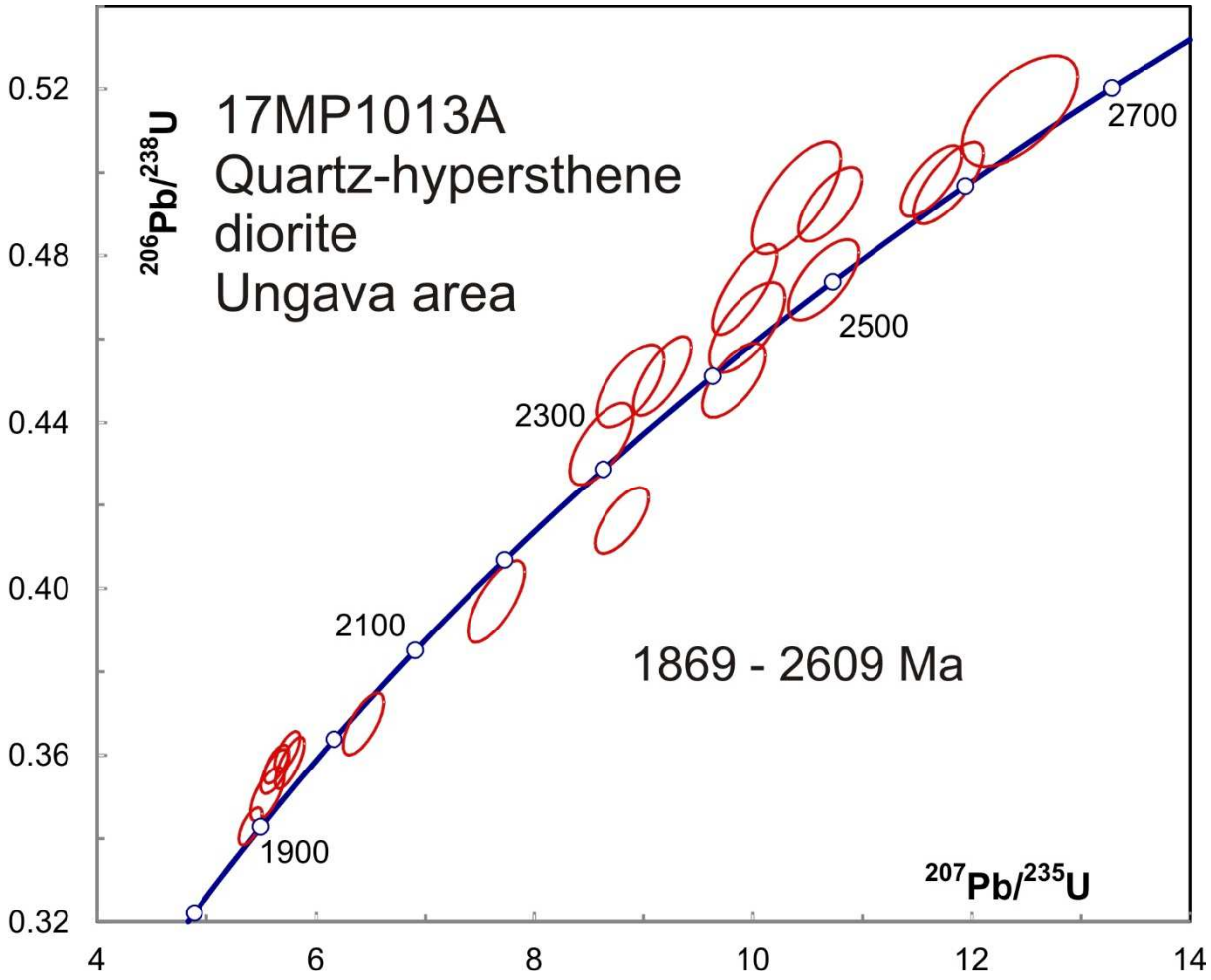


Fig 13-3. Concordia plot showing U-Pb isotopic data on zircon from quartz-orthopyroxene diorite sample 17MP1013A.

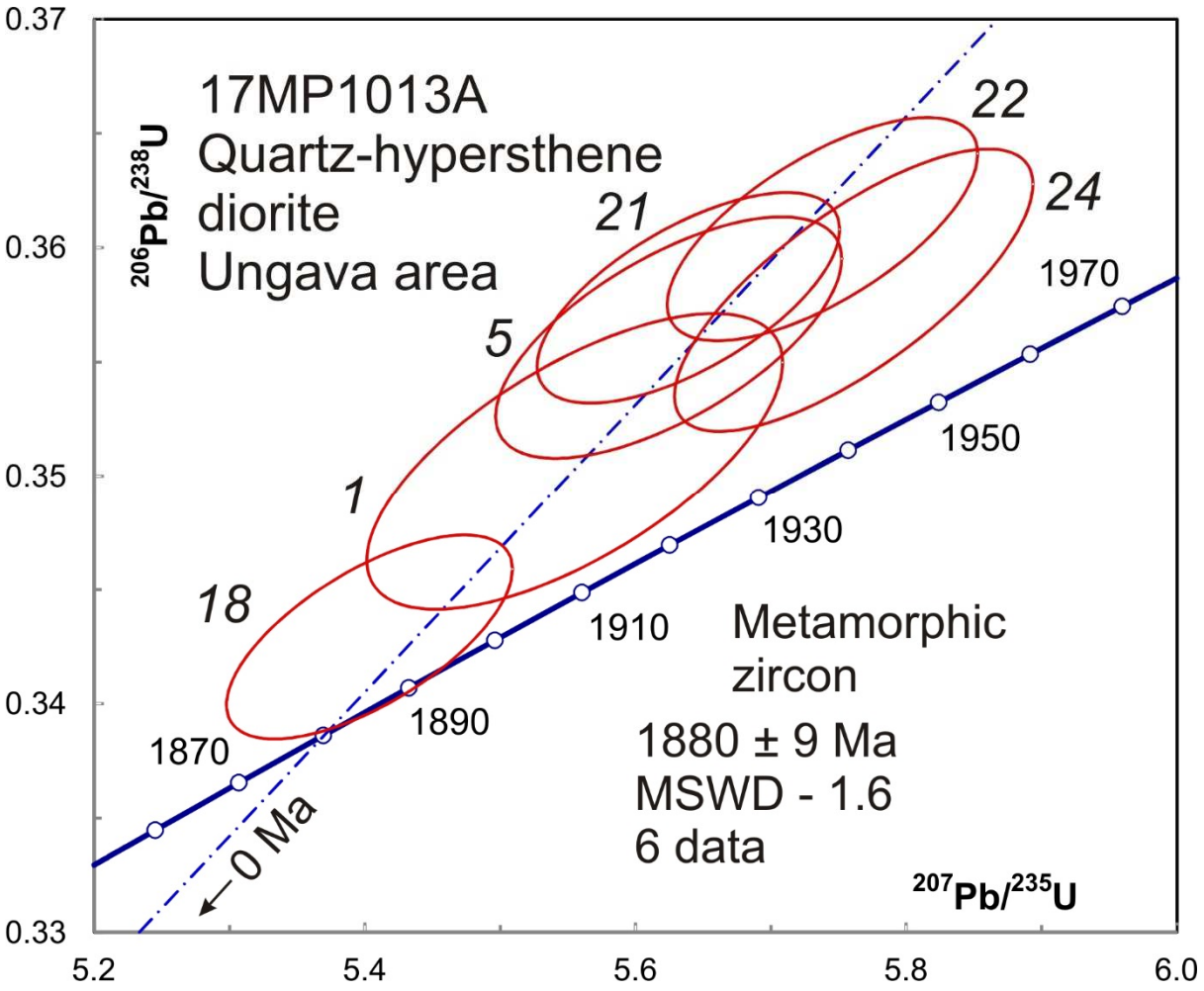


Fig 13-4. Concordia plot showing U-Pb isotopic data on low Th/U (metamorphic) zircon from quartz-orthopyroxene diorite sample 17MP1013A. Spot numbers are given in italics.

### *3-14 17LP2023A: Porphyritic quartz monzodiorite, Nallujuaq Suite, Ungava Area*

Zircon from this sample is abundant and similar to the previous plutons from the Ungava area in being subrounded and highly fractured (Fig 14-1). BSE images show unzoned zircon, with rare cores (grain 76, Fig 14-2) and possible thin higher U overgrowths on some (e.g. grains 26, 31). U-Pb analyses on 52 spots scatter from 2551 Ma to 1837 Ma (Fig 14-3). Data are generally more clustered in the older part of the age range but a small cluster of data overlap at the youngest age, giving an average of 1841 ± 10 Ma based on 4 data (Fig 14-4). There is no obvious difference between the youngest spots and the older ones. The Th/U ratios of most of the spots are near the upper range for magmatic zircon from felsic rocks (1.0) but the youngest grains have extraordinarily high ratios of 2-5 (Table 1). This suggests that they represent zircon crystallization from a highly fractionated partial melt and that they date this event. The protolith is late Archean but must have undergone a prolonged period of metamorphic heating that resulted in diffusional Pb loss.

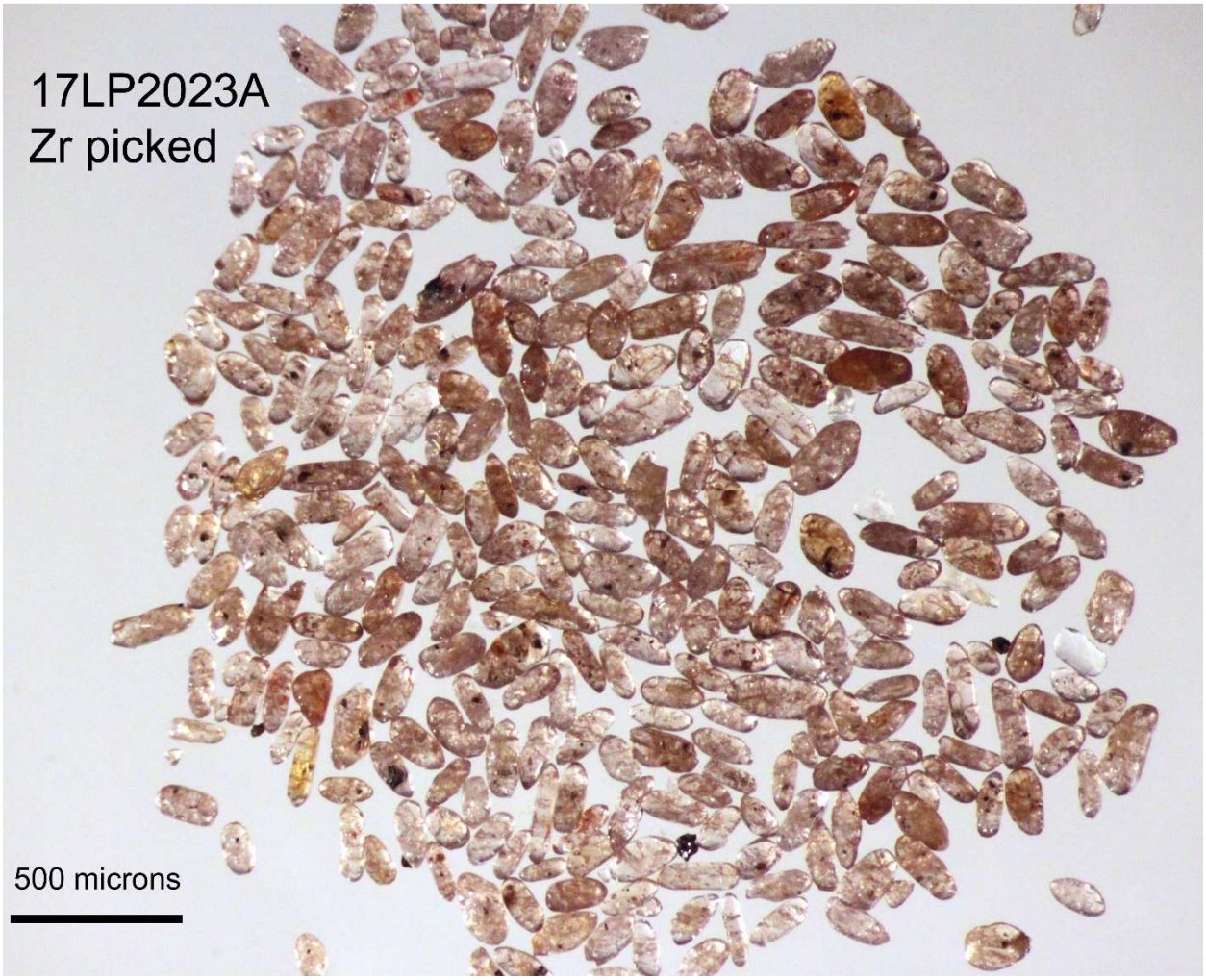


Fig 14-1. Picked zircon from porphyritic quartz monzodiorite sample 17LP2023A.

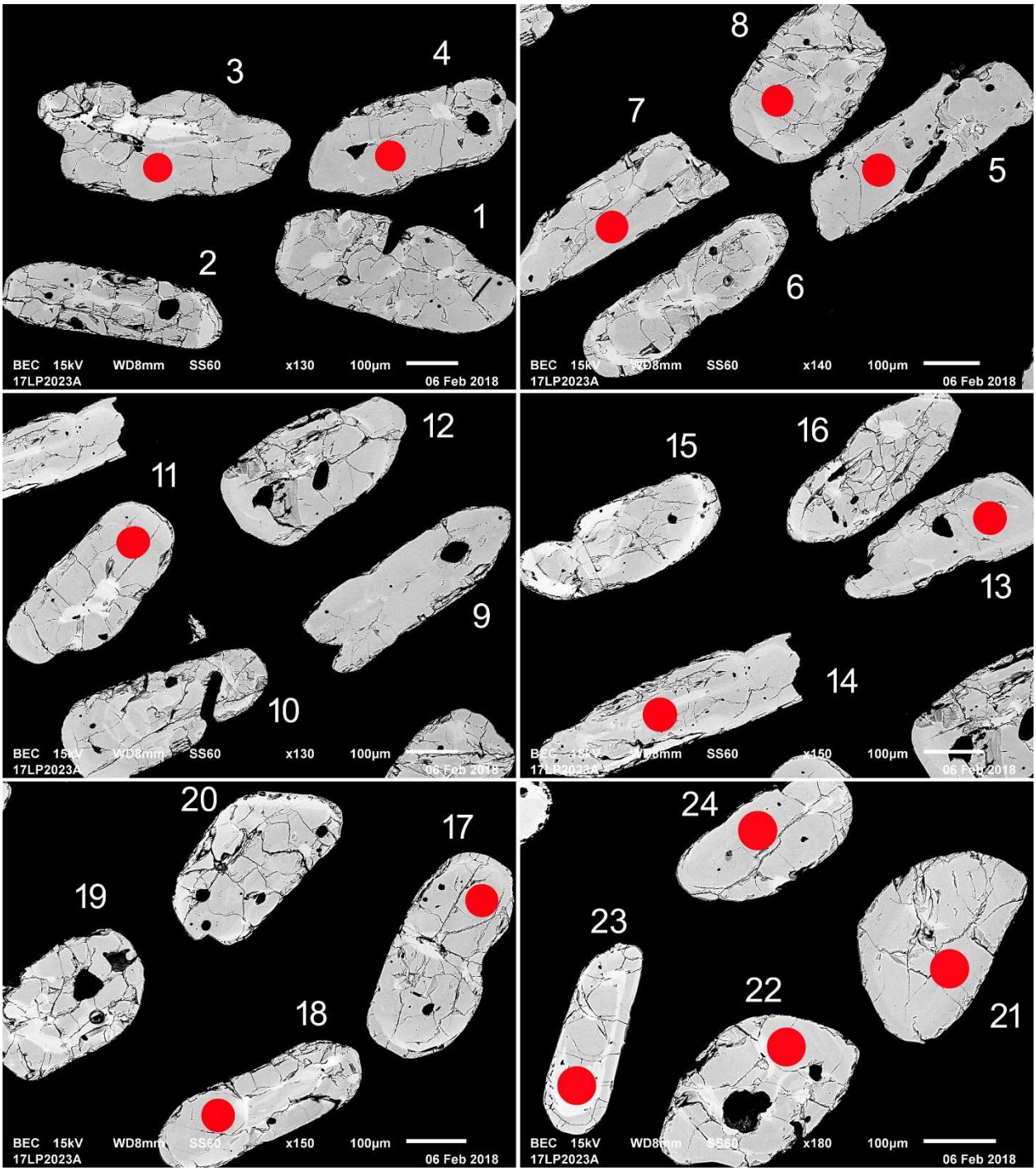


Fig 14-2-1 BSE images of selected grains from porphyritic monzodiorite sample 17LP2023A. The red spots represent the approximate locations of laser ablation pits.

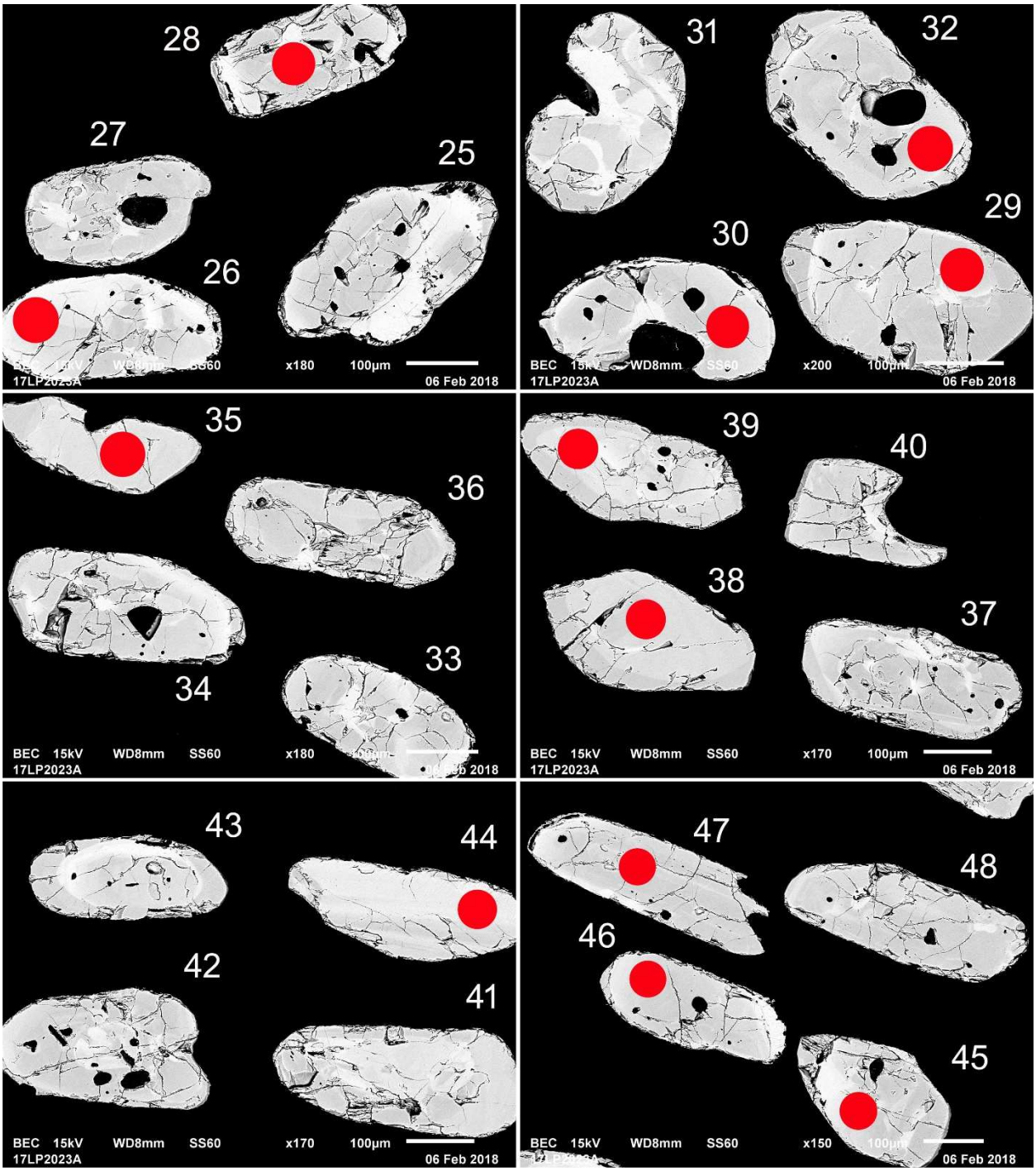


Fig 14-2-2 BSE images of selected grains from porphyritic monzodiorite sample 17LP2023A. The red spots represent the approximate locations of laser ablation pits.

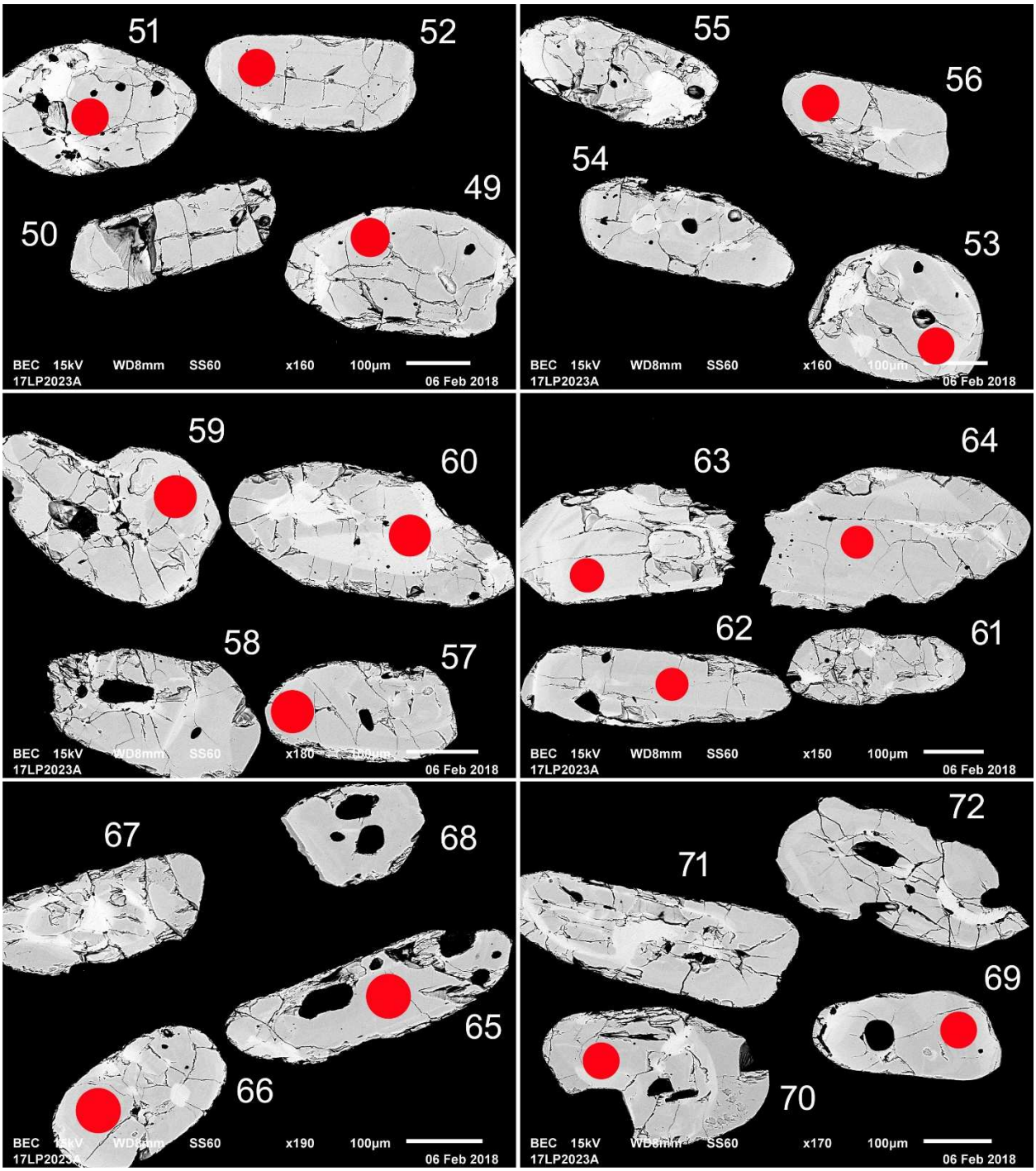


Fig 14-2-3 BSE images of selected grains from porphyritic monzodiorite sample 17LP2023A. The red spots represent the approximate locations of laser ablation pits.

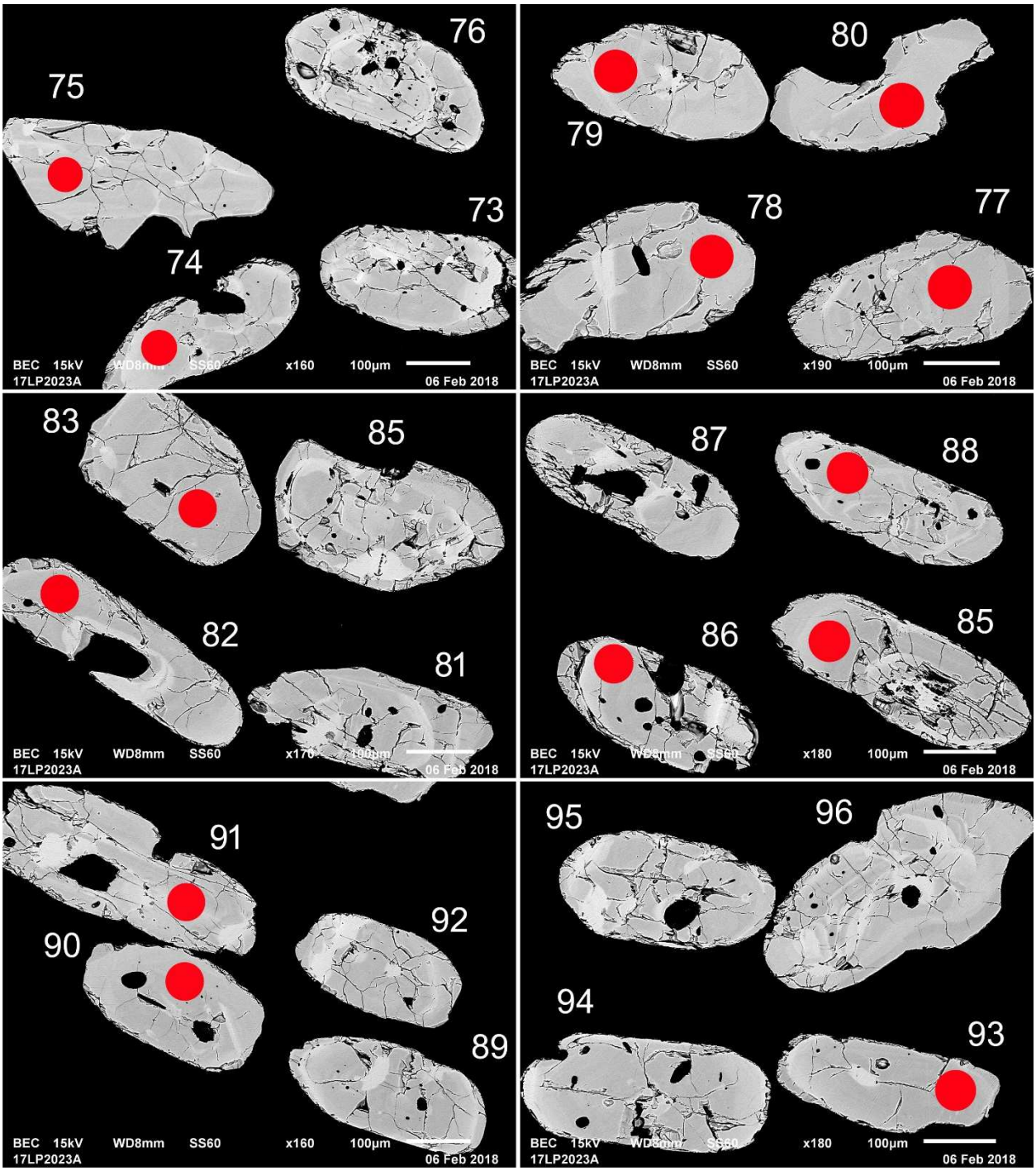


Fig 14-2-4 BSE images of selected grains from porphyritic monzodiorite sample 17LP2023A. The red spots represent the approximate locations of laser ablation pits.

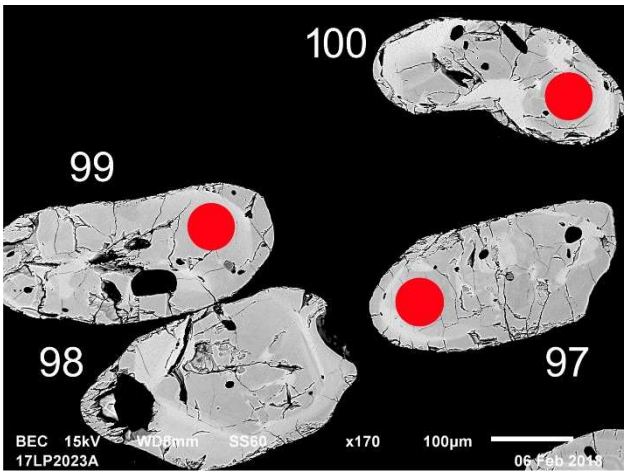


Fig 14-2-5 BSE images of selected grains from porphyritic monzodiorite sample 17LP2023A. The red spots represent the approximate locations of laser ablation pits.

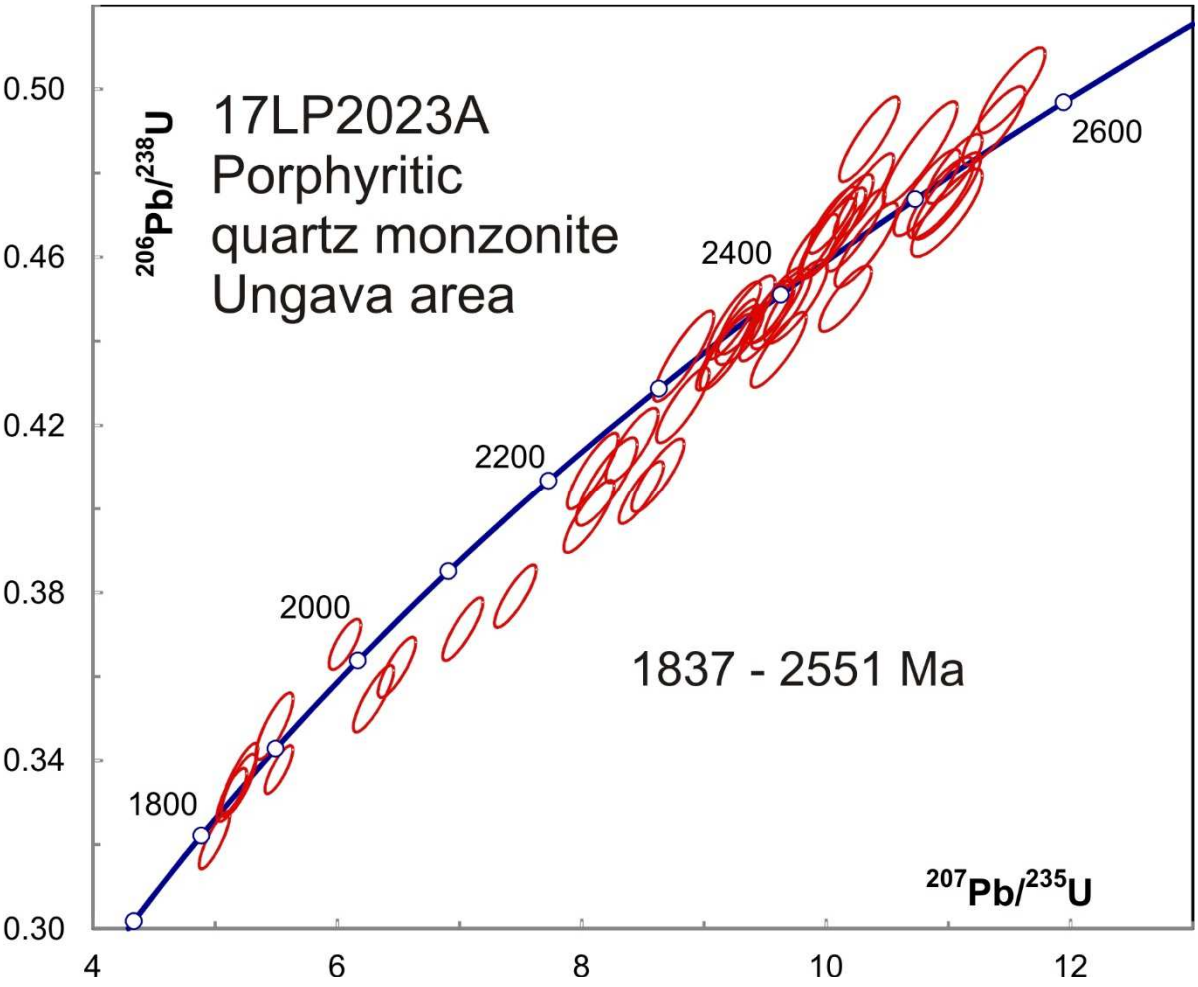


Fig 14-3. Concordia plot showing U-Pb isotopic data on zircon from monzodiorite sample 17LP2023A.

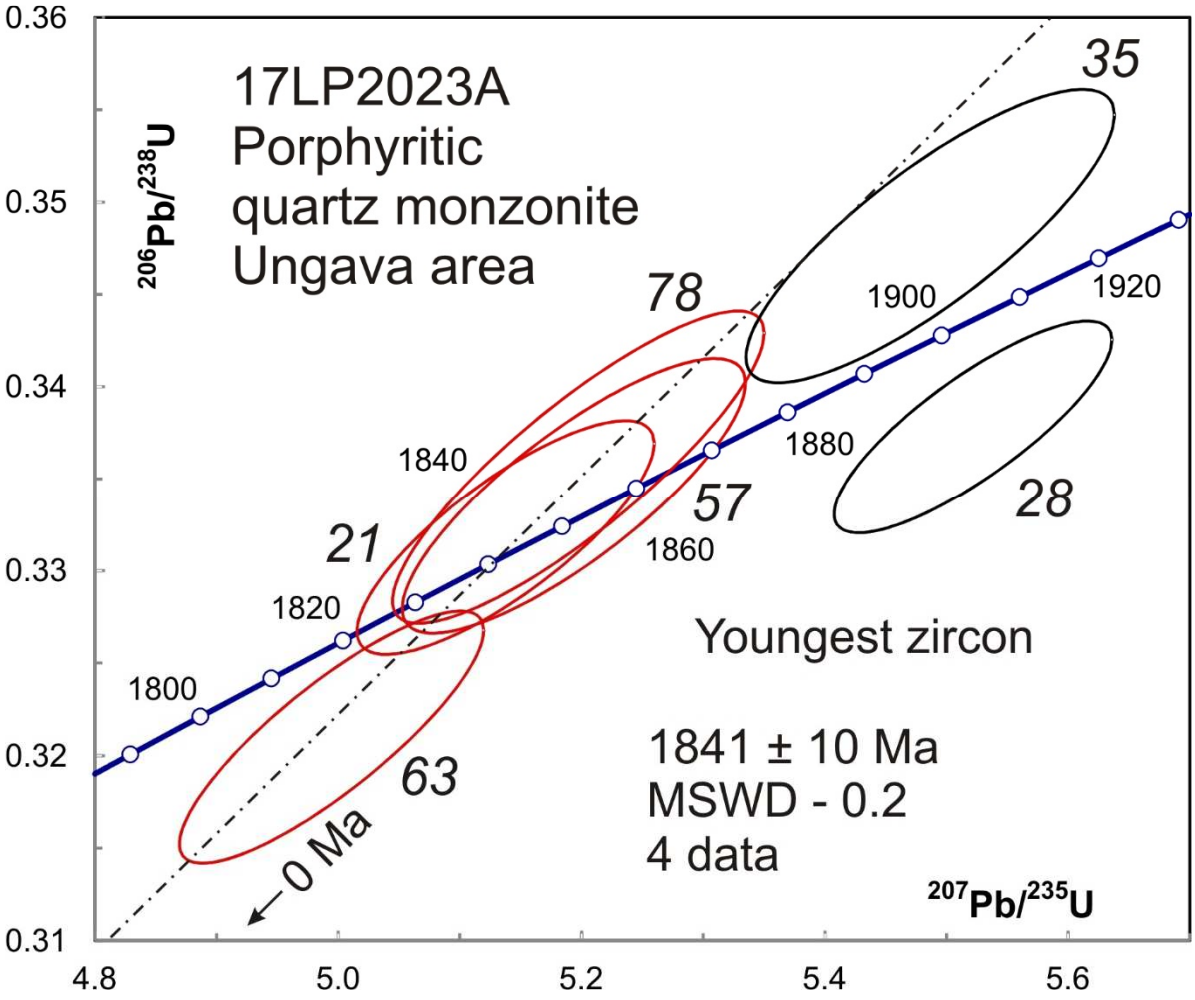


Fig 14-4. Concordia plot showing U-Pb isotopic data on youngest zircon from monzodiorite sample 17LP2023A. The black ellipses are not included in the age average. Spot numbers are in italics.

### *3-15 17LP2157A: Monzonite, Suluraaq Suite, Ungava Area*

Zircon recovered from this rock is subrounded and fractured, similar in appearance to the previous two samples (Fig 15-1). BSE images show a similar unzoned or patchy appearance (Fig 15-2). Most U-Pb data cluster within error except for two, which are discordant and obviously older (Fig 15-3), although these two spots do not appear to be different from the others. The other data give an average age of 1889 ± 4 Ma (Fig 15-4). A line between the two older data projects to about 3.8 Ga, although this number is heavily dependent on the degree of discordance, which is poorly controlled, so it may not be meaningful. Th/U ratios are highly variable ranging from about 0.2 to 2 with one value up to 3.5 (Table 1), although there is no correlation with age. The data suggest that the pluton was emplaced during the Paleoproterozoic and involved mixing two magmas, a normal felsic melt with crustal Th/U, and a high Th/U melt similar to that which formed the youngest zircon phase in quartz monzonite sample 17LP2023A, although the bulk of zircon in this rock appears to be Archean.

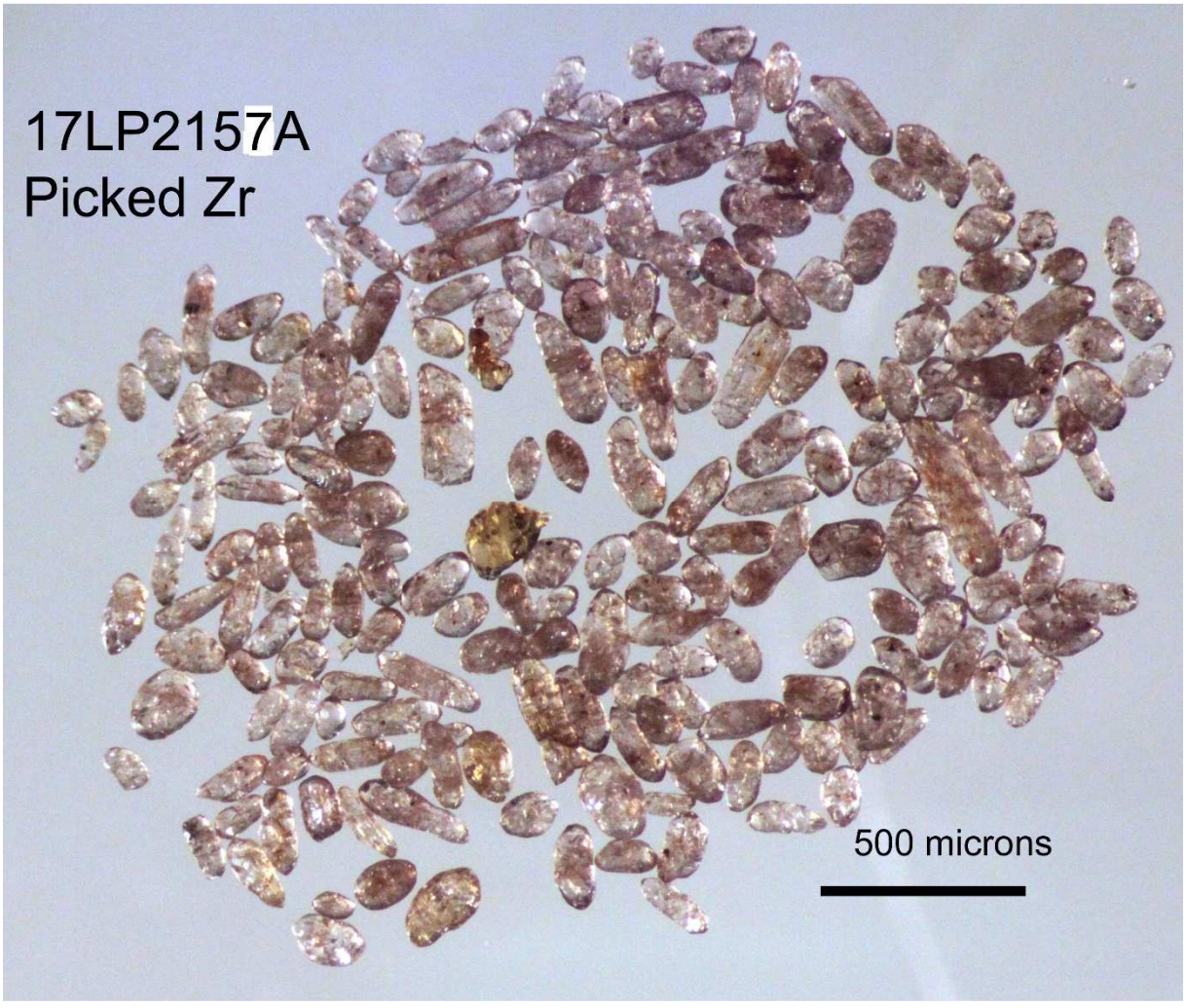


Fig 15-1. Picked zircon from monzonite sample 17LP2157A.

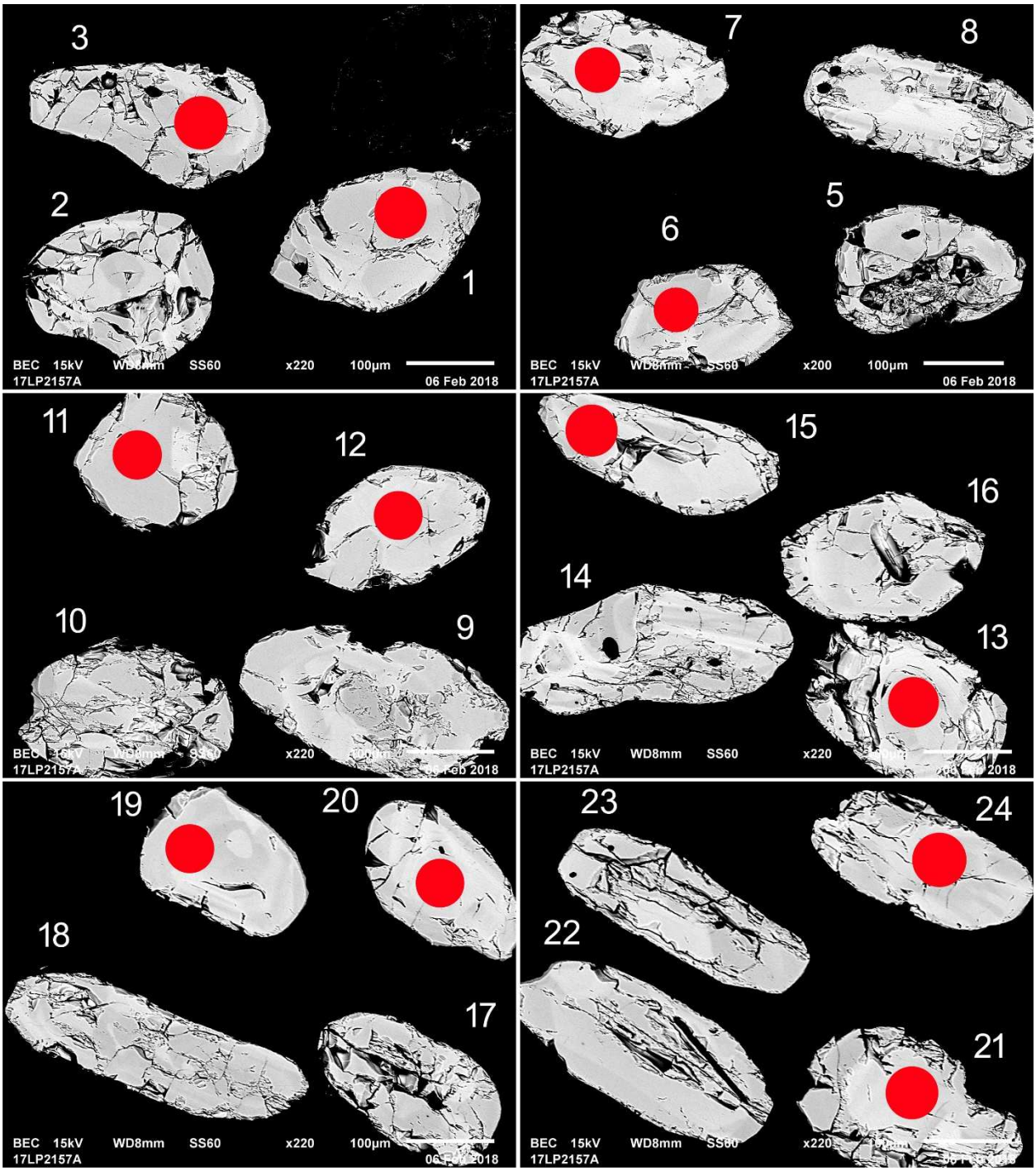


Fig 15-2-1 BSE images of selected grains from monzonite sample 17LP2157A. The red spots represent the approximate locations of laser ablation pits.

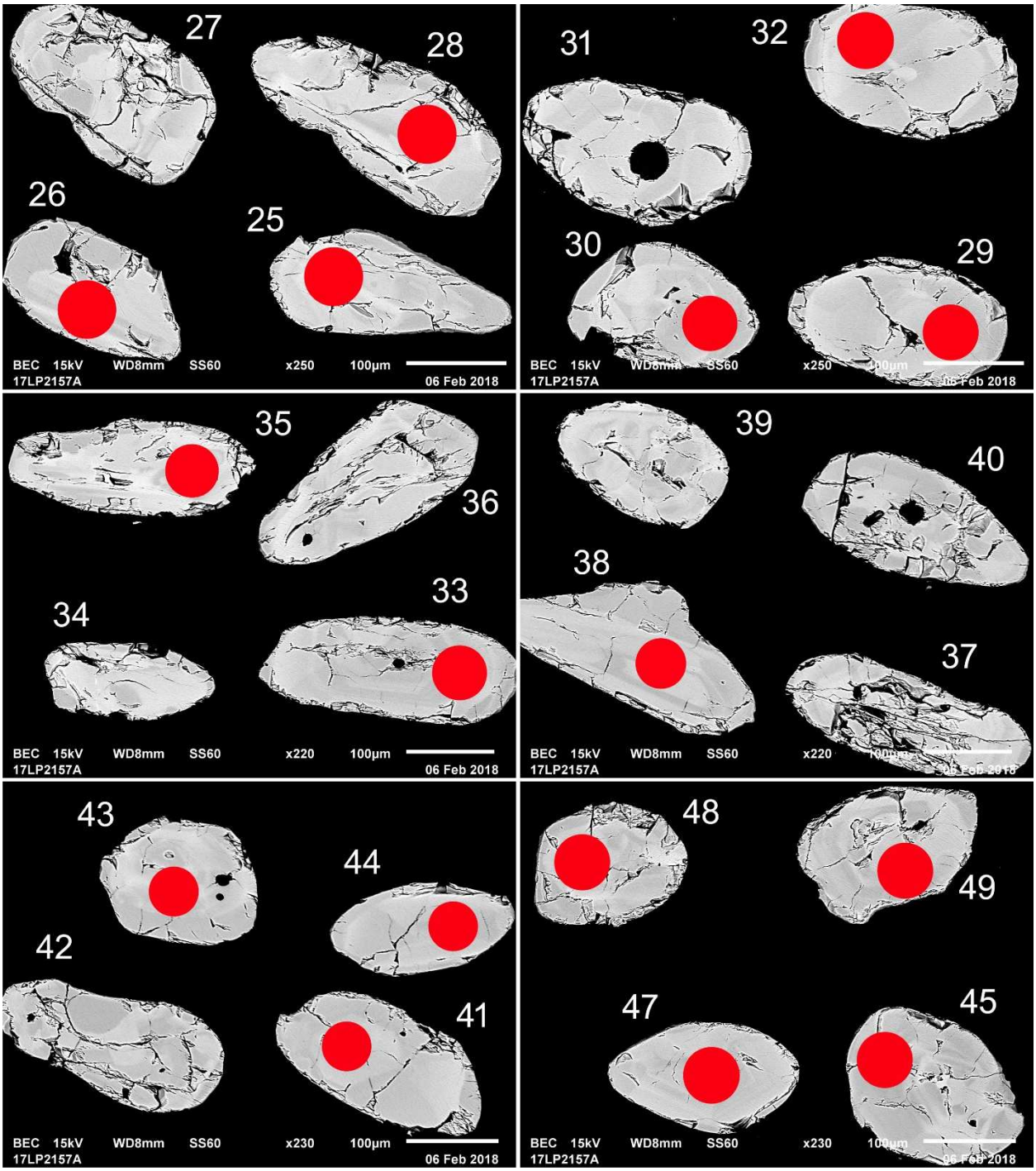


Fig 15-2-2 BSE images of selected grains from monzonite sample 17LP2157A. The red spots represent the approximate locations of laser ablation pits.

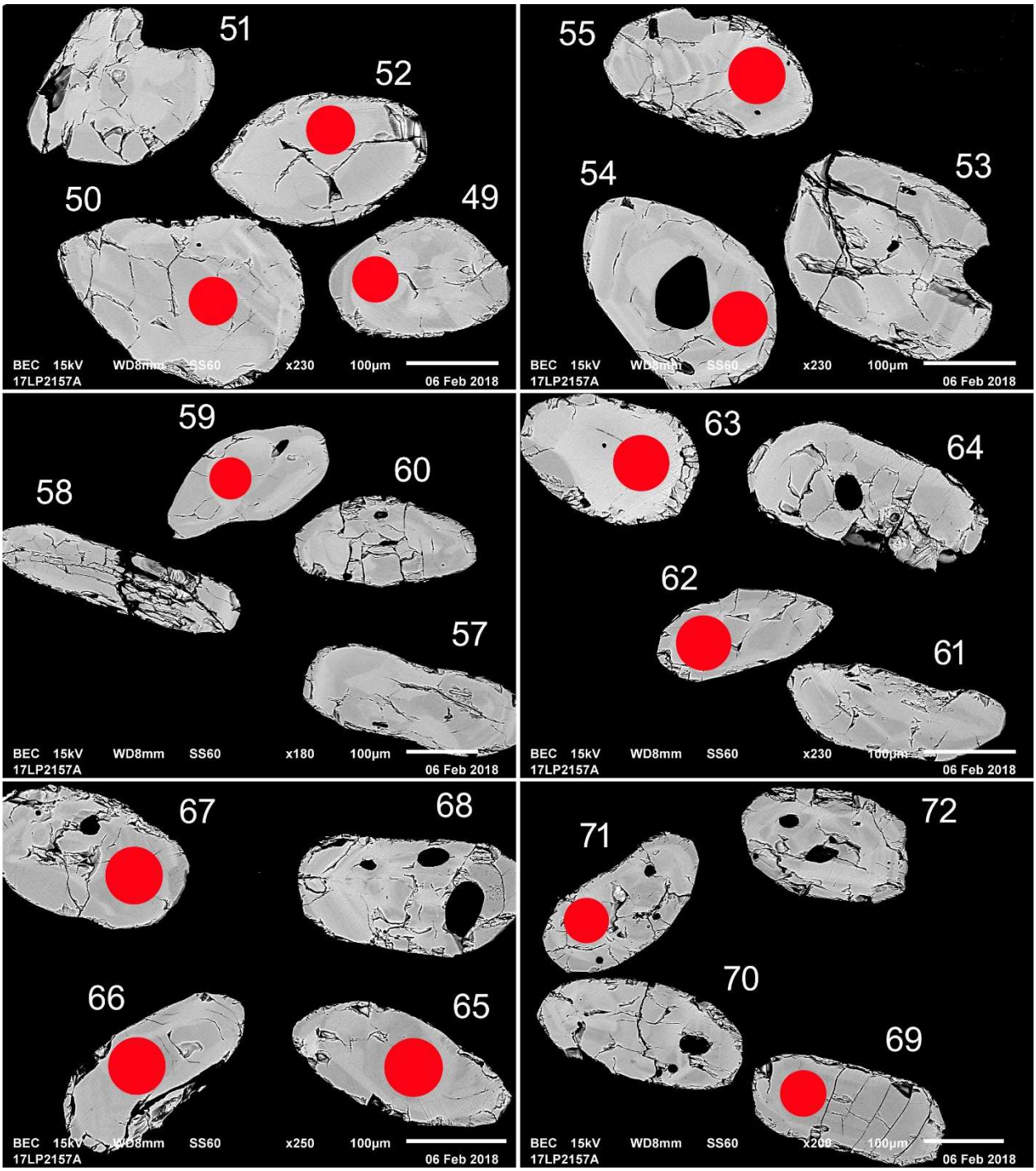


Fig 15-2-3 BSE images of selected grains from monzonite sample 17LP2157A. The red spots represent the approximate locations of laser ablation pits.

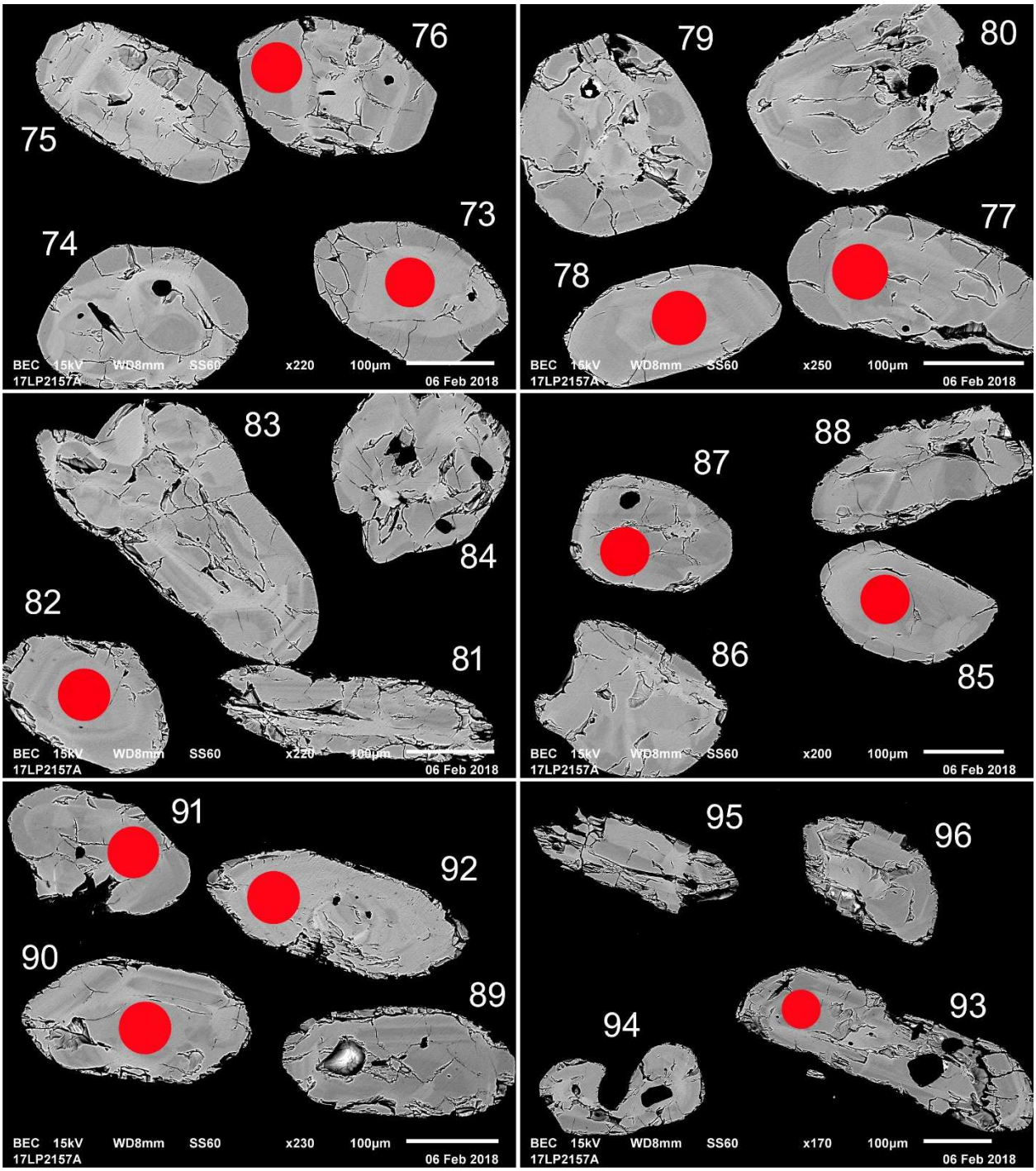


Fig 15-2-4 BSE images of selected grains from monzonite sample 17LP2157A. The red spots represent the approximate locations of laser ablation pits.

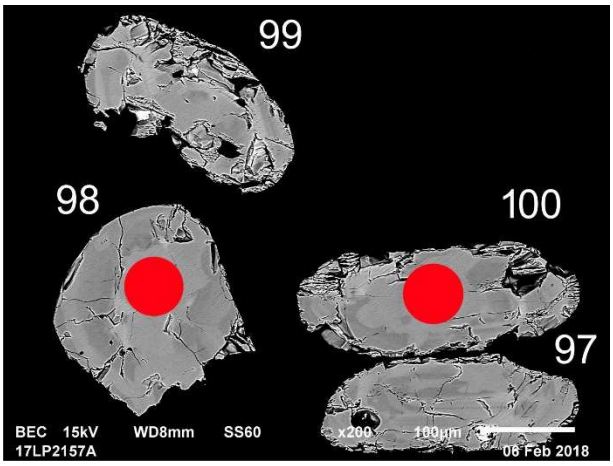


Fig 15-2-5 BSE images of selected grains from monzonite sample 17LP2157A. The red spots represent the approximate locations of laser ablation pits.

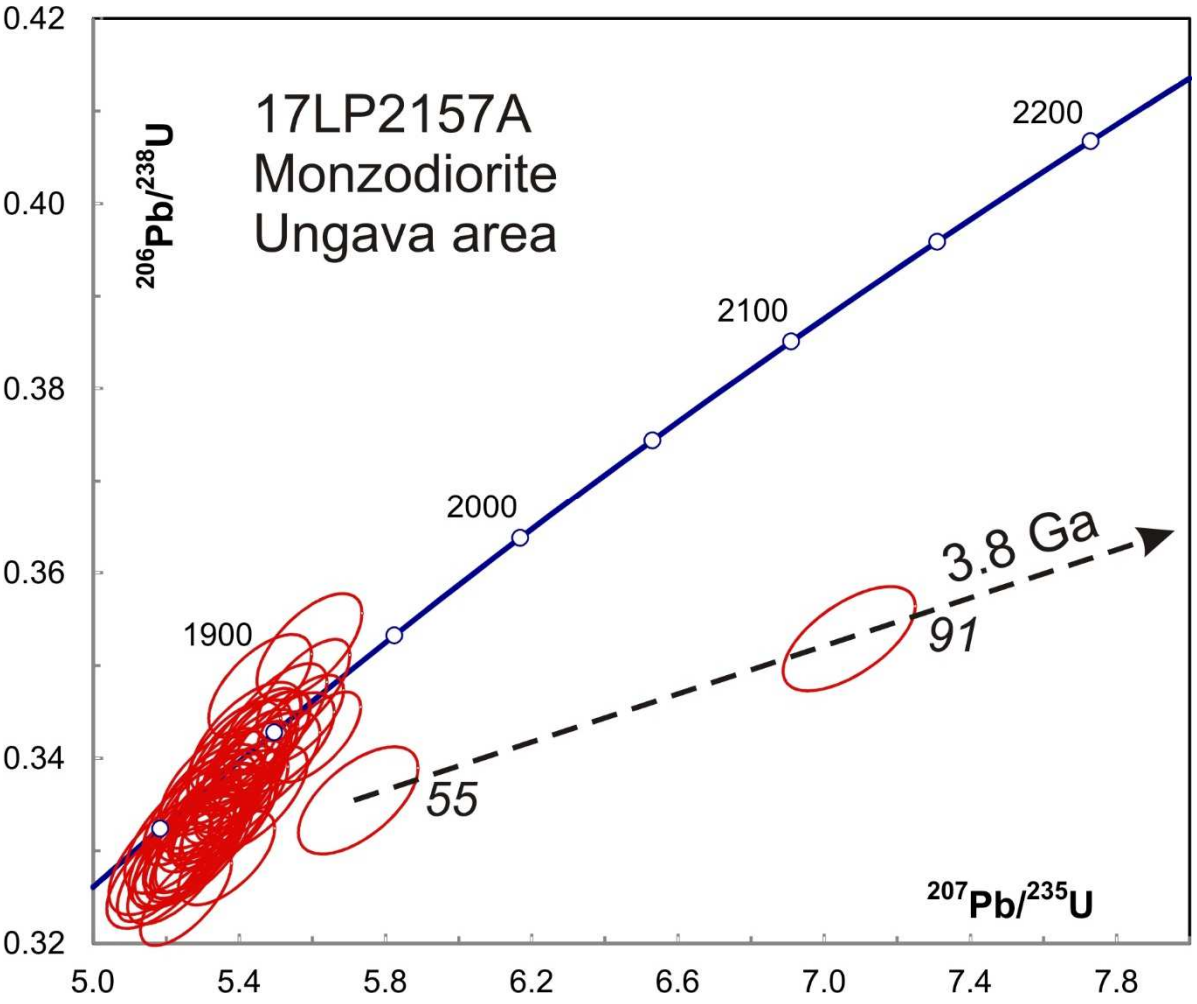


Fig 15-3. Concordia plot showing U-Pb isotopic data on zircon from monzonite sample 17LP2157A. Numbers of two oldest spots are in italics.

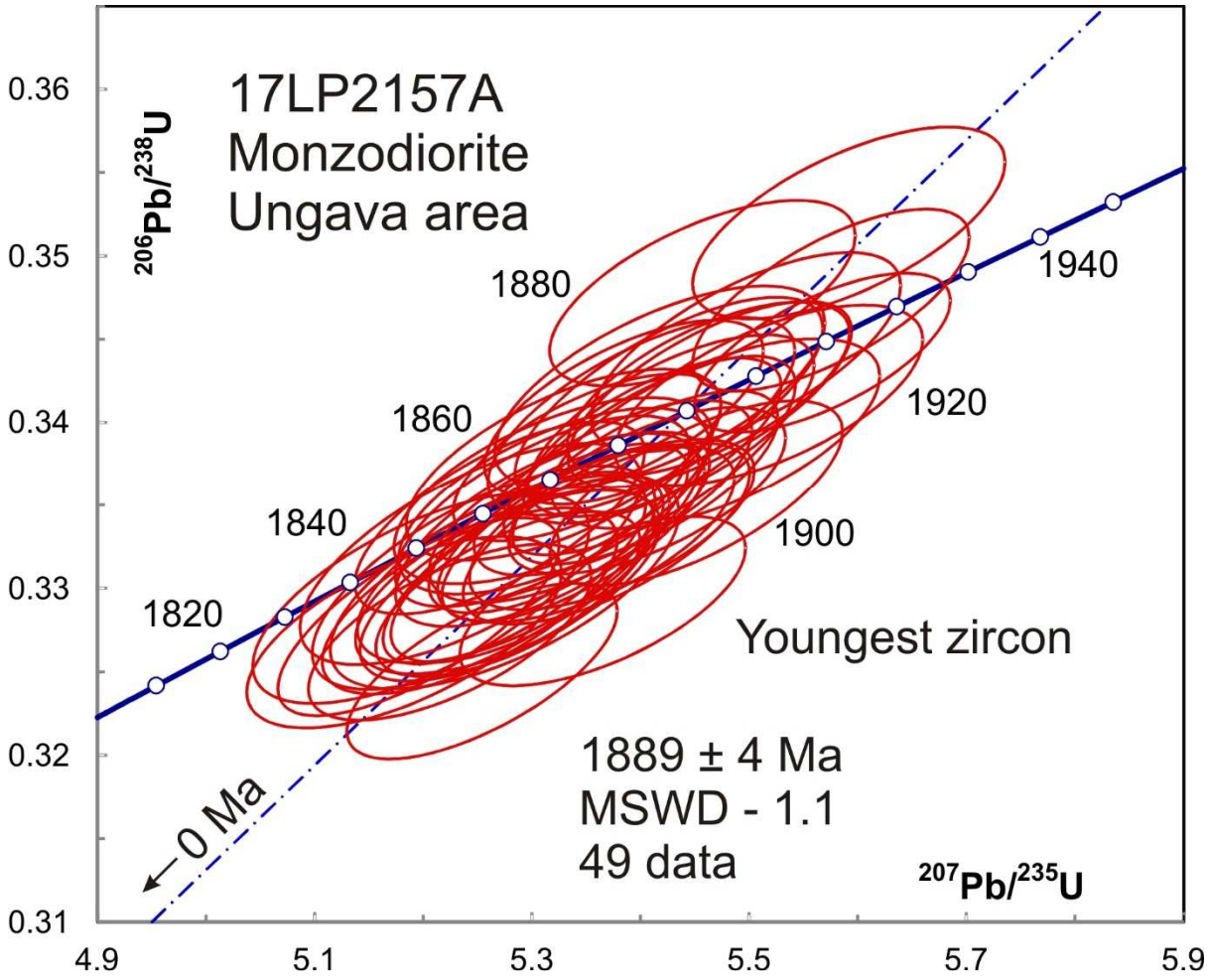


Fig 15-4. Concordia plot showing U-Pb isotopic data on zircon from monzonite sample 17LP2157A. The 3 oldest data are omitted from the full data set.

### *3-16 17MP1092A: Quartz monzodiorite, Suluraaq Suite, Ungava Area*

Zircon from this rock is similar in morphology to the previous Ungava plutons but fresher and less cracked (Fig 16-1). BSE images show unzoned grains that often have higher U cores, some of which show relict oscillatory zoning (Fig 16-2). Despite the presence of cores, all of the analyses overlap with an average age of 1844 ± 6 Ma, except for one analysis from a core that may be slightly older (Fig 16-3). Th/U ratios of all the spots are in the normal range for zircon resulting from igneous crystallization of a felsic rock (Table 1). Either the cores lost all older Pb by diffusion or magmatic crystallization was interrupted and continued under conditions that did not promote oscillatory zoning.

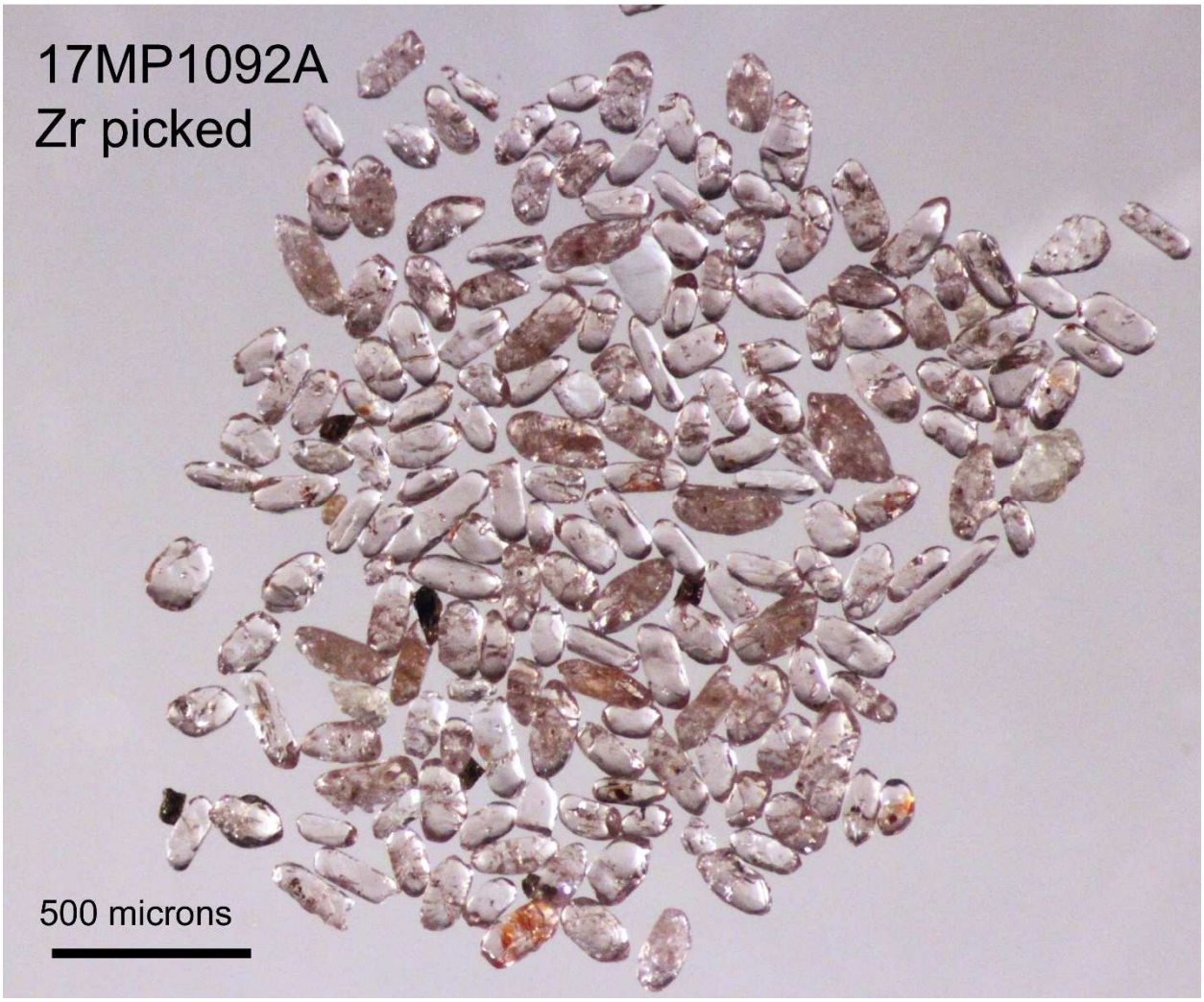


Fig 16-1. Picked zircon from quartz monzodiorite sample 17MP1092A.

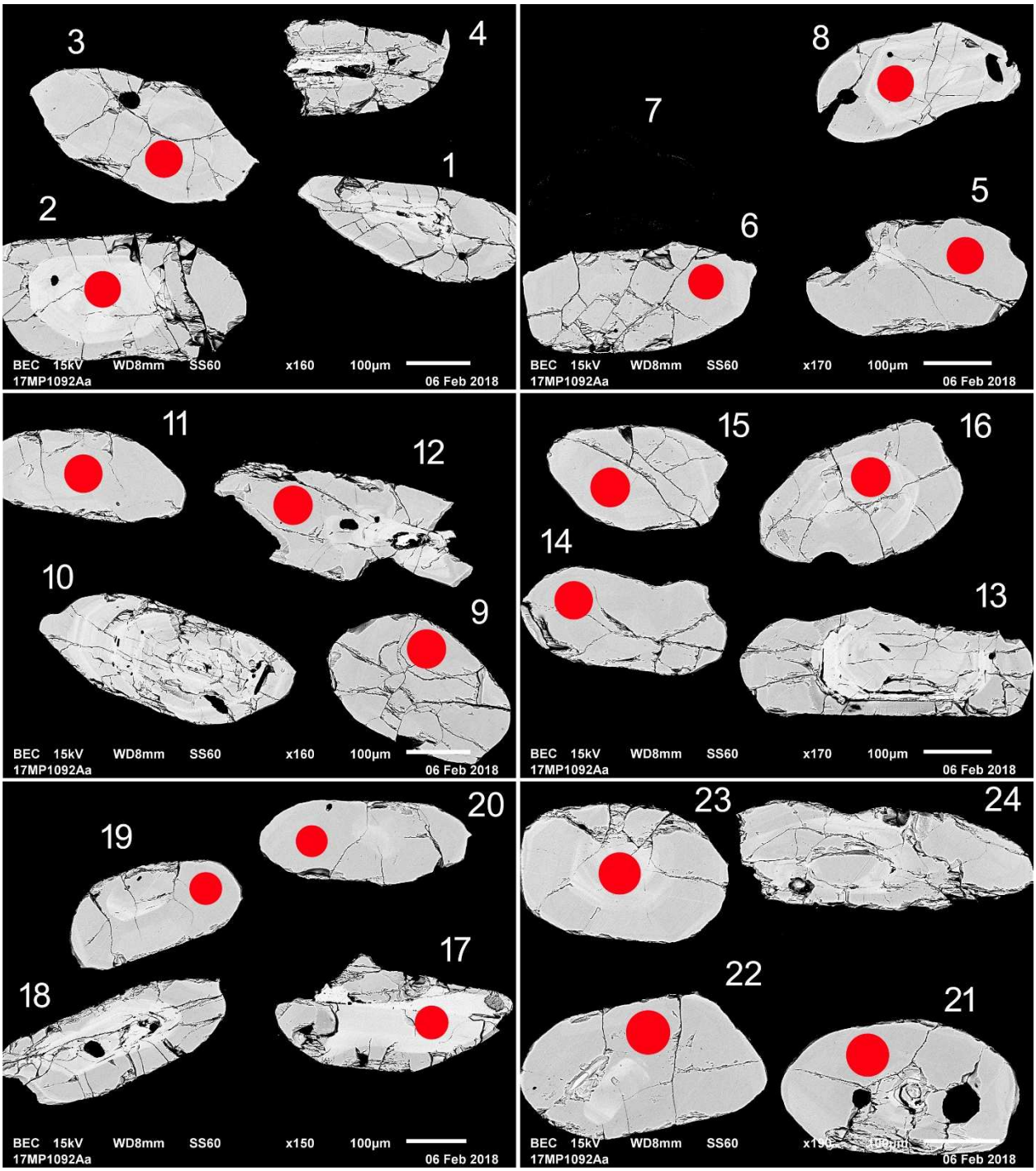


Fig 16-2-1 BSE images of selected grains from quartz monzodiorite sample 17MP1092A. The red spots represent the approximate locations of laser ablation pits.

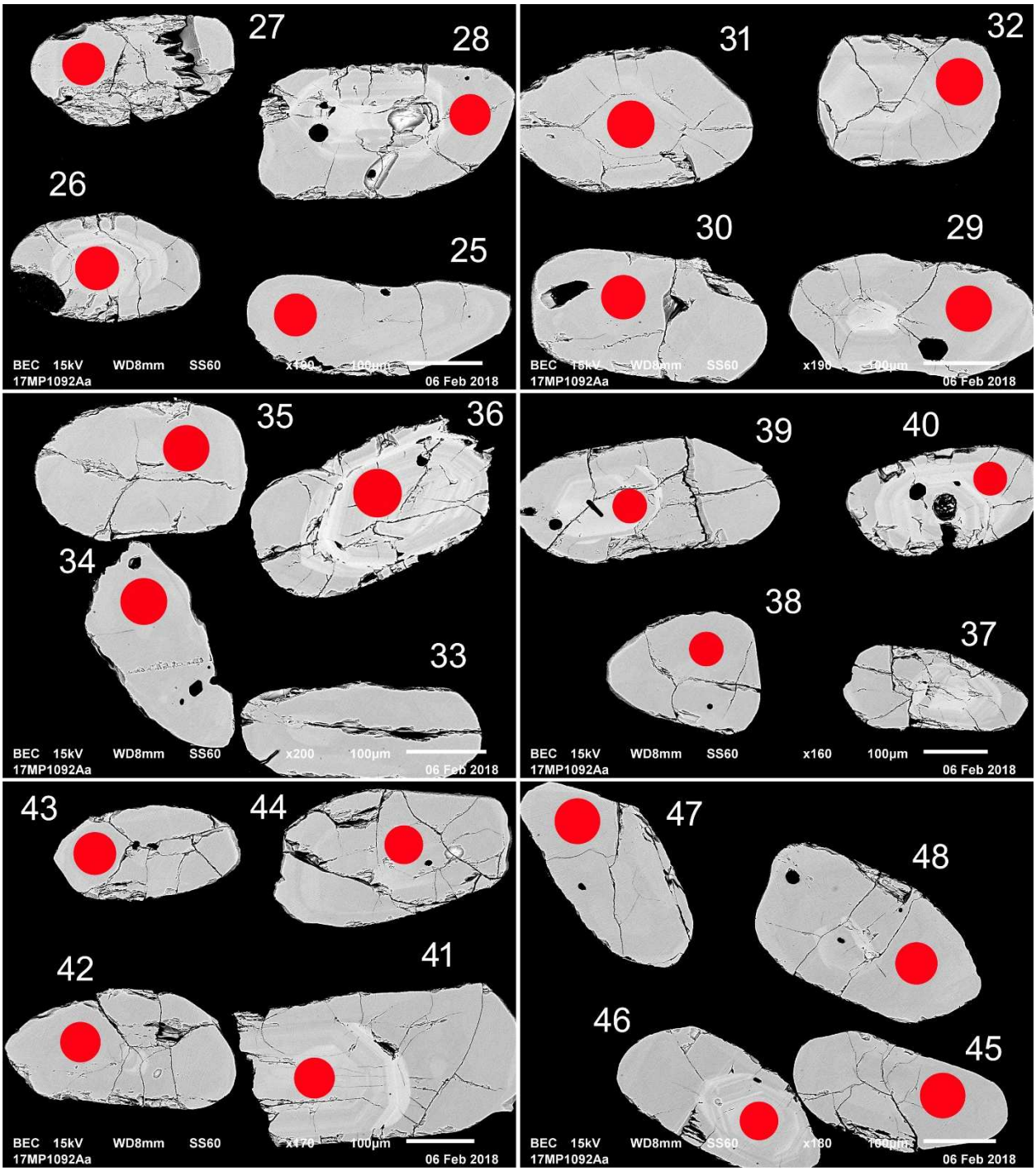


Fig 16-2-2 BSE images of selected grains from quartz monzodiorite sample 17MP1092A. The red spots represent the approximate locations of laser ablation pits.

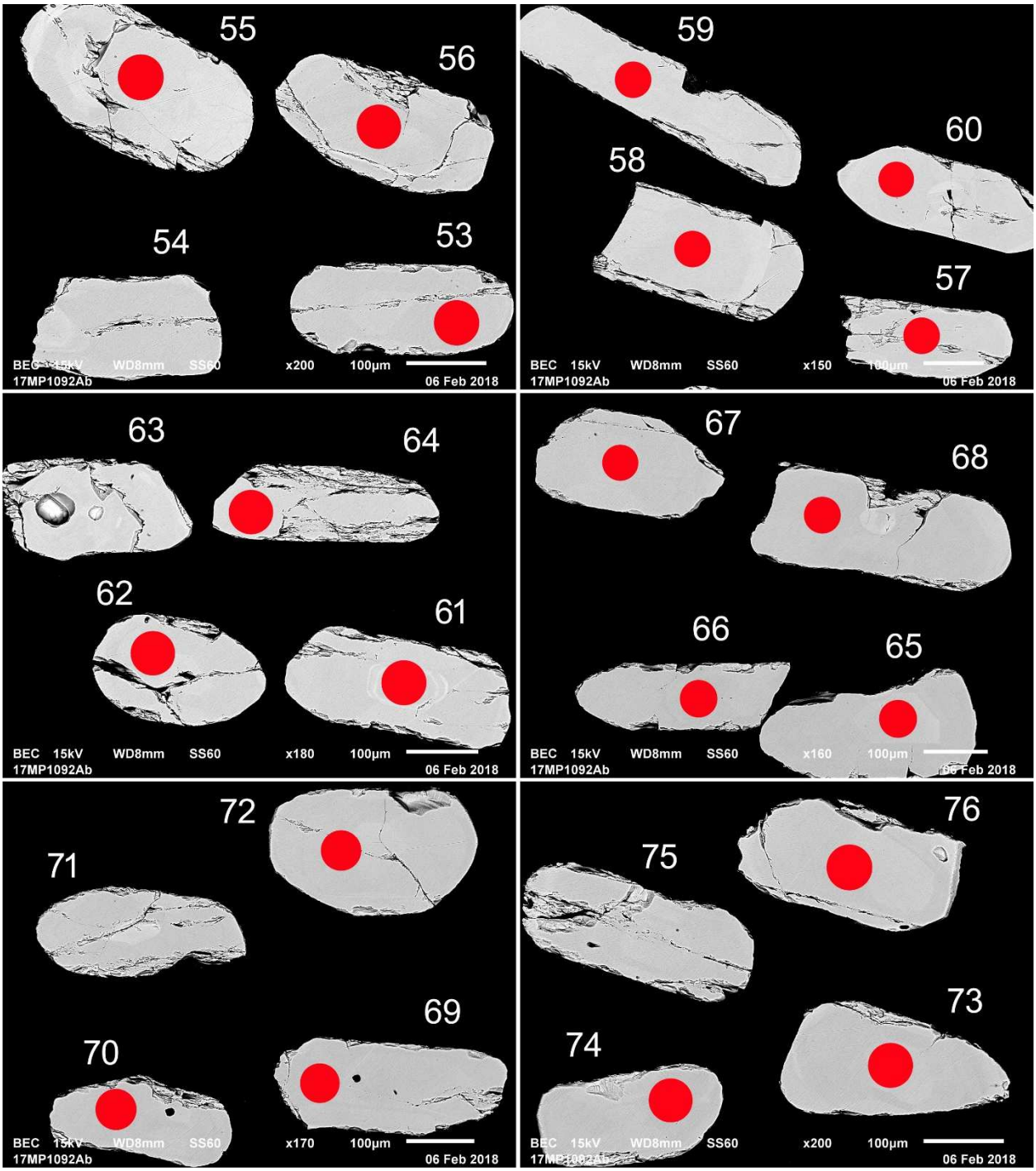


Fig 16-2-3 BSE images of selected grains from quartz monzodiorite sample 17MP1092A. The red spots represent the approximate locations of laser ablation pits.

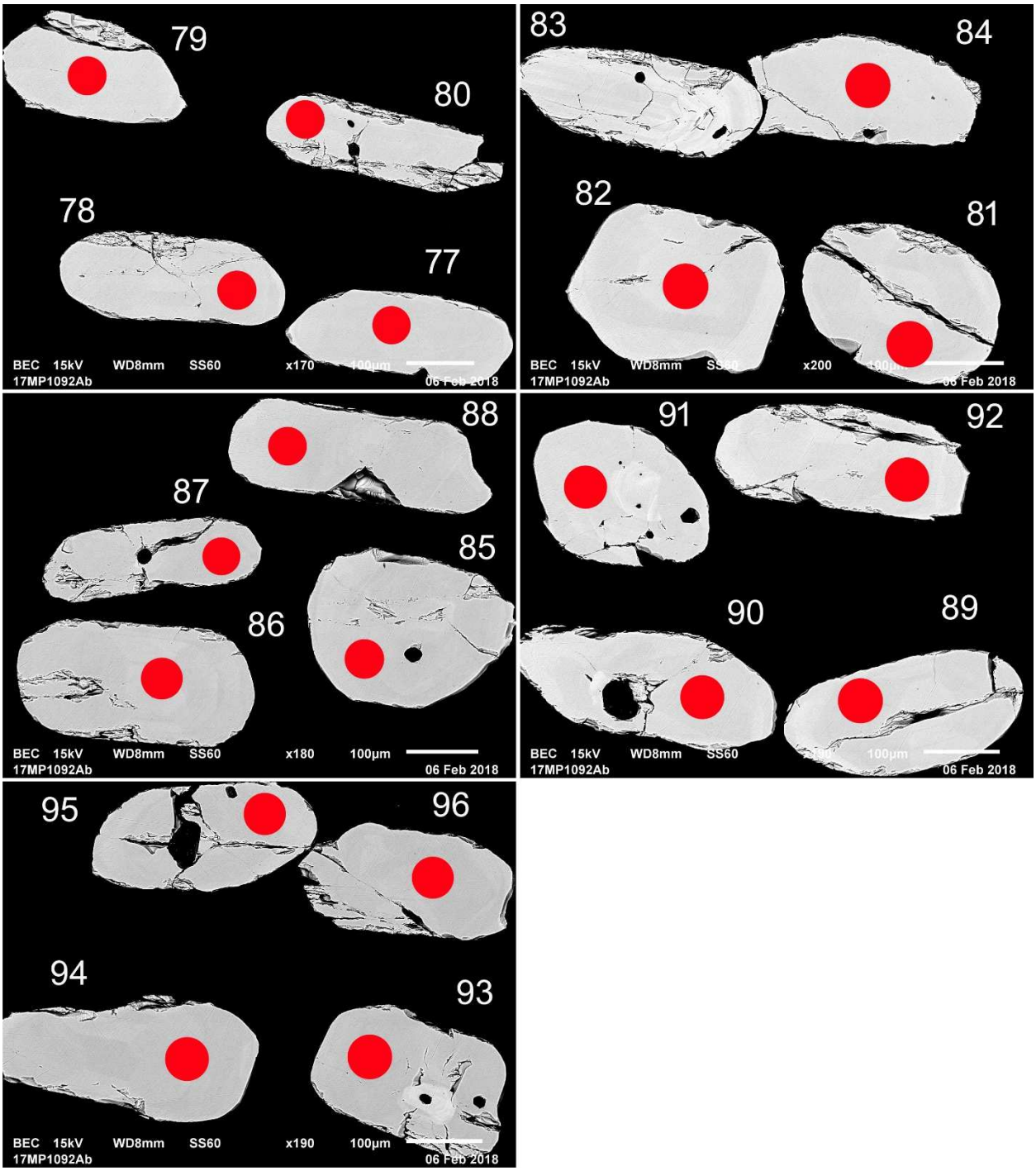


Fig 16-2-4 BSE images of selected grains from quartz monzodiorite sample 17MP1092A. The red spots represent the approximate locations of laser ablation pits.

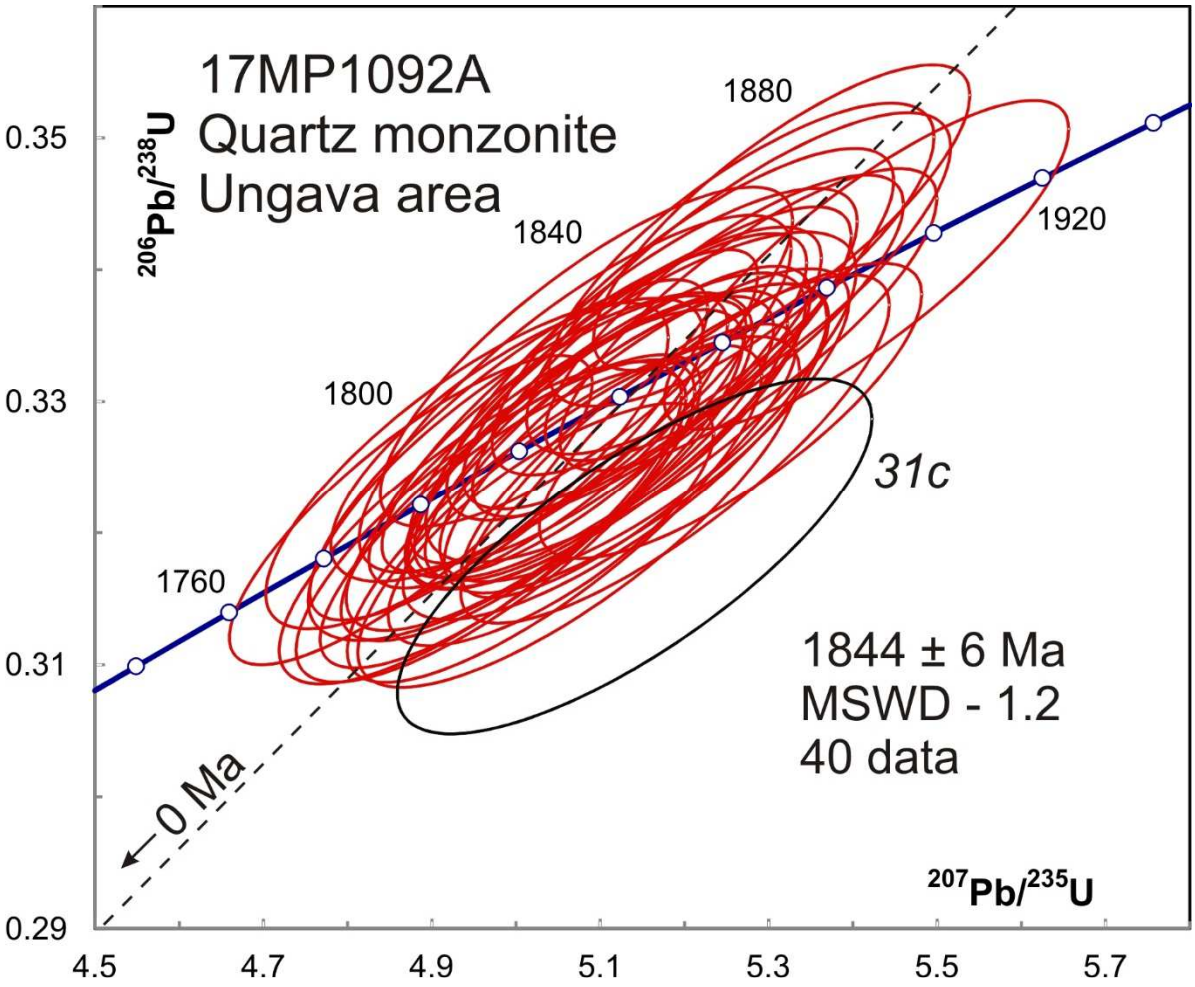


Fig 16-3. Concordia plot showing all U-Pb isotopic data on zircon from quartz monzodiorite sample 17MP1092A. The ellipse in black is omitted from the average. Its spot number is given in italic.

### *3-17 17CT5021A: Enderbite, Pingasualuit Complex, Ungava Area*

As with other samples from the area, the charnockite yielded abundant subrounded zircon that is generally fractured (Fig 17-1). BSE images show a patchy zonation that may in part be caused by remnants of high-U rims. Because of variable U concentrations, some analyses exceeded the limit of the detector and had to be rejected. Seventeen successful analyses are spread over ages from 2773 Ma to 1841 ± 24 Ma, the younger age being an average of the two youngest data, which overlap (Fig 17-3). Th/U ratios are variable but generally within the normal magmatic range (Table 1). The protolith appears to be Neoarchean but was heated long enough to cause diffusional loss of Pb from zircon during the Paleoproterozoic.

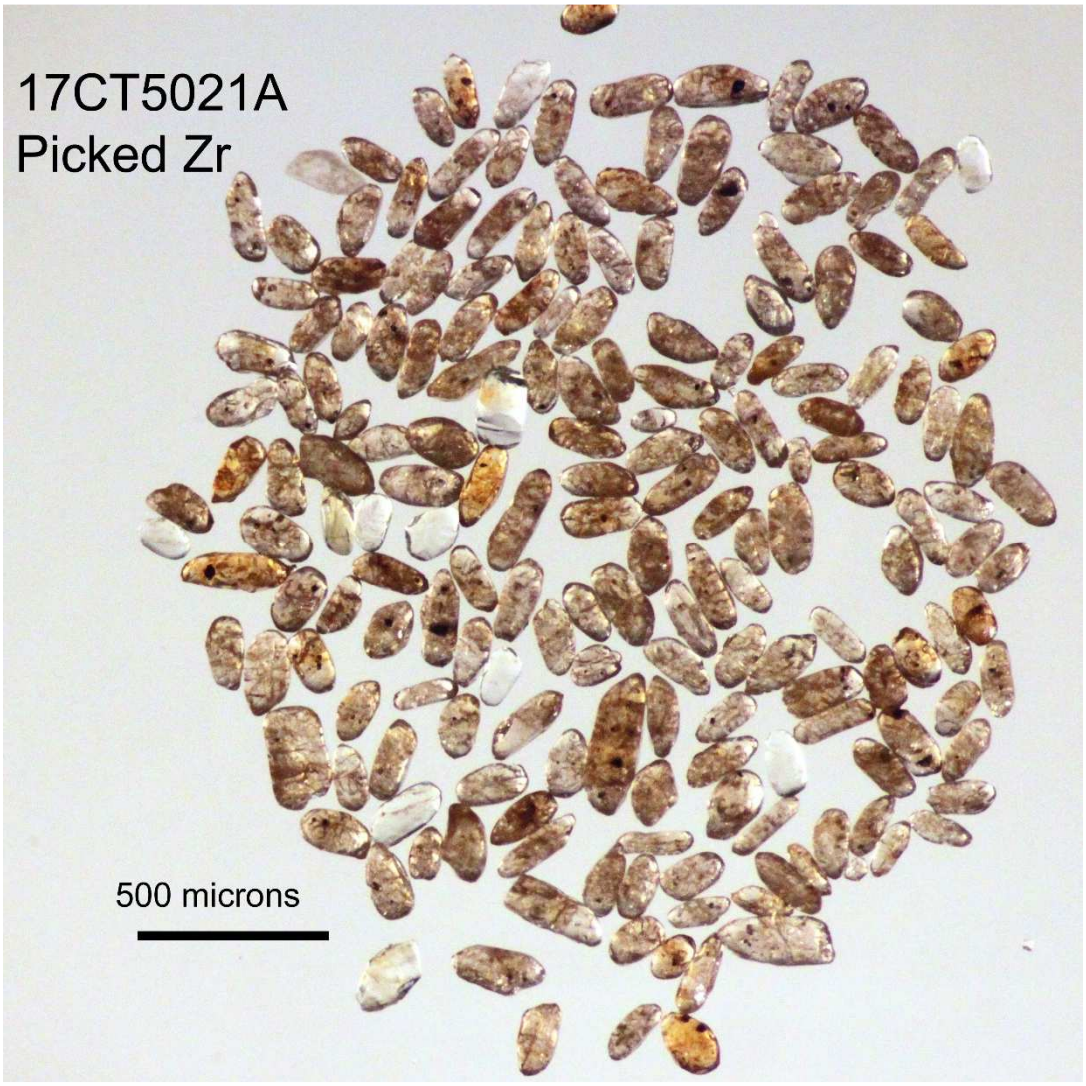


Fig 17-1. Picked zircon from enderbite sample 17CT5021A.

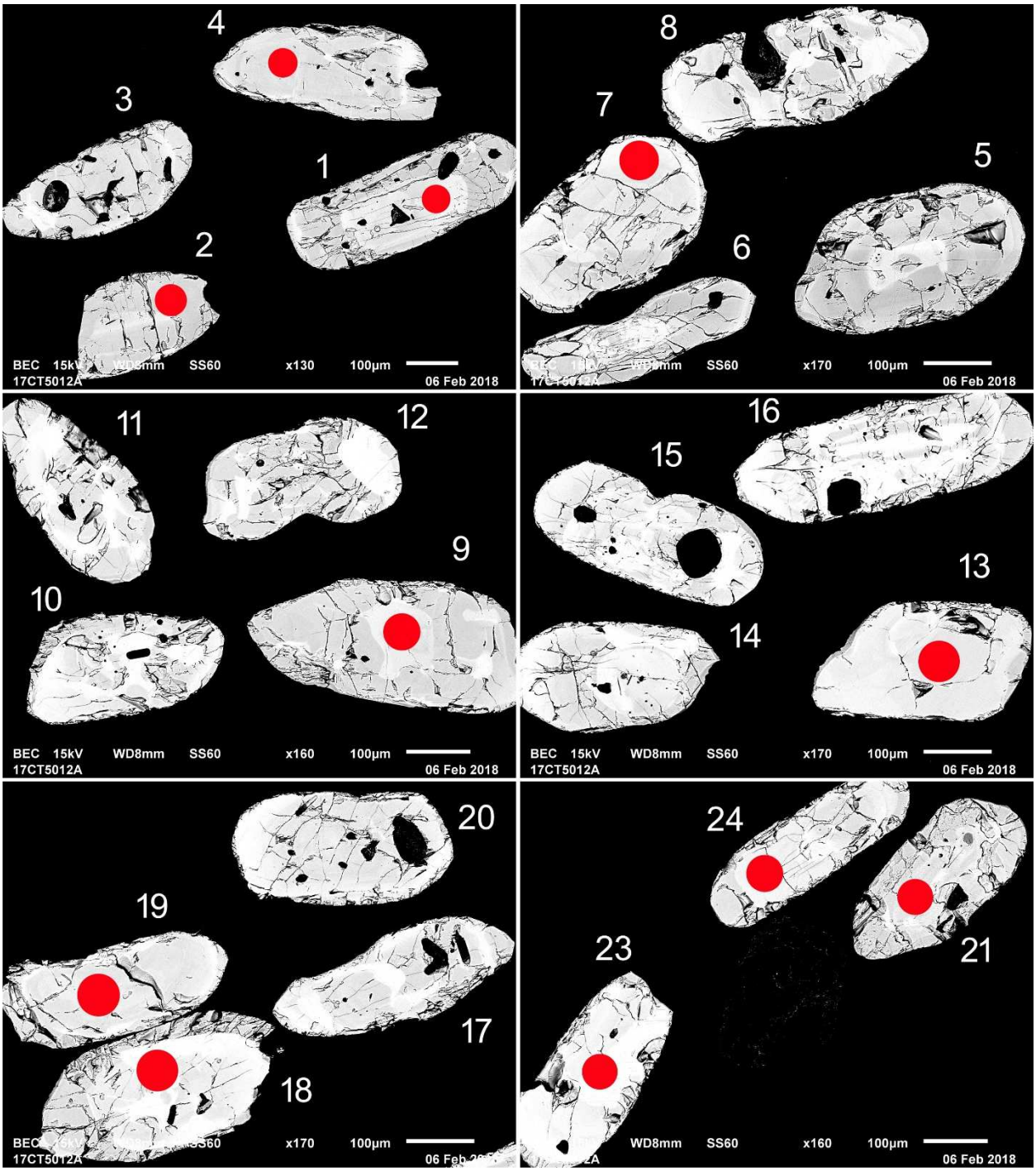


Fig 17-2-1 BSE images of selected grains from enderbite sample 17CT5021A. The red spots represent the approximate locations of laser ablation pits.

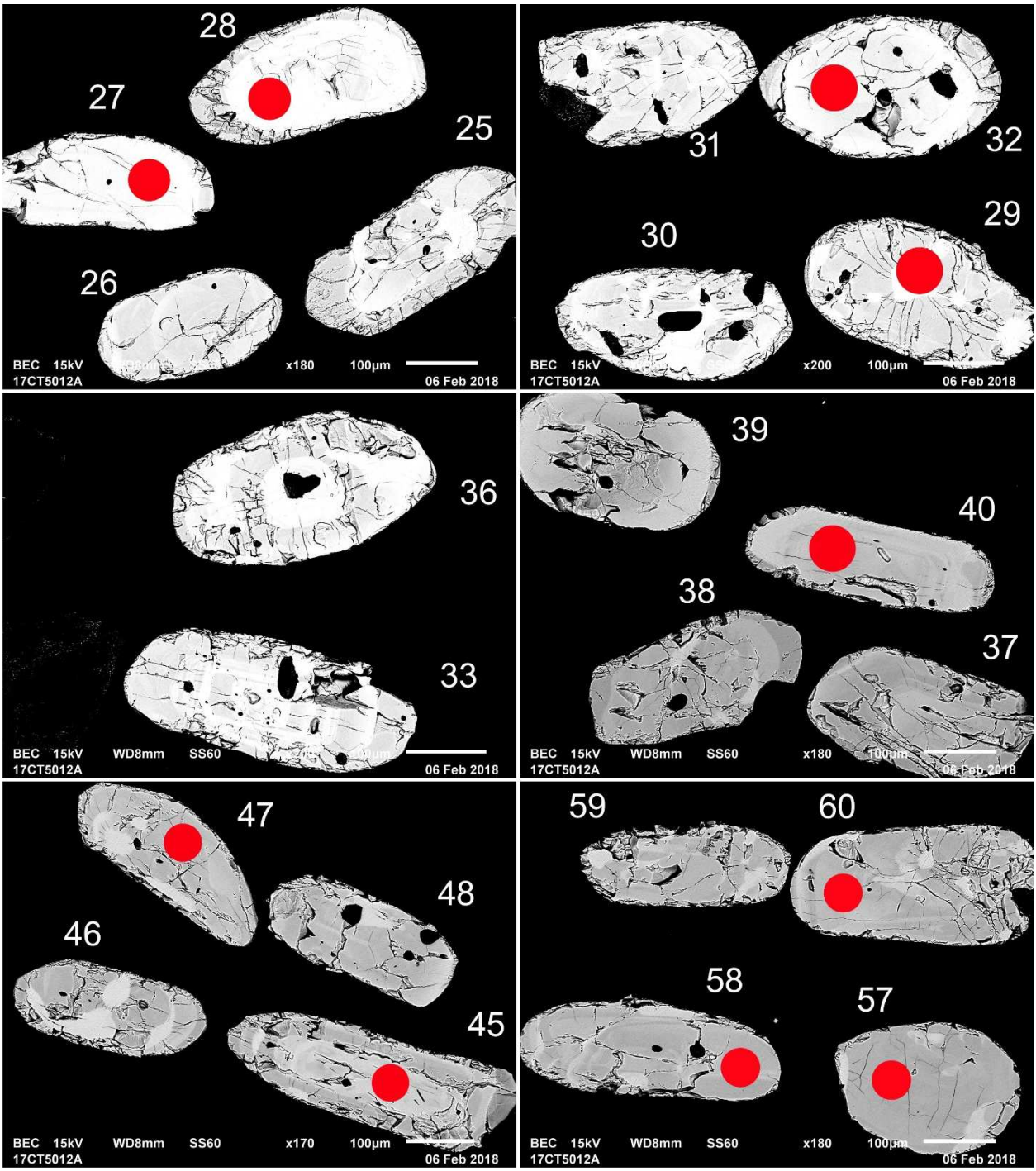


Fig 17-2-2 BSE images of selected grains from enderbite sample 17CT5021A. The red spots represent the approximate locations of laser ablation pits.

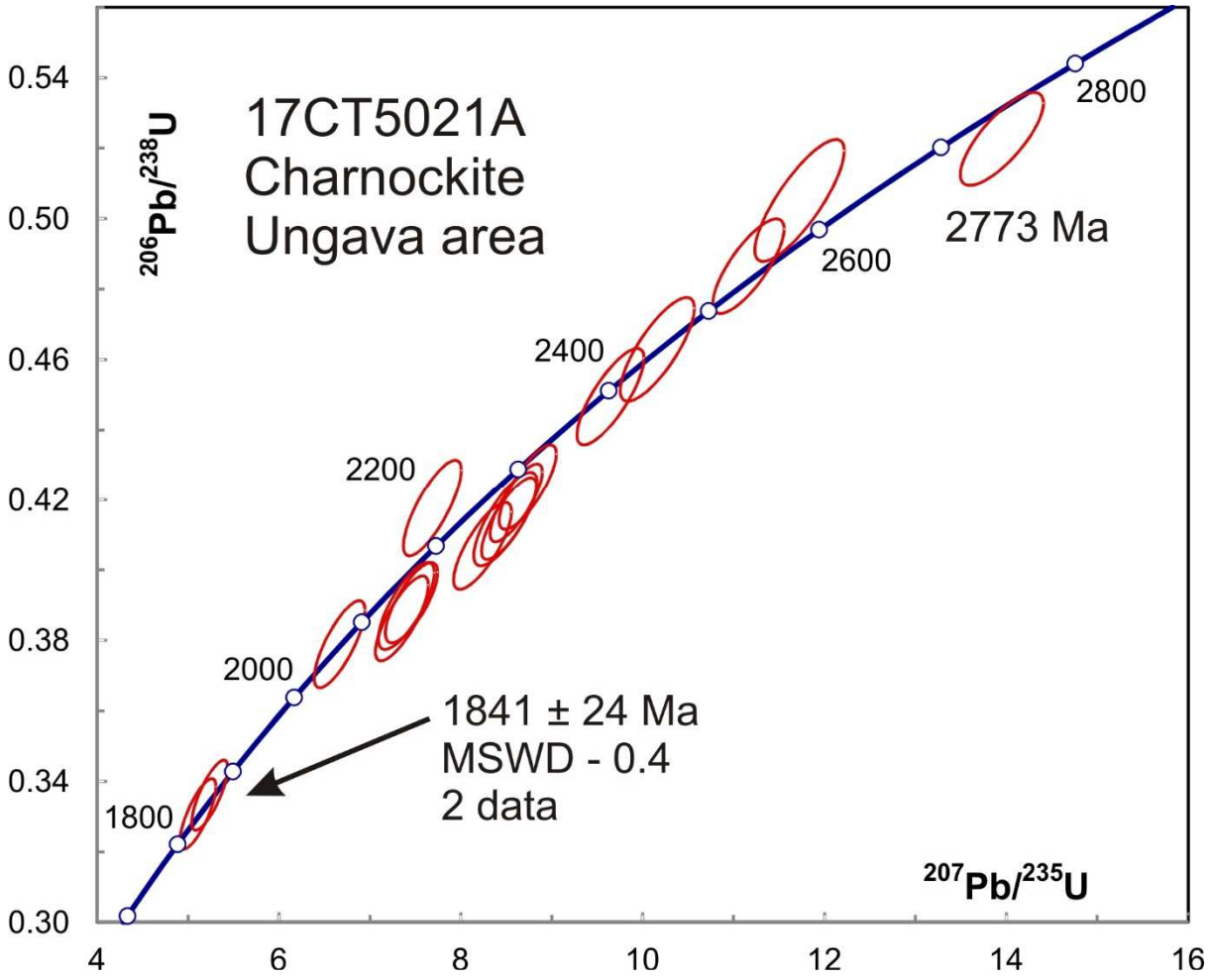


Fig 17-3. Concordia plot showing U-Pb isotopic data on zircon from enderbite sample 17CT5021A. The average $^{207}Pb/^{206}Pb$ age of the two youngest data is shown as well as the oldest age.

### *3-18 17BC6021A: Tonalite, Sainte-Hélène Complex, Ungava Area*

This sample yielded the familiar population of subrounded, short-prismatic, cracked zircon seen in other rocks from the area (Fig 18-1). BSE images show that fine magmatic oscillatory zoning is preserved in many zircon grains (Fig 18-2). This suggests that the sample did not attain as high a level of metamorphic heating as the other samples. U-Pb analyses indicate that the pluton probably crystallized at about 2794 ± 21 Ma (Fig 18-3). Th/U ratios are uniformly in the magmatic range and the youngest spots are on areas with well-developed zoning so the spread in ages is probably due to limited diffusional Pb loss during the Paleoproterozoic, rather than a younger phase. The lower concordia intercept of 1650 ± 150 Ma gives a rough estimate of the age of resetting but may not be reliable because of the difficulty in controlling Pb/U measurements.


Fig 18-1. Picked zircon from tonalite sample 17BC6021A.

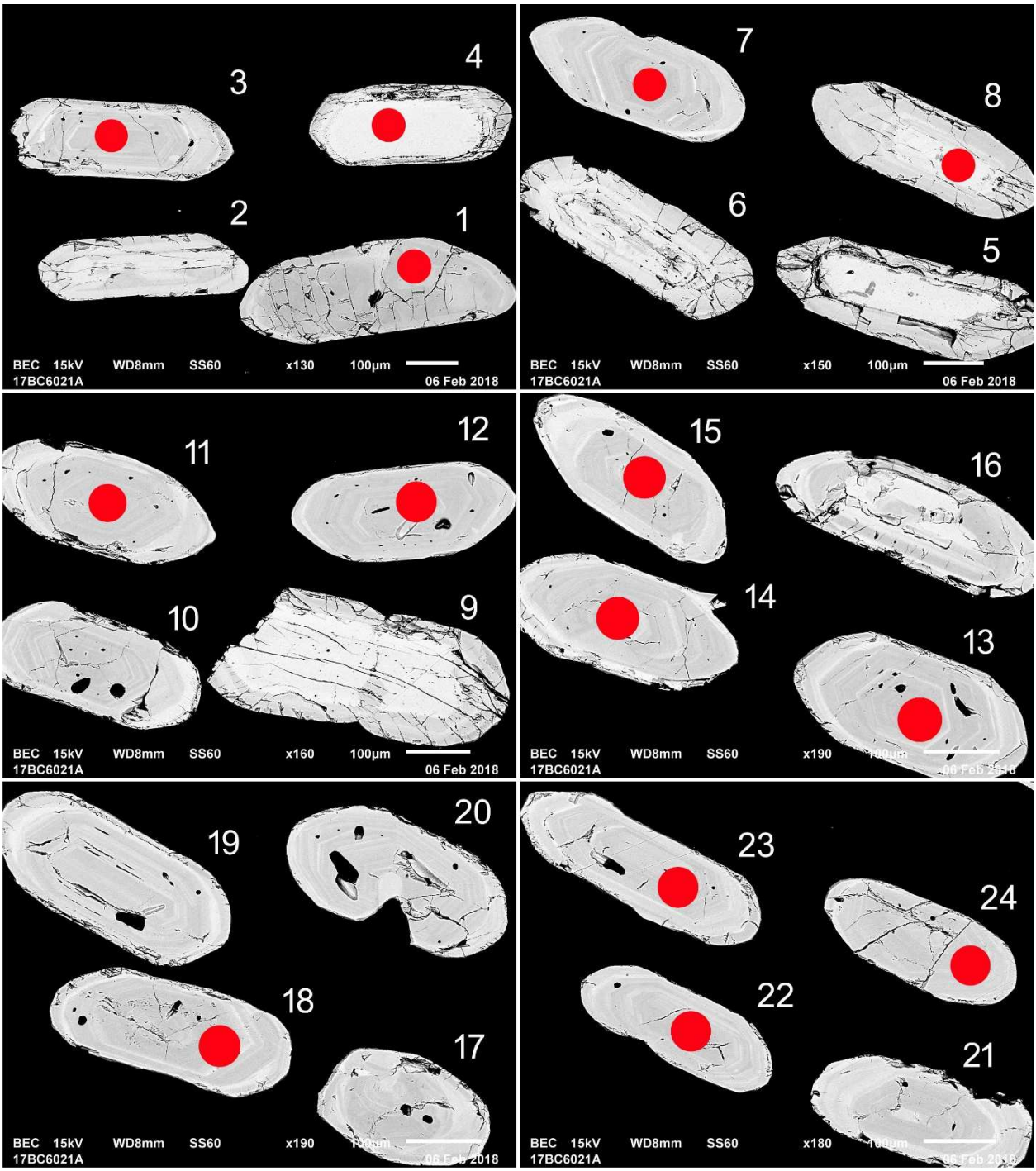


Fig 18-2-1 BSE images of selected grains from charnockite sample 17BC6021A. The red spots represent the approximate locations of laser ablation pits.

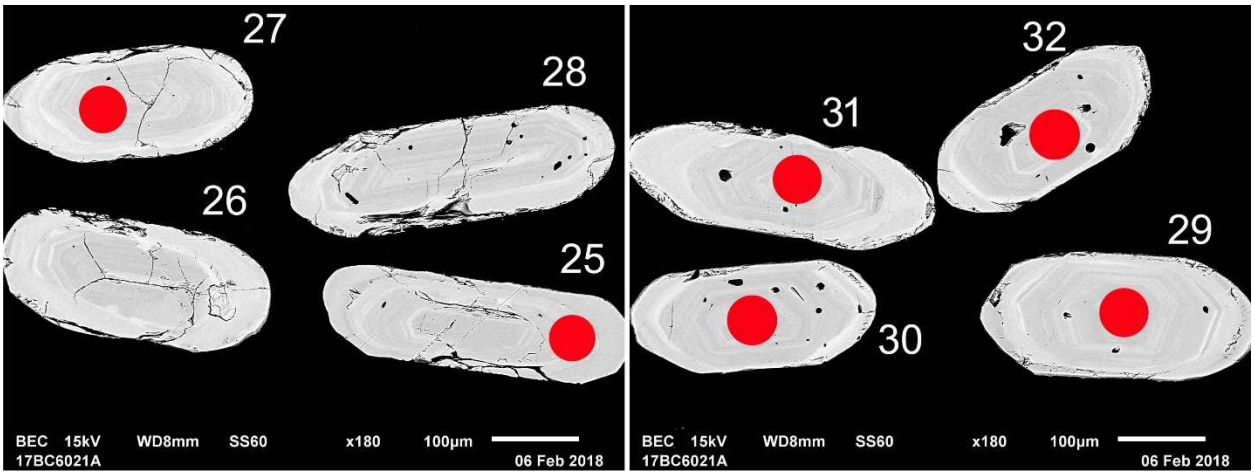


Fig 20-2-2 BSE images of selected grains from charnockite sample 17BC6021A. The red spots represent the approximate locations of laser ablation pits.

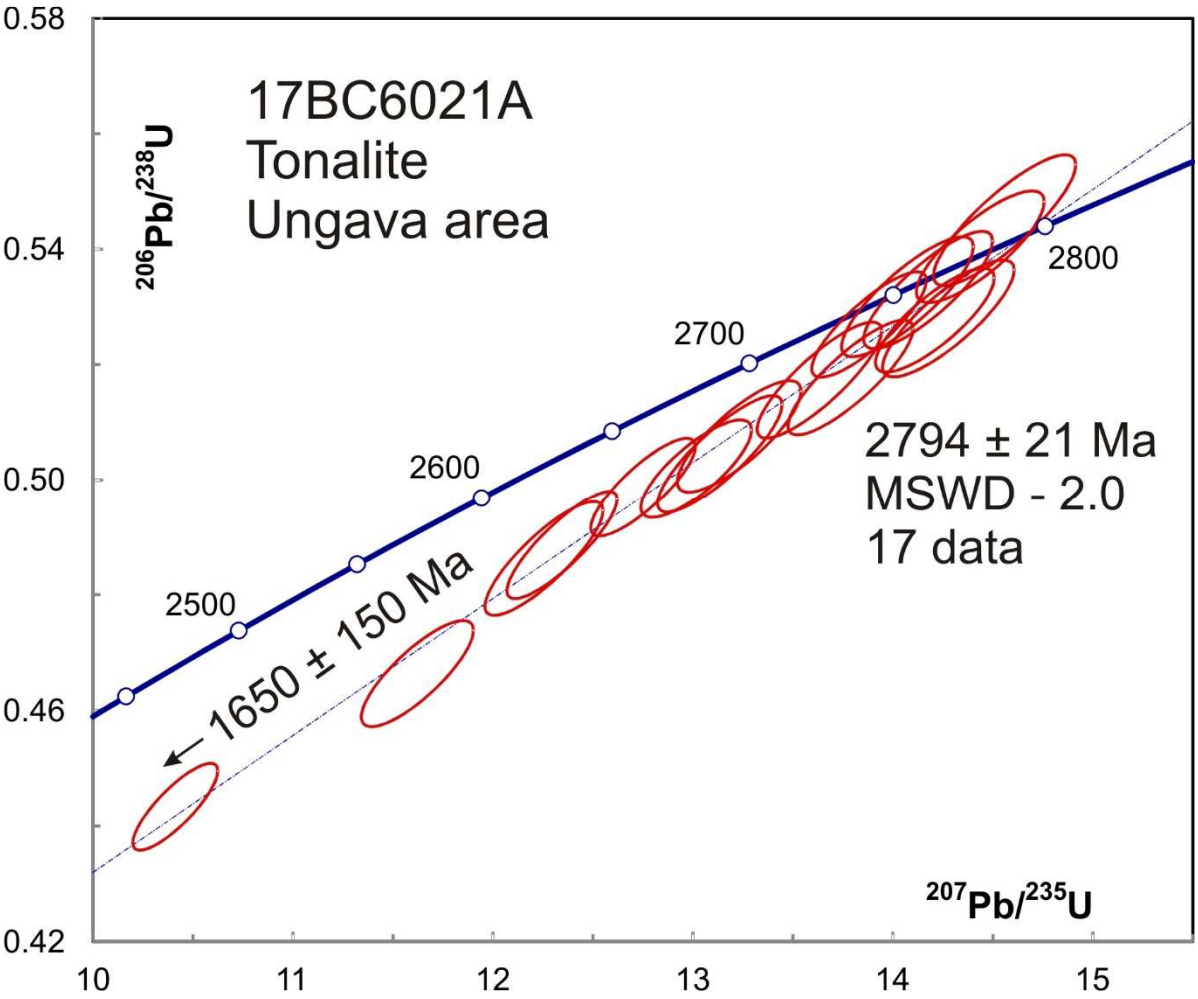


Fig 18-3. Concordia plot showing U-Pb isotopic data on zircon from tonalite sample 17BC6021A.

## REFERENCES


Davis, D.W. 2002. U-Pb geochronology of Archean metasediments in the Pontiac and Abitibi subprovinces, Quebec, constraints on timing, provenance and regional tectonics. Precambrian Research, 115: 97-117.

Jaffey, A.H., Flynn, K.F., Glendenin, L.E., Bentley, W.C. & Essling, A.M. 1971. Precision measurement of half-lives and specific activities of 235U and 238U. Physical Review 4: 1889-1906.

Ludwig, K.R. 2003. User's manual for Isoplot 3.00 a geochronological toolkit for Excel. Berkeley Geochronological Center Special Publication 4, 71 p.

Ludwig, K.R. 1998. On the treatment of concordant uranium-lead ages. Geochimica et Cosmochimica Acta 62: 665-676.

Oberthur, T., Davis, D.W., Blenkinsop, T.G. and Hohndorf, A. 2002. Precise U–Pb mineral ages, Rb–Sr and Sm–Nd systematics for the Great Dyke, Zimbabwe—constraints on late Archean events in the Zimbabwe craton and Limpopo belt. Precambrian Research, 113: 293-305.

Tomlinson, K.Y., Davis, D.W., Stone, D. & Hart, T.R. 2003. U-Pb age and Nd isotopic evidence for crustal recycling and Archean terrane development in the south-central Wabigoon subprovince, Canada. Contributions to Mineralogy and Petrology, 144: 684-702.